TEXTILE RESEARCH JOURNAL

Publication of

TEXTILE RESEARCH INSTITUTE

VOLUME 30 NOVEMBER 1960 NUMBER 11

TEXTILE RESEARCH JOURNAL

Volume 30 *November 1960* Number 11

Editor: **Richard K. Toner**

Production Editor: **Candida Frenking**

Advisory Board

Herbert J. Ball
Earl E. Berkley
John Boulton
C. H. Fisher
Walter J. Hamburger
Milton Harris
R. M. Hoffman
Harold P. Lundgren
Herman Mark
Edward R. Schwarz
George Switlyk
Helmut Zahn

TEXTILE RESEARCH JOURNAL, published monthly at Prince and Lemon Streets, Lancaster, Pa., is devoted to the interest of research in textile and allied industries. It is published by Textile Research Institute.

Manuscripts and communications should be sent to the Publications Department, P.O. Box 625, Princeton, N. J.

Second-class postage paid at Lancaster, Pa.

Subscription rates: $25.00 per year; additional for postage, 50 cents to Canada, $1.00 to all other countries. Single copies, $2.50 each.

Contents copyright © 1960 by Textile Research Institute. Advertising rates applied on request.

IN THIS ISSUE

The Tensile Properties of Twisted Single Fibers. *R. W. Dent and J. W. S. Hearle* 805

A Computer for the Automatic Processing of Fiber, Yarn, and Fabric Stress–Strain Data. *W. J. Thorsen* 827

The Relation Between Crystallite Orientation and Mechanical Properties of Mercerized Cottons. *B. R. Shelat, T. Radhakrishnan, and B. V. Iyer* 836

A Measure of the Variation in Blend Proportions Along Blended Yarns and its Relation to the Number of Doublings Used in Processing. *P. G. Walker* 843

The Stabilizer in Hydrogen Peroxide Bleaching. *David M. Cates and Winnifred H. Cranor* 848

The Kinetics of Wool Dyeing—Some Effects of Alcohols on Wool Dyeing Rates. *J. A. Medley and M. W. Andrews* 855

Sodium Chlorite Bleaching. *Heinz Hefti*

Part I 861

Part II 867

Action of Oxidizing Agents on Cellulose and Hydrocellulose. *W. B. Achwal and G. M. Nabar* 872

The Heat Treatment of Orlon Acrylic Fiber to Render it Fireproof. *W. G. Vosburgh* 882

The Mechanical Properties of Ortho- and Para-Like Components of Lincoln Wool Fibers. *M. Feughelman and A. R. Haly* 897

LETTER TO THE EDITOR

Setting Wool Textiles with Ethanolamine. *N. H. Koenig, W. L. Wasley, and C. E. Pardo, Jr.* 901

REPRINT REQUESTS SHOULD BE DIRECTED TO THE AUTHORS

SEE ARTICLES FOR ADDRESSES

NOVEMBER 1960
VOL. 30 NO. 11

TEXTILE RESEARCH JOURNAL

The Tensile Properties of Twisted Single Fibers[1]

R. W. Dent[2] and J. W. S. Hearle

Department of Textile Industries, Manchester College of Science and Technology, University of Manchester, England

Abstract

Single fibers were twisted to various amounts prior to tensile testing. The variations with twist in tenacity, breaking extension, modulus, and contraction or contractive stress on twisting have thus been measured. Experiments were carried out for both constant-tension and constant-length twisting; subsidiary experiments show the effect of other factors. The results are compared with those of other workers; explanations of them are offered.

Introduction

In a twisted yarn the individual fibers or filaments must themselves be twisted, and their mechanical properties may be different from those of untwisted filaments; this is one example of the complex combinations of strain to which fibers may be subject in use. While there have been many investigations of the simple tensile properties of fibers, there have been few in which tensile strain has been combined with other forms of strain. The present investigation was concerned with the determination of the properties of fibers which had been twisted immediately prior to the tensile test. Incidentally, values of the contraction due to twisting under constant tension (or of the contractive force due to twisting at constant length) and of the breaking twist were also found.

Apart from its direct practical implications, the work represents a further contribution to the complete study of the mechanical properties of fibers under the influence of stresses in all directions. The experimental data are presented in terms of specific stresses and tenacities in g./tex, extensions as percentages, and twist factors in tex$^{\frac{1}{2}}$ turns/cm. The twist factor, which is the accepted measure of "hardness of twist" in yarns, is related to the angle of twist by the equation

$$\tau\sqrt{c} = \tfrac{1}{2}\sqrt{10^5/\pi v}\tan\theta \qquad (1)$$

where τ = twist in turns/cm., c = fiber denier in tex, v = specific volume of fiber in cm.^{3}/g., θ = twist angle = $\tan^{-1}(2\pi r/h)$, r = fiber radius, and $h = 1/$twist in turns per centimeter = length for one turn of twist. It follows that fibers of different diameters, but with the same specific volume, will have the same surface twist angle and contain the same distribution of shear strains through their cross sections if they are twisted to the same twist factors. Equation 1 applies strictly only for fibers of circular cross section; for other fibers it will give values of θ which

[1] The work described in this paper formed part of a thesis presented by R. W. Dent to satisfy the requirements for the M.Sc. Tech. degree.

[2] Present address: Courtaulds Limited, Coventry, England.

are too low. The errors will not be large and are in general neglected.

Review

Little comprehensive work on the subject has been reported. Most of the earlier work involved twisting at constant tension; some reports refer only to single tests, which are of limited value for variable materials such as textile fibers. Many of the earlier references quote breaking loads in grams and twists in turns/unit length; these are of little help in making comparisons among fibers of differing fineness, so they have been converted to values of tenacity in g./tex and twist factors in tex$^{\frac{1}{2}}$ turns/cm. The results of the earlier studies are summarized in Tables I–III.

The most extensive work has been reported by Husung [9], who investigated the whole twist range up to break due to twist alone, and did several tests to obtain each mean value. He worked on staple

TABLE I. Variation of Tenacity with Twist Factor (Constant-Tension Twisting)

Fiber	Tenacity in g./tex at twist factor (tex$^{\frac{1}{2}}$ turns/cm.) of: 0	5	10	20	40	80	Breaking twist factor, tex$^{\frac{1}{2}}$ turns/cm.
Viscose staple 0.44 tex [9]	17.1	17.0	16.9	16.6	15.5	9.4	101
Viscose staple 0.42 tex [9]	14.7	14.7	14.6	14.3	13.0	0	80
Acetate staple 0.47 tex [9]	11.65	11.6	11.6	11.5	10.8		75
Lanital staple 0.47 tex [9]	5.8	5.8	5.8	5.8	5.47	3.9	128
Cuprammonium staple 0.47 tex [9]	14.8	14.8	14.75	14.6	13.4		78
Cotton (Banilla) 0.18 tex [20]	35	35	34.5	33.75	30		
Cotton (Cambodia CO.1) 0.16 tex [20]	25.5	25.55	26	26.25	26.25		
Cotton (Aligarh A.19) 0.29 tex [20]	19	19.25	19.5	19.5	17.5		
Nylon filament 1.70 tex [1]	48.25	48.5	48.5	48.5			
Viscose filament 0.16 tex [4]	18.5	18.5	18.5	18.5	16.75		
Abaca staple 42 tex [10]	60.5	57.5	52				
Sisal staple 43 tex [10]	39.5	39	38				
Henequen staple 50 tex [10]	30	29	28.5				

TABLE II. Variation of Breaking Extension with Twist Factor (Constant-Tension Twisting)

Fiber	Breaking extension, %, at twist factor (tex$^{\frac{1}{2}}$ turns/cm.) of: 0	5	10	20	40	80
Viscose staple 0.44 tex [9]	30	29.75	29.5	28.5	24.4	
Viscose staple 0.42 tex [9]	30.75	30.75	30.5	28	20	
Lanital staple 0.47 tex [9]	84.5	84.5	84.5	84	81	57
Acetate staple 0.47 tex [9]	38	37.5	36.5	34.5	28	
Cuprammonium staple 0.47 tex [9]	27	26	25	22.5	17	0
Nylon filament 1.70 tex [1]	18	18.5	19	19.5		
Acetate filament 0.42 tex [26]	32	32.25	32.5			
Nylon, high tenacity 0.69 tex [26]	15.25	15.5	15.75	16.25		

TABLE III. Contraction and Contractive Stress in Twisting

Fiber	Contraction, %, in constant-tension twisting at a twist factor (tex$^{\frac{1}{2}}$ turns/cm.) of: 0	10	20	40	60	80	100
Viscose staple 0.44 tex [9]	0	0	0	0.5	3	6.5	12
Viscose staple 0.40 tex [3]	0	0.5	1.5	7.5			
Cotton (Banilla) 0.18 tex [20]	0	0.5	1.0	6.0			
Cotton (Cambodia CO 1) 0.16 tex [20]	0	0.5	1.0	5.0			
Cotton (Aligarh A.19) 0.29 tex [20]	0	0.5	1.0	5.25			
	Contractive stress, g./tex in constant-length twisting:						
Nylon filament 1.67 tex [8]	0	1.5	4.0	11.5	20	24.5	

rayons: acetate, cuprammonium, Lanital (a regenerated protein fiber), and viscose from various sources. The testing conditions were 1.0 cm. specimen length and a constant tension of 0.5 g. during twisting. His results (Tables I and II) show that both tenacity and breaking extension decrease as twist is increased and that they fall off more rapidly at higher twists. He also did some preliminary measurements on the contraction obtained by twisting (Table III) but did not pursue this as his results were too variable. The method of sampling was to weigh the fibers, then split them up into several groups depending on the fineness. His results surprisingly indicate that the tenacity at any twist increases with fineness and that the corresponding breaking extension increases for coarser fibers. This odd effect with the breaking extension may be connected with the difficulty he experienced in obtaining contraction values. The dependence of the tenacity on fineness indicates a constant breaking load, which can be explained, as failure is a property of the weakest point in the fiber, not of the over-all length; therefore it is the minimum denier along the specimen, not the fiber average, which is important.

Among others who have investigated limited twist ranges, Nakval and Ahmed [20] worked on five grades of Indian cotton. They used a specimen length of 1.0 cm. twisting at 15–20 turns/min. They did large numbers of tests at each value of twist up to 100 turns/cm. and studied the effect of twist on the distribution of breaking load. They concluded that there was a slight initial increase in strength followed by a decrease. The effect was different for the different grades of cotton which were of various lengths and also of different finenesses. They did not measure the breaking extension, but they did measure the contraction due to twist and found that this increased with increasing twist, again the rate of increase being dependent on the grade. The results (Tables I and III) indicate that all the grades have similar properties. They found also that the strength distribution at any one twist was a Pearsons type I curve and that this distribution was the same whether whole fibers or cut middles were used. Also this distribution was the same at higher twists, except that the variance and skewness increased, as it did also for the contraction values. They found that the correlation between the strength and contraction was zero.

Alexander and Sturley [1] studied nylon monofilaments with a test length of 50 cm. and a constant rate of traverse of 12 in./min. The twist was heat set. These authors found that the breaking load and extension were practically constant over the range that they investigated.

Conrad and Berkley [4] quote some results obtained on filament viscose using means of 18 tests which show a decrease in tenacity with increasing twist. Kaswell and Platt [10] have tested three leaf fibers (Abaca, Sisal, and Henequen) over a small range; they also found a decrease in strength from means of 50 tests.

Thakur [26] found that the breaking extension was constant for filament acetate and increased slightly over a small twist range for filament nylon. He also showed that twist affected the shape of the load–elongation curve, decreasing the initial modulus and smoothing out the inflexion at the yield point, as shown in Figure 1.

Tänzer [24] tested wool, but he took only single tests, so his results are very varied; he did not con-

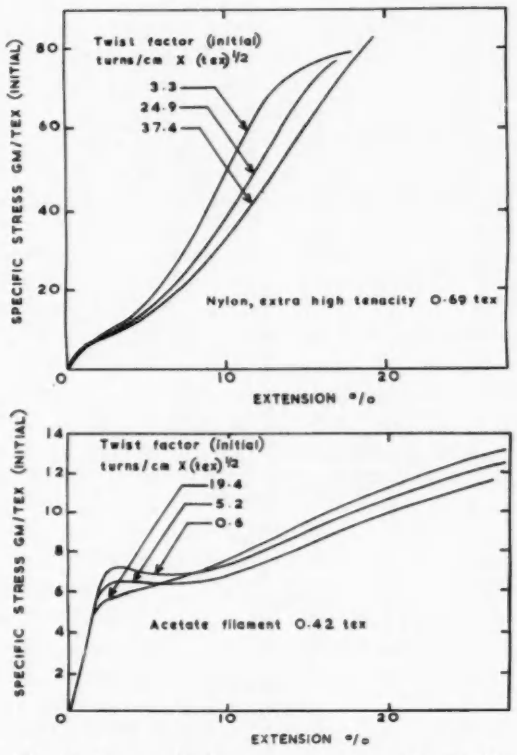

Fig. 1. Changes in the stress–strain curve due to twist (constant-tension twisting) [26].

sider the individual fiber fineness, so that his results cannot be converted for comparison with others. They do, however, indicate a decrease in strength and breaking extension with increasing twist.

Further results by Breuer [3] showing the increase in contraction with increased twist at constant-tension twisting are given for filament viscose in Table III. The investigation of constant-length twisting is very sparse, but Fuchino, Nakazato, and Matsuda [8] did some work with nylon monofilament; they indicate the manner in which the contractive stress increases in the fiber as the twist is increased (Table III). More results showing this increase for different fibers such as Perlon, viscose, glass fiber, wool, and cotton are given by Frenzel and Perner [7]. Their results show that the shape of the contractive stress–twist curve differs for different fiber types.

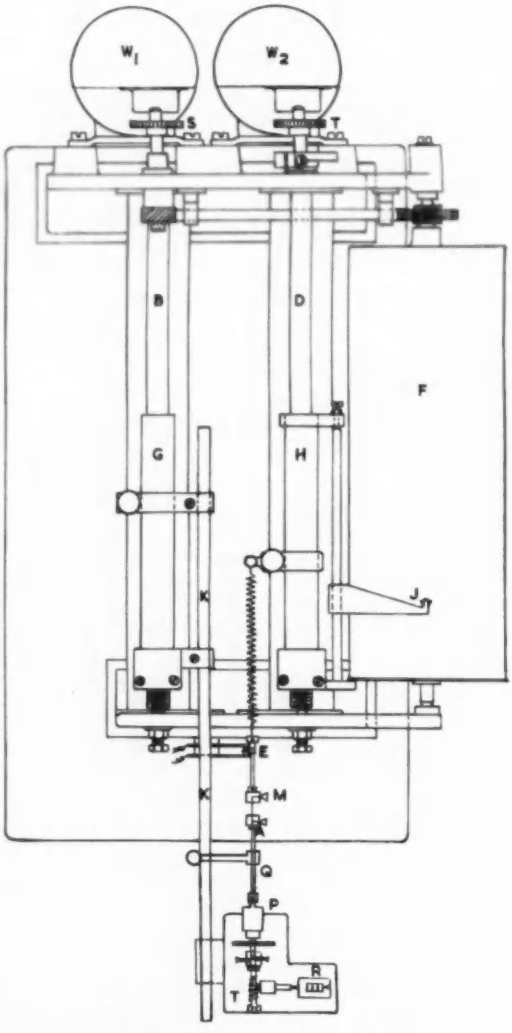

Fig. 2. Diagram of apparatus.

Extensive work has been carried out on the purely tensile properties, which can be regarded as a special case of the more general combination of tensile and torsional stresses acting on a fiber where the torsion is equal to zero; most of this work is reviewed by Meredith [16].

When sufficient twist is put into the fiber, it will rupture due to shear stress alone. This is again a special case of fiber rupture due to combined stresses, with the tensile stress being equal to zero. This breakage occurs at a certain twist; at this twist the fiber has either contracted or is subject to a tensile stress, depending on the method of twisting. These values of twist and contraction (contractive stress) depend on the type of fiber and its molecular state, just as the tensile properties vary for the different types of fiber. In fact, the use of fiber resistance to twist has been suggested several times as a means of comparing fibers and augmenting information on tensile properties.

Krais [11] suggested that the breaking twist in turns per centimeter was dependent only on the type of fiber being twisted. Deppe [6] and Tänzer [24] gave values of the breaking twist for wool but showed that the value increased for finer fibers. Vinckers [27] with cotton; Breuer [3] with wool, staple rayon, Perlon, and Artilana; Husung [9] with regenerated staple fibers; and Schwab [22] for various rayons all gave values of breaking twist and verified that finer fibers need more turns to break them.

It has been suggested by several people that, as the breaking twist in turns per unit length is dependent on fiber fineness for one type of fiber, it could be a quick accurate measure of quality. This has been noted by Tänzer [24] for wool and by Das, Guha, and Wareham [5] for bast fibers.

However, twist angle is more fundamental than turns per unit length, as it removes the effect of fineness. Husung [9] suggested this and defined the breaking twist angle θ_B, as $\tan^{-1}(2\pi r/h_B)$, where h_B is the fiber length (cm.) containing one complete turn of twist at break. The breaking twist factor may be calculated from Equation 1.

Koch [12] has pursued this work and supports

the view that the breaking twist angle is a fundamental property of the fiber structure. The angle given by Koch was the complementary angle α_B, where $\alpha_B = 90° - \theta_B$. He confirmed the decrease in breaking turns for coarser fibers, while the breaking angle remained constant. He has also shown that the breaking twist angle is less for more brittle fibers and for more highly oriented or drawn high-tenacity forms of rayon and synthetic fibers, and that usually θ_B is less for the filament form than for the staple form of any one type of fiber.

He used constant-tension twisting on a 1-cm. specimen length. The constant tension was 10^8 dynes/cm.^{2} for all fibers, except for Perlon, where higher tensions of 2.5 to 5.0 $\times$ 10^8 dynes/cm.^{2} were necessary to avoid snarling; the rate of twisting was 240 turns/min. of Z twist. His values converted to θ_B are given in Table IV, where the ranges of values are due to different types, processes, and sources of each fiber.

Each of the values is the mean of 50 tests. Koch determined statistically that this was the smallest accurate sample. Husung [9] used a sample of 10–20 and realized that single values, as used by previous workers, were inaccurate. His values are also given in Table IV and were obtained by constant-tension twisting on a 1-cm. specimen with a constant tension of 0.6 g.

TABLE IV. Values of Breaking Twist Angle θ_B, in Degrees

Fiber	Koch [12]	Husung [9]
Regenerated protein	62–58.5	
Polyamide staple	63–56	
Polyester staple	59	
Polyamide filament	55.5–47.5	
Polyester filament	50–42	
Acetate staple and filament	46–40.5	37.5
Cuprammonium staple	42–40	36.5
Wool	41.5–38.5	
Silk	39	
Viscose staple and filament	39.5–35.5	43.5
Cotton	37–34	
Cuprammonium filament	35–33.5	
Polyacrylic	34.5–33	
Viscose high tenacity	33.5–31.5	27
Viscose extra high tenacity	23	
Flax	21.5	
Glass	5–2.5	

Experimental Method

Apparatus

The apparatus used in the present investigation is illustrated in Figure 2. Single fibers 2.0 cm. long were twisted to various amounts and then subjected to a tensile test by use of a Cambridge Textile Extensometer, at a constant rate of extension of 0.20%/sec. This rate of extension, which was found to be the most suitable in order to cover the whole range of fibers satisfactorily, considering the limitations of the instrument, was obtained by reducing the speed of the extension motor W_1 by having a resistance of 1050Ω in series with it and by reducing the speed of the screw B by using a gear ratio of 1:9 at S.

When this instrument is used at constant rate of extension, the spring extension motor W_2 runs intermittently, under the control of the electric contacts at E. The springs and the gear ratio from the motor were chosen so as to give the best load–elongation curves for each type of fiber tested. For most fibers, the modulus decreases rapidly at higher strains. This means that the rate of extension of the spring which is chosen for the initial elastic region is too high after the yield point has been passed, causing a very jerky trace. This can be avoided by decreasing the speed of running of the spring motor, by increasing the resistance in its external circuit, at the appropriate stage of the test.

The twisting head consisted of a small motor P, driving through a reduction gear to a vertical twisting shaft or spindle Q, carrying at its top end the lower fiber holder, M, and at its bottom end a worm-driven revolution counter, R. This assembly was mounted on a "Perspex" block T, and clamped onto the rod K, extending from the extension motor carriage G. Thus the twisting head and the lower fiber holder move as a whole depending on the fiber extension or contraction.

The motor circuit consisted of a 4½-volt battery, a rheostat, and a reversing switch. At full speed, the motor rotor revolved at approximately 6000 rpm; using a reduction gear 8/27, this drove the external shaft at 780 rpm. This was further reduced to 230–270 rpm by reducing the rotor speed by placing a resistance of 19Ω in series with it. The twisting was all in the S direction.

Several methods of holding the fibers were tried. The method finally adopted was to cement the fibers with Durofix onto a U-shaped piece of card. This gives a standard length mounted at standard tension, probably less than 0.25 g., and gives ease of handling so that the fibers can be easily and safely stored. This card was then placed in two Perspex clamps in the machine, and tightly clamped to give the extra strength which Durofix lacks when used alone. The

card can very quickly be slotted into the clamps and these can then be rapidly tightened by wing-nuts. When the card is firmly clamped the side limb of the card can be cut away to leave a 2.0-cm. free length of fiber between the two sets of clamp jaws.

Fibers Tested

A wide range of samples was selected, in an effort to represent the whole range of the more important commercial fibers; for convenience and accuracy in testing, longer and coarser varieties of each type of fiber were used.

The full list of fibers tested was as follows:

Natural Fibers

Sudan Cotton
Sea Island Cotton
Crossbred Wool
Merino Wool

Regenerated Fibers

Filament viscose	500/50/S bright—Courtaulds
Fibro (viscose)	18 den. 2 in. tow bright—Courtaulds
Tenasco	150/40/S bright—Courtaulds
Dicel (acetate)	140/26/2.5 Z bright—Courtaulds
Celafibre (acetate)	15 den. 3 in. staple dull (crimped)—Courtaulds
Tricel (triacetate)	200/50/2.5 Z bright pink—Courtaulds

Synthetic Fibers

Nylon 15 den. monofilament/0.5 Z, Samples A and B	B.N.S.
Extra high tenacity nylon 840/136/1 Z	B.N.S.
Terylene 25/3/0.75 Z (1)	I.C.I.
Terylene 25/12/0.75 Z (2)	I.C.I.
High tenacity Terylene 125/24/0.75 Z	I.C.I.
Acrilan 15 den. 3 in. staple (crimped)	Chemstrand

Procedure

Prior to testing, each sample was allowed to condition for at least 24 hr. in a standard atmosphere ($68 \pm 2°$ F. and $65 \pm 2\%$ RH); all tests were carried out under these conditions.

The method of fiber extraction depended on the form in which the fiber sample was stored. With filament yarns the whole yarn was carefully cut to a 3-cm. length; then the individual filaments were separated, taking care to avoid straining. With the staple fibers, which were all in random masses, the single fibers were first carefully extracted and then tensioned to just remove any crimp and cut to 3 cm. Cotton, however, was too fine for this method, so a tuft was carefully combed out till all the fibers in it were longer than about 3.5 cm. This tuft was then clamped between two glass plates set approximately 3.1 cm. apart and then the whole tuft cut. The cutting was done by two razor blades set 3.0 cm. apart in a wooden block.

For each type of fiber some 50–60 separate fibers were tested. Thus, for the continuous filament yarns with less than 50 filaments, at least one entire cross section of filaments was tested. However, with the staple fibers it was impossible to select a fully representative sample and so random selection was employed. This would result in a length-biased sample with wool, as the coarser fibers are longer and an unconscious biasing towards coarser fibers would occur. The cotton sample was necessarily length-biased due to the method of selecting only the longer fibers and due to using cut middles.

The 3-cm. lengths of each fiber were weighed on a cantilever microbalance [13, 14] of appropriate sensitivity and the fiber denier calculated. The fibers were then placed in order on a black velvet pad; when the entire sample of 50–60 fibers had been assembled, they were mounted onto the U-shaped cards. The fibers were stuck in series of 10, a notation and order being employed so that the linear density of each fiber was known throughout. The fibers were attached at one end, and when the adhesive set, the other end was slightly tensioned, if necessary, and any crimp removed before fixing this end by Durofix also. Care was taken that no Durofix coated the fiber across the gap, as this would set hard and effectively reduce the specimen length as well as perhaps strengthen the fiber.

In order to mount a 2.0-cm. specimen, the original 3.0-cm. length is needed to provide an overlap to stick to the black mounting card and also to hold while mounting. Also, when being weighed, the fibers were manipulated by tweezers, and some, in particular acetate and viscose, tended to get damaged. If the specimens are always held by the ends, the center is undamaged, so the mounted 2.0-cm. specimen is in good condition. The whole 3.0 cm. is weighed and the linear density found for 3.0 cm. This is assumed to equal the average tex for the center 2.0 cm.

Single fibers were selected in turn for testing, fitted into the Perspex holders, and clamped. Then

the card was cut away, leaving the 2.0-cm. fiber slack between the two jaws. The fiber motor was advanced slowly and intermittently, with the spring motor switched off, until the crimp was removed and the contact broken. It was then reversed a little to allow for any machine overrun. Thus, the fiber is firmly fixed in the machine, exactly 2.0 cm. long, taut, but under no stress or strain.

The twist was inserted at approximately 250 rpm, the upper jaw being stationary and the lower jaw rotating on the twisting shaft. The two jaws are carefully lined up so that the twisting is not eccentric, in order to avoid abrasion and remove any tendency for jaw breaks. The twist put in was varied on consecutive fibers, the amount increasing from none up to breaking twist, usually in steps of 7.5 or 15.0 turns/cm. One fiber was tested to find the likely breaking twist and then the steps were arranged so that 9 or 10 fibers at different twists were tested in one series, more tests being made near the breaking twist. The sample was usually of 45–55 fibers and 5 or 6 full series were tested one after the other.

The twisting was of two types, one at constant tension and the other at constant length.

Constant-tension twisting. The constant tension in grams was calculated from the fiber denier and the required specific stress; prior to twisting the fiber was stressed to this amount at a slow rate of loading.

When the fiber was loaded, twisting took place; the fiber was allowed to contract, with the extension motor running intermittently as the contacts closed. A gear ratio of 2/1 from the fiber motor was needed to give speeds greater than the maximum required contraction rate.

When the required twist had been put in, the twister was stopped and the tensile test undertaken. The rate of extension was 0.20%/sec. and the gear ratio from the fiber motor had to be changed to 1/9. This was done quickly by having two separate gear trains on two arms, either of which could be the carrier wheel or intermediate in the train. To make the change, the required gear train is just swiveled into position and locked by a wing nut. The return to the zero position after the fiber had broken could be speeded by using the 2/1 train.

Constant-length twisting. This is somewhat simpler, and a stress develops in the fiber as twisting progresses. The rate of loading is fixed by the gear ratio calculated for the subsequent tensile test; in all cases this was enough to ensure that the stress, which developed while twisting, could increase. The switching was such that the spring motor could run intermittently operated by the contacts, although the extension motor was switched off. The fiber motor gear ratio was set at 1/9 throughout and the faster rate of extension of the 2/1 arm used only as a quick return mechanism after the tensile test.

Results for Constant-Tension Twisting

Choice of constant tension. When the fiber is twisted under a zero tension and contraction is allowed, it is found that, after a certain amount of twist, the fiber snarls up on itself and contracts until the distance between the jaws is zero, but the fiber is still unbroken. The fiber protrudes in a snarled configuration at right angles to its original vertical direction. Due to the snarling, the fiber is able to absorb a very large amount of twist without breaking. If the fiber is pretensioned slightly, much more twist can be inserted before this snarling occurs, and the fiber tends to break before it has fully contracted onto itself. Increasing the initial tension still further enables the twisting to proceed without any snarling at all prior to fiber breakage.

A preliminary investigation was undertaken to establish the minimum values of the tensions needed to prevent snarling for all the fiber samples to be tested. The values are given in Table V. The values given are not very accurate and tend to be rather high. This is because the limiting initial tension for each type of fiber is not clear-cut and varies from fiber to fiber. The tension which will prevent snarl-

TABLE V

Fiber	Fineness, tex	Tension to prevent snarling, g.	Specific stress, g./tex
Nylon fil (B)	1.62	7.5	4.8
Nylon, extra high tenacity	0.67	3.0	4.5
Terylene, fil (1)	0.91	2.7	3.0
Terylene, fil (2)	0.23	0.7	3.0
Terylene, high tenacity	0.55	2.0	3.6
Cotton (Sudan)	0.14	0.1	0.7
Viscose, high tenacity	0.48	0.3	0.6
Viscose fil	1.12	0.45	0.4
Viscose staple	1.97	0.4	0.2
Triacetate fil	0.43	0.3	0.7
Acetate fil	0.62	0.3	0.5
Acetate staple	1.69	0.7	0.4
Acrilan staple	1.64	0.5	0.3
Wool (cross-bred)	1.76	0.35	0.2

TABLE VI. Constant Tensions Reported by Other Workers

Research workers	Fibers	Initial tension	Specific stress, g./tex
Husung [9]	Staple rayons	0.5 g.	1.0–1.5
Koch [12]	Perlon	(2.5–5.0) × 10^8 dynes/cm.^{2}	2.5–5.5
	All other fibers	1.0 × 10^8 dynes/cm.^{2}	1.3–1.6
Breuer [3]	All fibers	0.5 g.	1.0–1.2
Vinckers [27]	Cotton	0.57 g.	3.2
Tänzer [24]	Wool	2.0 g.	0.7–1.5

ing for one fiber will not necessarily do the same for the next fiber of the same type.

It can be seen from the table that nylon and Terylene show a greater tendency to snarl than the other fibers.

It is interesting to compare the values of tension needed to prevent snarling with those predicted by the theory of elastic stability. Timoshenko [25] quotes the following formula for the stability of a rod of flexural rigidity EI and length l under a combined twisting couple M_t and compressive force P:

$$\frac{M_t^2}{4(EI)^2} + \frac{P}{EI} = \frac{\pi^2}{l^2}$$

For a rod under tension, the sign of P must be changed and we have

Tension to prevent snarling (or buckling)

$$= \frac{M_t^2}{4EI} - \frac{\pi^2}{l^2} EI$$

No measurements of twisting couple were made during this work, but approximate values can be calculated from the maximum values of torque shown in Morton and Permanyer's [17, 18] torque–twist curves and from the dimensions of the fibers tested. Values of flexural rigidity were calculated from the fiber dimensions and from values of modulus given by Meredith [14]; no account was taken of the shape factor. By substitution of the appropriate values, the predicted tensions needed to maintain stability were calculated for four of the fibers: nylon filament, (B) 9 g.; viscose, high tenacity, 0.2 g.; viscose filament, 0.8 g.; and acetate, 0.3 g. The agreement with the experimental values given in Table V is good—surprisingly so in view of the approximations involved. It was found that the second term in the above expression was negligible for these specimens. The equation indicates that the tension needed to prevent snarling should be proportional to the square of the fiber count in tex. However, the only results for which this can be tested, those for Terylene (1) and (2), suggest that the tension is directly proportional to the count. An investigation directed towards this aspect of the subject would be needed to check this result.

When choosing the initial tensions to be used, a safety margin of at least 25% was allowed in the selected values. The values of the tension finally used in this work were 6.0 g./tex for nylon fibers, 5.0 g./tex for Terylene, and 1.0 g./tex for all other types of fiber. These values are sufficiently in excess of the quoted results in Table V to account for any random fibers which would require higher tension values.

It will be noted that the tensions above are in terms of specific stress where previous workers have quoted pure loads. Their values are of interest and are listed in Table VI.

It will be noted that the values of specific stress are between 0.7 and 1.6 g./tex in most cases, which agrees quite well with the value of 1.0 g./tex in the present work. The only exceptions in the table are the 2.5–5.5 g./tex for Perlon, a polyamide fiber, and 3.2 g./tex for cotton.

Prior to testing the fibers, the spring was calibrated at the initial rate of loading by the use of standard 5-g. weights to enable spring extensions to be converted directly into loads in grams. This enabled each fiber to be tensioned to its appropriate load for the twisting. The value of this load was obtained from the known tex of the fiber and the initial tensioning value in g./tex. In practice, initial tensions slightly in excess of the chosen values were used. The average values used were 6.4, 5.3, and 1.1 g./tex.

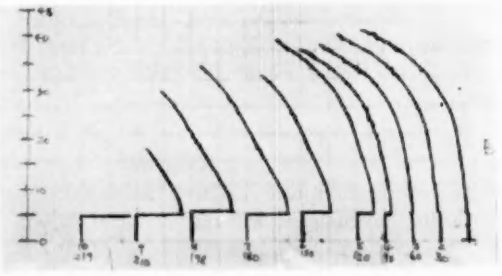

Fig. 3. A typical series of results (constant-tension twisting).

Typical Test Results

One typical set from the results for the filament Terylene sample is shown in Figure 3. Below the stress–strain curve for each fiber can be seen the serial number describing the fiber and, below this, the number of turns inserted into the fiber. On the left-hand side the spring calibration is shown. Any fibers which broke at the jaws were neglected. However, these were very infrequent, especially as the experimental technique improved.

The general shape of an individual result is shown (somewhat exaggerated) in Figure 4. OA is the stress–strain curve when the initial tension is put into the fiber, AB is the contraction when twisting occurs, and BC is the final stress–strain curve of the twisted fiber, C being the breaking point. In the actual results, Figure 3, some effects due to creep can be seen at the point corresponding to B.

The "original" values are defined as those based on the original unstrained 2.0-cm. specimen length. Thus, as the fiber denier had been predetermined on the 2.0-cm. length, the original breaking extension, contraction, tenacity, and twist factor could be easily found. The values noted from each trace were CY, CZ, and XB. CY was read directly in grams from the spring calibration and, on dividing by the tex, gives the tenacity; CZ (breaking extension) and XB (contraction) were noted as percentages of the original 2.0-cm. length.

When the 50–60 individual readings were plotted, graphs such as Figure 5a were obtained. These show definite trends, but there is a scatter of the individual readings. This scatter was much more for the staple man-made fibers, and much more again for the staple natural fibers. This increased variability is expected and is similar to that shown for all the fiber properties. It can also be seen from the figure that odd points lie far from the general trend line. To lessen their influence and condense the data, means were taken of groups of five or more readings. More individual readings were taken in a group at higher twists, as the scatter was then much more pronounced. These means show much less scatter, and when the 7–9 group means were plotted the results were clearly shown. This simplification for the viscose sample is shown in Figure 5b.

These curves are typical and show the general trend observed with all fibers. The scheme used in the diagrams is shown simply in Figure 6. The lines O_1A_1 and O_2A_2 represent the initial tensioning, lines A_1M_1 and A_2M_2 represent the twisting, and lines L_1M_1 and L_2M_2 represent the fiber breakage. The course taken by the load and extension in one individual fiber, twisted to an intermediate amount, is shown by the thickened line. O_1 and O_2 represent the original zero load and extension conditions in the fiber. O_1A_1 and O_2A_2 show the effect of putting the initial tension on the fiber, the fiber being extended positively. A_1B_1 and A_2B_2 show the twisting, the load remaining constant while the fiber contracts to B_2. B_1C_1 and B_2C_2 then show the effect of the tensile test, the load and extension increasing at a constant twist factor until the fiber breaks at C_1C_2.

Original, Nominal, and Actual Results

Although the use of the original values is the simplest way to deal with the test data, it has no basis on theoretical grounds. There are two other possibilities: to use values based on either the fiber

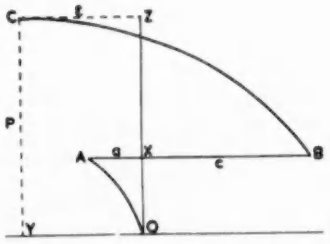

Fig. 4. Schematic diagram of trace (constant-tension twisting).

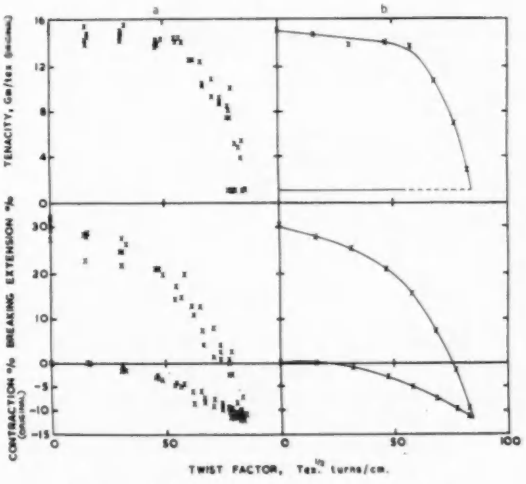

Fig 5. Original and smoothed test results.

length immediately prior to the tensile test or the actual length when breakage occurs. These are called the initial (or nominal) and the final (or actual) values, respectively. The differences in the respective values can be easily deduced from Figure 4, and are given in Table VII. P and ϵ are the measured load and extension at break; while c is the measured contraction due to twisting to a twist angle θ, and a is the measured extension due to tensioning. It will be noted that the nominal and actual extension and contraction values are identical. On theoretical grounds, the use of actual values is preferable, but for practical considerations of the use of twisted fibers, the nominal tenacity and twist factor based on the length prior to the tensile test, not on the final extended length, are preferable.

To show the effect of the different types of calculation, the different values are plotted for filament nylon in Figure 7. The curves for nylon show quite large differences, as this is one of the extreme cases, where the values of c and a are large.

TABLE VII. Comparison of Methods of Calculating Results

	"Original" values	"Nominal" values	"Actual" values
Linear density, tex	T	$T/(1-c)$	$T/(1+\epsilon)$
Twist, turns/cm.	t	$t/1-c)$	$t/(1+\epsilon)$
Twist factor, tex$^{\frac{1}{2}}$ turns/cm.	$F=t\cdot T^{\frac{1}{2}}$	$F/(1-c)^{\frac{1}{2}}$	$F/(1+\epsilon)^{\frac{1}{2}}$
Tenacity, g./tex	$S=P/T$	$(1-c)S$	$(1+\epsilon)S$
Breaking extension	ϵ	$(\epsilon+c)/(1-c)$	$(\epsilon+c)/(1-c)$
Contraction	c	$(c+a)/(1+a)$	$(c+a)/(1+a)$

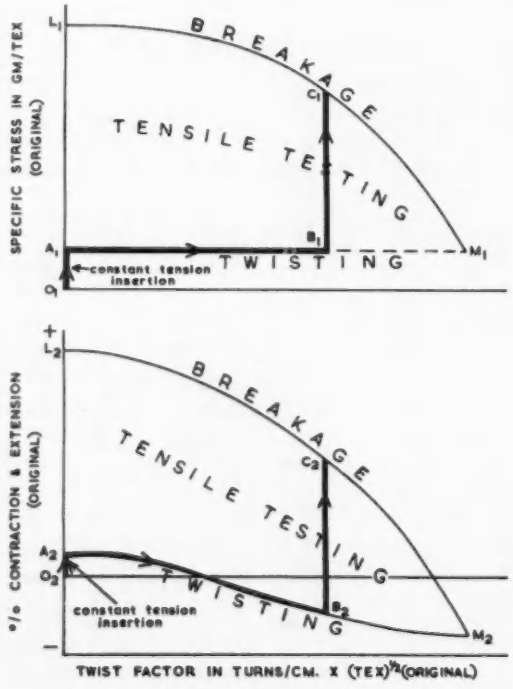

Fig. 6. Form of curves for constant-tension twisting.

Rupture Properties

Curves of the original values of tenacity, breaking extension, and contraction are shown in Figures 8, 9, and 10, and of the nominal values in Figures, 11, 12, and 13. The curves for most fibers show the same general trends. The tenacities decrease little for about half the twist range, but then fall rapidly, while the breaking extensions decrease over the whole range at an ever-increasing rate, except for nylon and Terylene, which show an increase in nominal breaking extension up to quite high twist factors.

The original breaking twist factors lie between 80 and 100, except for filament Terylene and wool,

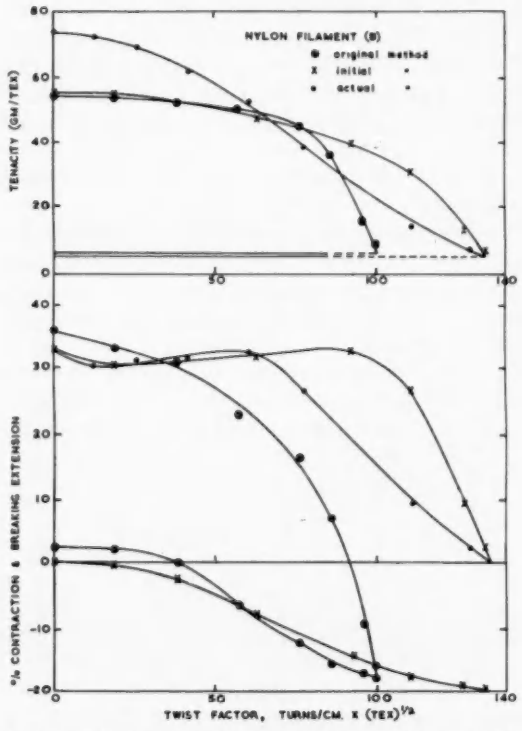

Fig. 7. Effect of different methods of calculating test data.

which can take more twist. There is no correlation at all between the tenacity at zero twist and the breaking twist factor, while from examination of Figure 10 it appears that the more extensible fibers at zero twist tend to have higher values of breaking twist, while the less extensible fibers contract less.

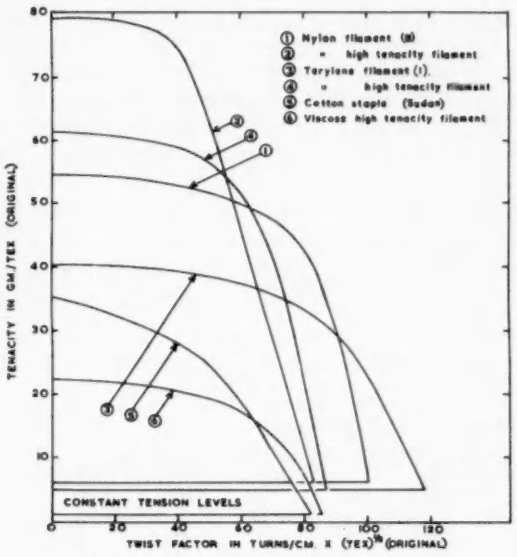
① Nylon filament (B)
② " high tenacity filament
③ Terylene filament (I)
④ " high tenacity filament
⑤ Cotton staple (Sudan)
⑥ Viscose high tenacity filament
CONSTANT TENSION LEVELS
TENACITY IN GM./TEX (ORIGINAL)
TWIST FACTOR IN TURNS/CM. x (TEX)^½ (ORIGINAL)

Fig. 8. Variation of tenacity with twist factor (constant-tension twisting; original values).

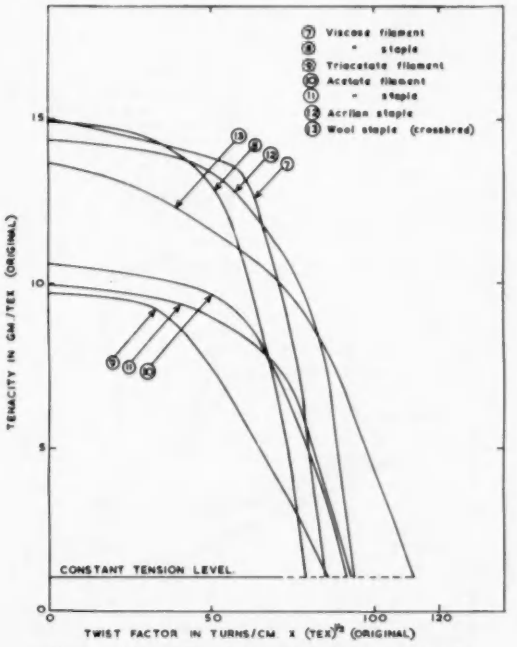

Fig. 9. Variation of tenacity with twist factor (constant-tension twisting; original values).

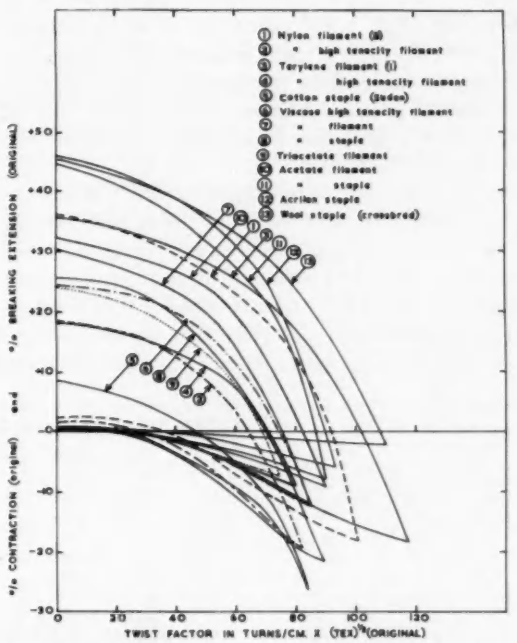
① Nylon filament (B)
② " high tenacity filament
③ Terylene filament (I)
④ " high tenacity filament
⑤ Cotton staple (Sudan)
⑥ Viscose high tenacity filament
⑦ " filament
⑧ " staple
⑨ Triacetate filament
⑩ Acetate filament
⑪ " staple
⑫ Acrilan staple
⑬ Wool staple (crossbred)
% BREAKING EXTENSION (ORIGINAL) and % CONTRACTION (original)
TWIST FACTOR IN TURNS/CM. x (TEX)^½ (ORIGINAL)

Fig. 10. Variation of breaking extension with twist factor (constant-tension twisting; original values).

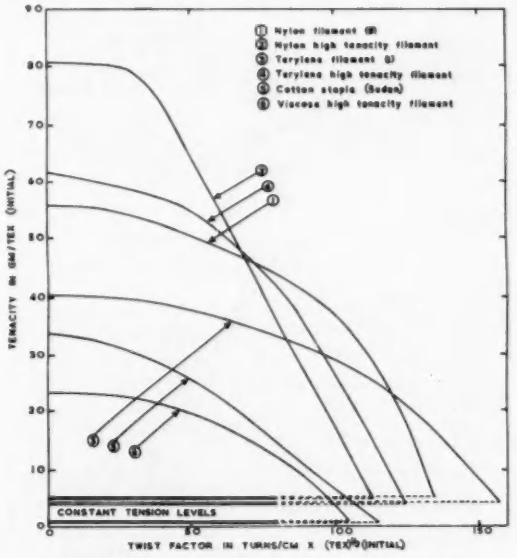
① Nylon filament (B)
② Nylon high tenacity filament
③ Terylene filament (I)
④ Terylene high tenacity filament
⑤ Cotton staple (Sudan)
⑥ Viscose high tenacity filament
CONSTANT TENSION LEVELS
TENACITY IN GM./TEX (INITIAL)
TWIST FACTOR IN TURNS/CM. x (TEX)^½ (INITIAL)

Fig. 11. Variation of tenacity with twist factor (constant-tension twisting; nominal values).

It can be noted also that wool and cotton bound the other fibers, i.e., the rayons and synthetic fibers. Wool has a high extension at zero twist, a high breaking twist factor, and a small contraction at the breaking twist, while cotton has a small extension at zero twist and a small breaking twist factor, but a large breaking twist contraction. The contraction curves differ for the different fibers, and the breaking twist contraction values vary from 2% for wool to 26.5% for cotton.

Comparing particular types of fiber, it appears that the high-tenacity forms of nylon and Terylene have lower breaking twist factors than the corresponding filament fibers, but there is no significant difference between the staple and filament forms of viscose and acetate. It can also be seen that all the high-tenacity forms show a greater breaking twist contraction, and filament forms have bigger contraction values than the corresponding staple form.

Shape of the Stress–Strain Curve

The effect of twist can be shown by plotting the actual curves at different twists on the same axes. This is done in Figure 14 for the original values, showing the various effects with different fibers. The selection of the individual curves was made from those having the average tex value and having the average tenacity and contraction values. In other words, typical curves are plotted, showing as little as possible the effect of tex, tenacity, or other fiber variations.

As the twist is increased, all irregularities in the

TABLE VIII. Variation of Initial Modulus with Twist Factor

Fiber	Initial modulus, g./tex, at twist factor (tex$^{\frac{1}{2}}$ turns/cm.) of:							
	0	20	40	60	80	100	120	140
Cotton, Sudan	360	375	385	390	395	400	410	
Nylon filament (B)	255	285	290	275	250	220	180	
Terylene filament (1)	1125	990	885	790	720	660	610	560
Viscose filament	440	430	400	330	250	120		
Acetate filament	330	280	240	200	165	140		
Wool, crossbred	230	230	230	220	200	170		

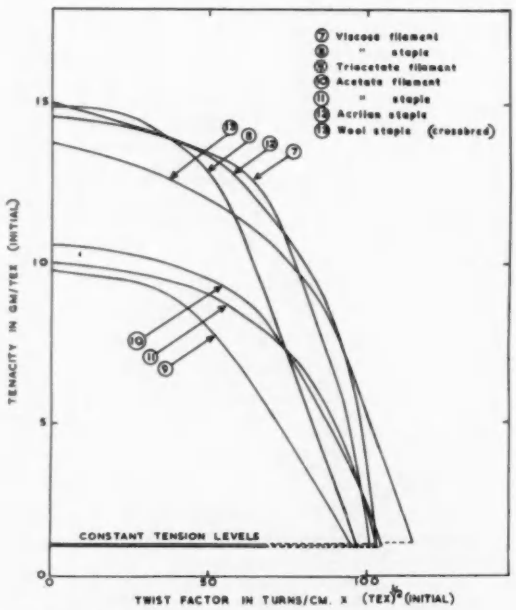

Fig. 12. Variation of tenacity with twist factor (constant-tension twisting; nominal values).

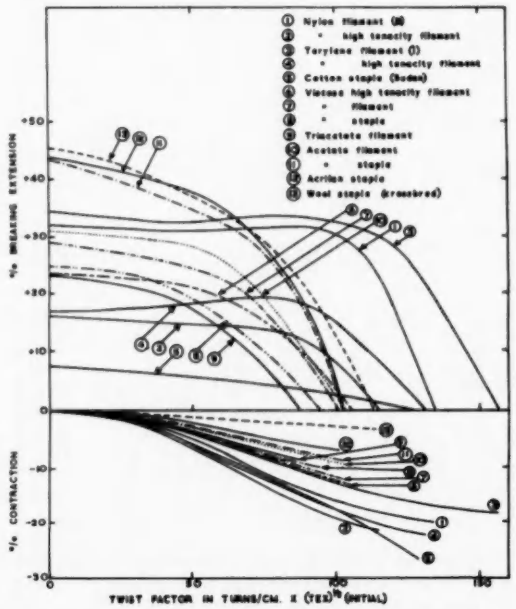

Fig. 13. Variation of breaking extension with twist factor (constant-tension twisting; nominal values).

stress–strain curve are diminished and the slope tends to a mean value. Thus with wool, acetate, and viscose the pronounced yield point disappears; with nylon and Terylene, the flow regions at larger extensions also diminish. The slope tends to a constant value which is less than the mean slope of the original zero twist curve. Thus the initial slopes for cotton and nylon increase, and then decrease at higher twists, while for all other fibers, the initial Young's moduli decrease. The small contraction of wool and the large values reached by cotton can be clearly seen.

The variation of initial modulus is shown in Table VIII. It decreases throughout for all fibers except nylon and cotton.

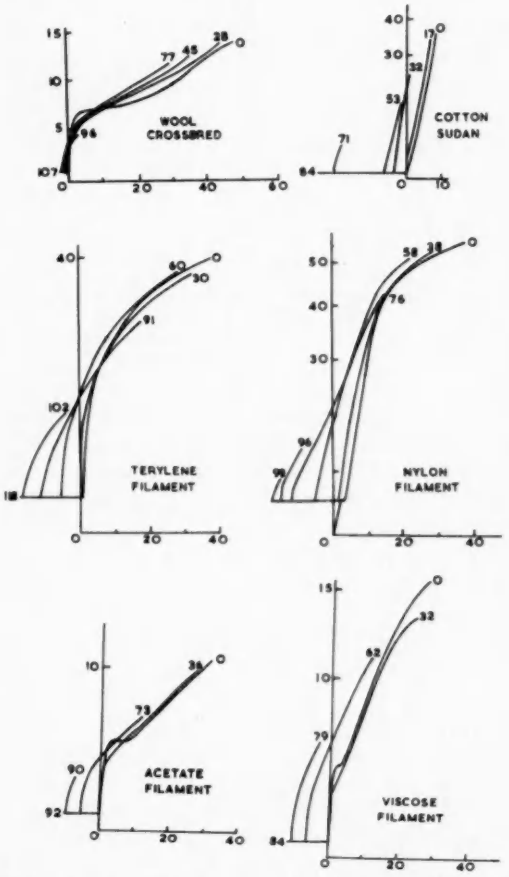

Fig. 14. Stress–strain curves (original values). Ordinate values are specific stress in grams per tex and abscissa values are percent strains. The numbers against curves are twist factors.

To give an idea of the effect of twist on the slope of the stress–strain curves over the whole range of extensions, three-dimensional diagrams are plotted in Figure 15 for the different forms of curves. Viscose and wool are not included, as they are very similar to acetate. The three variables are the modulus of elasticity, twist factor, and the percentage extension. These diagrams were obtained by measuring the slope of the stress–strain curve at particular extensions for the different twists.

The notable features of the curves are that the elastic modulus decreases at higher extensions for all fibers except cotton. This decrease is less at higher

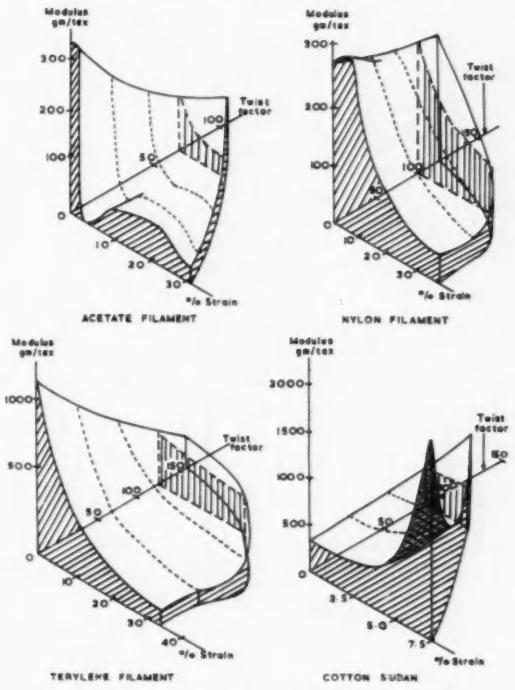

Fig. 15. Isometric diagrams of modulus.

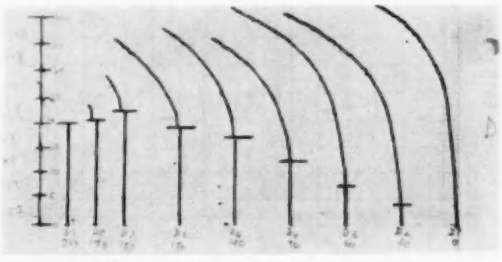

Fig. 16. Typical series of results (constant-length twisting).

twists. With cotton the elastic modulus increases at higher extensions, this increase being less at higher twists.

It must be noted that all the work on the shape of the stress–strain curve is only approximate. This is due in the first place to difficulties in selecting a representative curve for that twist, and also in then measuring slopes from the curve. The values are really comparative only and are designed to illustrate the different trends with the various fibers.

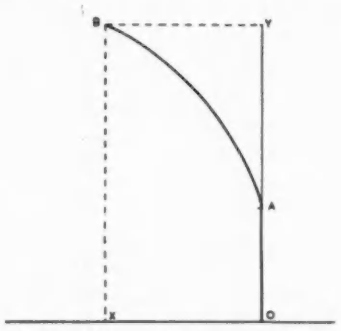

Fig. 17. Schematic diagram of trace (constant-length twisting).

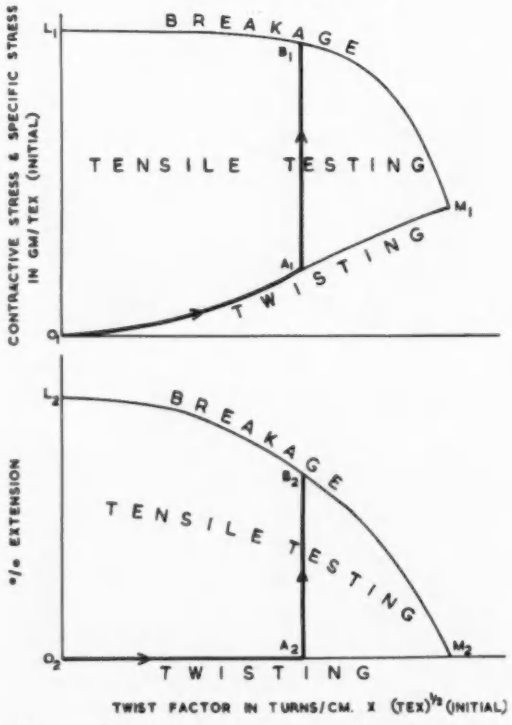

Fig. 18. Form of curves for constant-length twisting.

Results for Constant-Length Twisting

Typical test results. Again, the tests using constant-length twisting were made in sets of 10; a typical set from the results for filament Terylene is shown in Figure 16. The notation against each test is the same as it was in the work at constant tension.

The general shape of an individual result is shown in Figure 17. OA is the contractive stress, i.e., the increase in the fiber specific stress due to twisting, and AB is the stress–strain curve of the twisted fiber. On the photograph, Figure 16, effects due to the relaxation of stress can be seen at the point A at higher twists.

The values noted for each individual test specimen were BX, BY, and OA. BX and OA were noted directly in grams from the spring calibration and BY was noted as a percentage of the original 2.0-cm. length. As the fiber length does not alter during twisting, the length prior to the tensile test is still 2.0 cm., so for constant-length twisting the original values are the same as the nominal or initial values. Thus the nominal fiber tex was the predetermined one and the value of turns per centimeter was half the number of turns inserted. The experimental points were grouped and the mean curves obtained in the same way as for constant-tension twisting.

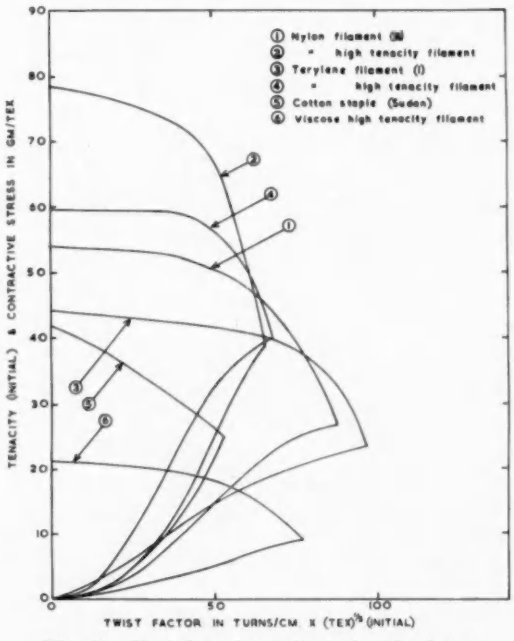
① Nylon filament (M)
② " high tenacity filament
③ Terylene filament (I)
④ " high tenacity filament
⑤ Cotton staple (Sudan)
⑥ Viscose high tenacity filament
TENACITY (INITIAL) & CONTRACTIVE STRESS IN GM/TEX
TWIST FACTOR IN TURNS/CM. x (TEX)½ (INITIAL)

Fig. 19. Variation of tenacity with twist factor (constant-length twisting).

The scheme used in the diagrams is shown in Figure 18. The lines O_1M_1 and O_2M_2 represent the twisting, and the lines L_1M_1 and L_2M_2 the fiber breakage. The changes in load and extension in one individual fiber are shown by the thickened lines. O_1A_1, O_2A_2 show that, during twisting, the fiber stress increases while the length is constant; A_1B_1, A_2B_2 represent the tensile test at constant twist factor.

Rupture properties. Curves showing the variation of tenacity, contractive stress, and breaking extension with twist factor are shown in Figures 19, 20, and 21.

As with constant-tension twisting, the fibers all show the same trend, both tenacity and breaking extension decreasing more and more rapidly as the twist factor increases. The breaking twist factors all lie between 65 and 95, except for wool, which is higher, and cotton, which is lower. The contractive stress curves are all similar, being sigmoidal in character, the stress increasing little at low twists, much at intermediate values, and then little again at high twists. The values of the specific stress developed due to twisting vary between 2.2 g./tex for wool and 40 g./tex for extra-high-tenacity nylon.

The more extensible fibers at zero twist have greater breaking twist factors, but not necessarily the weaker fibers. However, the stronger fibers under pure tension develop greater contractive stress forces under pure torsion. There is very little correlation between breaking twist factor and the contractive stress. On the breaking extension–twist curve, wool and cotton bound the man-made fibers.

The stress–strain curves. Selected stress–strain curves are again plotted on the same axes in Figure 22 and are generally similar to those for constant-tension twisting. Isometric diagrams of modulus can again be drawn, but these are very similar to Figure 15.

Subsidiary Experiments

The Influence of Fiber Fineness

By consideration of tenacities and twist factors, the direct effects of variations in fiber fineness should be eliminated. However, with cotton especially there was still a large variation in the results. This was as expected for the natural fibers. However, there will probably also be variations among samples of different deniers of the same man-made fibers, due to different skin–core ratios and other process factors.

Tests were therefore carried out on two filament Terylene samples with nominal linear density values of 0.926 and 0.231 tex. Both methods of twisting were used; the results are given in Table IX. The

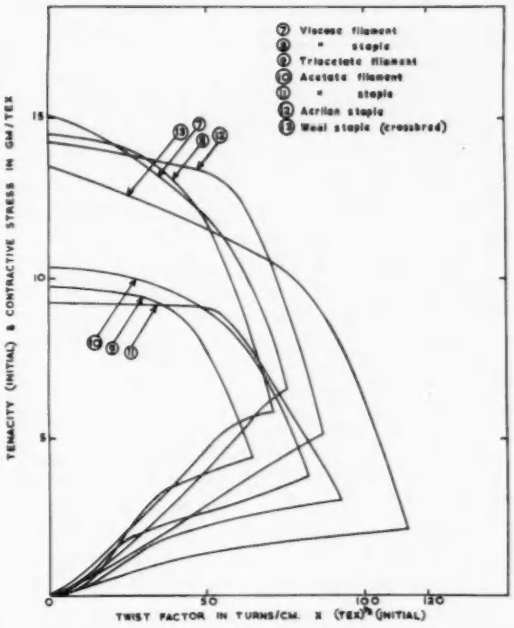

Fig. 20. Variation of tenacity with twist factor (constant-length twisting).

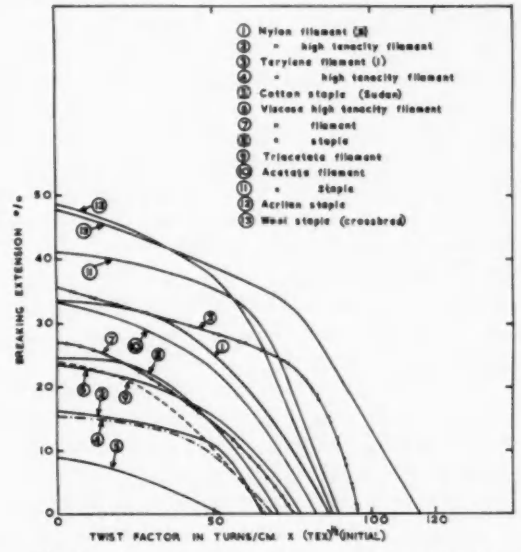

Fig. 21. Variation of breaking extension with twist (constant-length twisting).

TABLE IX

	Twist factor, tex$^{\frac{1}{2}}$ turns/cm.	Terylene, 0.23 tex	Terylene, 0.95 tex	Nylon, 1.62 tex	Nylon, 1.76 tex
Constant-tension twisting					
Tenacity, g./tex	0	38.5	40.5		
	40	37.75	38.5		
	80	37	37		
Breaking extension, %	0	35.75	34.5		
	40	35.5	32		
	80	38	35		
Contraction, %	0	0	0		
	40	1	2.5		
	80	9	9.5		
Constant-length twisting					
Tenacity, g./tex	0	42	43.75	54.5	46.5
	40	41	42.25	52.5	44.5
	80	35	36.5	35	33
Breaking extension, %	0	37.5	36	33.5	36
	40	33.5	30.5	28.5	27
	80	17.5	20.5	6	10
Contractive stress, g./tex	0	0	0	0	0
	40	13.5	12	10	9
	80	22	21	25.75	22

coarser sample was stronger and less extensible at zero twist in both cases, and as expected it gave larger values of contraction and contractive stress at the breaking twist. The coarse stronger sample had a lower breaking twist factor at constant length, but there was little difference at constant tension.

Further information was obtained for constant-length twisting by testing two bobbins of supposedly identical 15 den. monofilament nylon. The finenesses were found to be rather different; results are given in Table IX. In this case the finer filament gave higher strength and lower extension values at zero twist. The finer fiber sample also breaks at lower breaking twist factors, which again is opposite to the findings with the Terylenes of more widely different finenesses. However, in both cases, the stronger fiber had larger contractive forces and lower breaking twist factors. Of interest also are the results for wool and cotton, which have fibers of very different finenesses even in one sample. It was found that coarser wool fibers contracted more or developed a greater contractive force than the average, while for coarse cotton fibers, the opposite applied.

These opposite trends can again be explained when the correlation with strength is considered. It has been shown by Anderson and Cox [2] that, within one sample of wool, specific stress in grams per tex increases for coarser fibers, and this is the same as the relation found by Semple [23] among different strains. No work has been done on this effect within one sample for cotton, but Meredith [15] has found that, among different types of cotton, finer classes have greater specific strengths. By assuming that this applies within one sample, it can be seen that cotton and wool show different relations between fineness and strength. This evidence suggests that fiber strength or orientation has a greater effect on torsional properties than does fiber fineness.

TABLE X. Effect of Initial Tension

Fiber	Initial tension, g./tex	Breaking twist factor, tex$^{\frac{1}{2}}$ turns/cm.	Contraction, %, at breaking twist
Nylon filament	10	121	16
	30	77	4
	50	48.0	0
Terylene filament	10	130	10.4
	30	79	0
	50	66	0
Viscose filament	0	112	16
	5	76	3
	10	55	0
Acetate filament	0	125	16
	5	80	0
	10	47.5	0

The Effect of Initial Tension in Constant-Tension Twisting

The initial tension used must be sufficient to prevent snarling. In order to examine the effects of the initial tension, some experiments have been carried out on 2.0-cm. lengths of fiber twisted to break under various tensions. The results for filament nylon are given in Figure 23. As the initial tension

is increased, the extension due to the initial tension increases and the breaking twist factor decreases. The contraction during twisting at low tensions is high and gives a net contraction at break, but at high tensions the initial extension predominates.

Values of breaking twist factor and breaking twist contraction for various fibers are shown in Table X; these results have been corrected for the contraction at break. Where the extension due to the initial tension just equals the twisting contraction, the breaking twist factor was near the values obtained for constant-length twisting, the broken fiber length being the same, 2.0 cm., in both cases. When the initial tension is reduced below a certain value, snarling occurs, as indicated by the dotted lines in Figure 23. As the initial tension is further reduced, the snarling occurs at lower twist factors. This confirms the work on nylon fishing lines of Nakazato [19], who showed that the twist factor at the commencement of snarling was independent of the fiber fineness and who also considered a mechanism of double twisting or snarling.

The progress of snarling is interesting; it is shown diagrammatically in Figure 24. As the twisting starts, energy is developed in the fiber. If this is greater than the increase in potential energy which will accompany contractions against the constant tension, snarling occurs. The fiber forms a small U-shaped kink, any further twist being absorbed to twist this doubled kink. In the fibers, this kink was seen as a minute spot initially, Figure 24, and spreads in both directions (c) to the jaws (d). Fur-

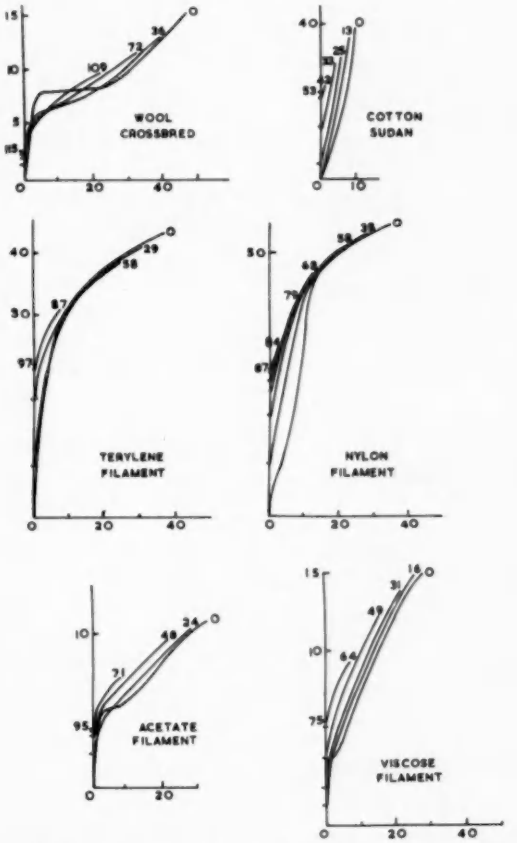

Fig. 22. Stress–strain curves. Ordinate values are specific stress in grams per tex and abscissa values are percent strains. Numbers against curves are twist factors.

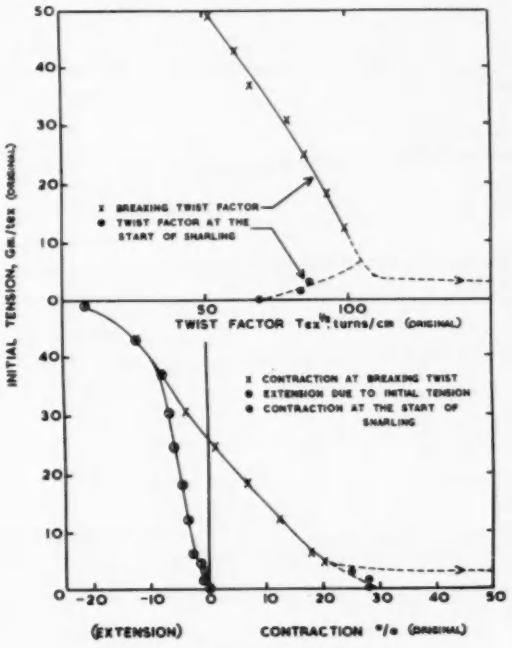
INITIAL TENSION, GM./TEX (ORIGINAL)
BREAKING TWIST FACTOR
TWIST FACTOR AT THE START OF SNARLING
TWIST FACTOR Tex^½ turns/cm (ORIGINAL)
CONTRACTION AT BREAKING TWIST
EXTENSION DUE TO INITIAL TENSION
CONTRACTION AT THE START OF SNARLING
(EXTENSION)
CONTRACTION %/o (ORIGINAL)

Fig. 23. Effect of initial tension.

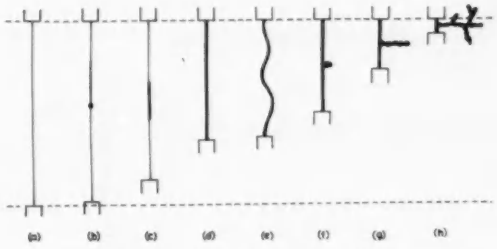

Fig. 24. Mechanism of snarling.

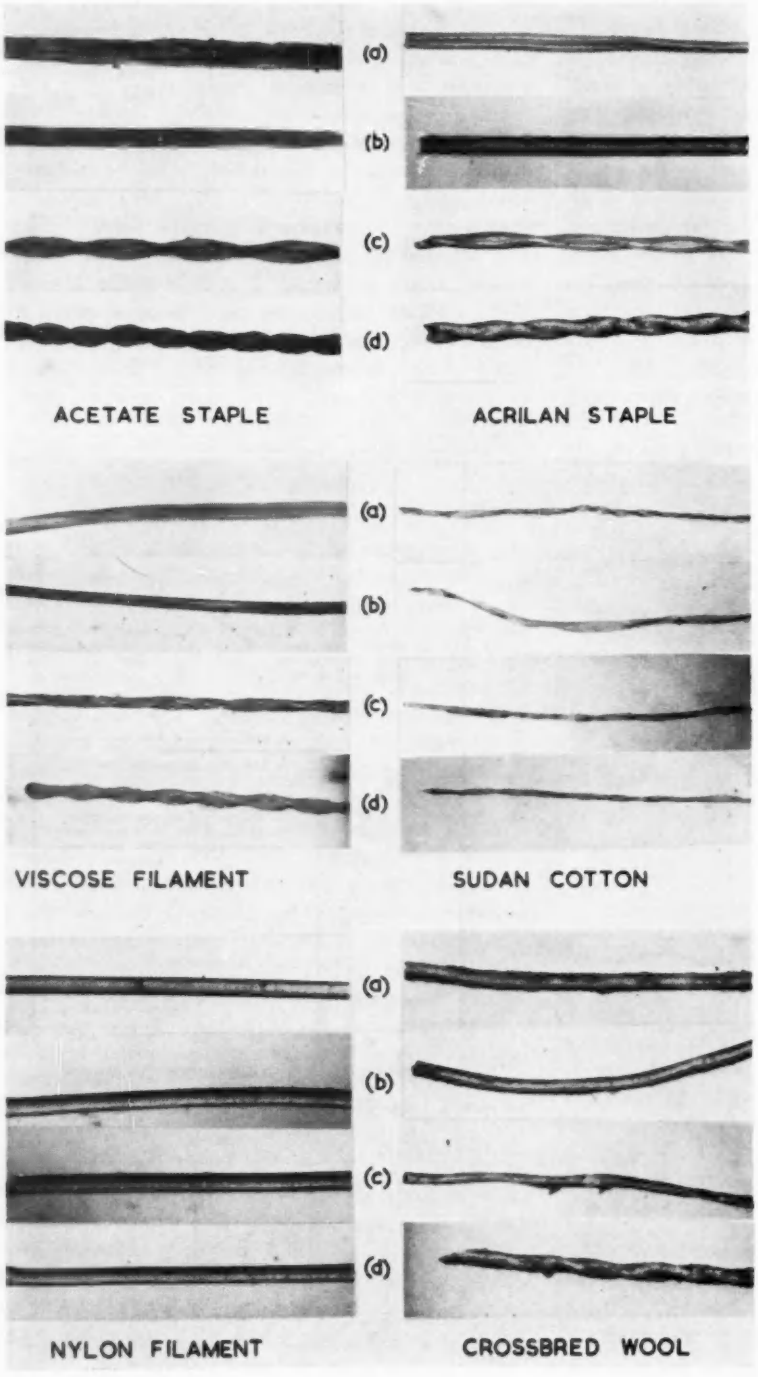

Fig. 25. Photomicrographs of fibers; (a) as obtained, (b) ruptured by tension, (c) ruptured by a combination of tension and torsion, and (d) ruptured by torsion.

ther twist now causes this thickened fiber to double-twist (e), which can be seen as a crimping of the thickened fiber into a sinusoidal form. As this is increased, a further kinking occurs (f), a new limb appearing off the stem of the thickened fiber, growing as twisting continues. All this time contraction is occurring; this process continues with more offshoots (h) till the distance between the jaws is zero.

This explains why, once snarling has started, the fiber can absorb more and more twist without breaking. It does this by assuming geometrical forms which entail no further twisting of the individual filaments, in such a way as to keep the fiber energy at a minimum.

The amount of twisting needed to produce sufficient energy to start snarling is different for different fibers and is reflected in the value of the constant tension required to prevent any snarling when the fiber is twisted up to break. Thus nylon and Terylene develop energy very quickly while other fibers do not or, if they do, they allow it to dissipate by twist setting.

The energy developed for a given twist factor is probably dependent on such fiber properties as the elastic recovery and the torsional rigidity. It has already been mentioned that the tendency to snarl, or the tension needed to prevent snarling, is dependent on the diameter or fineness of the fiber or filament. If the torsional rigidity were related to the snarling tendency, the square of the count would be important. However, our work tended to show that the energy due to twisting is probably related linearly to the fiber tex.

The Effect of Specimen Length

The effect of different specimen lengths in constant-length twisting was investigated for filament nylon, Terylene, viscose, and acetate; the results are given in Table XI, together with those of Breuer [3]. They all show the same trend; below about 3 cm. there is a large increase in breaking twist factor, while above 3 cm. there is very little decrease. It was also found that the breaking twist contractive stress was fairly constant for all the specimen lengths, any variation being random.

A theoretical curve for filament nylon based on Peirce's formula for yarn strength [21] is included in Table XI and agrees with the experimental results, save for a less marked change at short lengths. The curve was calculated from the experimental values of filament nylon at 2.0 cm. with a breaking twist factor of 87.0 and assuming a standard deviation of 3.0 $(\text{tex})^{\frac{1}{2}}$ turns/cm. This standard deviation was estimated from the scatter diagram at constant length and should be quite accurate. In constant-tension twisting, increasing the test length also decreases the breaking twist factor.

TABLE XI. Effect of Specimen Length

	Breaking twist factor ($\text{tex}^{\frac{1}{2}}$ turns/cm.) at test length (cm.) of:					
	0.5	1	2	5	10	20
Nylon filament	111	100	87	81	77	69
Terylene filament	137	115	95	91	90	—
Viscose filament	—	87	75	70	68	—
Acetate filament	—	93	82	76	74	—
Viscose staple (Breuer) [3]	60	57	54	52	—	—
Theoretical [21] (for nylon filament data)	91	89	87	85	84	73

Examination of Broken Fibers

The broken ends of fibers were examined under the microscope; Figure 25 shows photomicrographs of staple acetate, filament viscose, staple Acrilan, filament nylon, Sudan cotton, and crossbred wool fibers which have been broken (i) by a pure tension; (ii) by a combined torsion and tension, i.e., twisting the fiber to an intermediate value and then breaking by a tensile test; and (iii) by pure torsion, using constant-length twisting. Photomicrographs of untested, untwisted fibers are also shown.

From these it can be seen that for acetate, viscose, and Acrilan, a large plastic deformation has occurred; the fibers remain in their twisted form, even when broken. Nylon shows very little deformation and wool shows it only at high twists and then to a reduced degree. With the cotton fibers it is difficult to see clearly, as the fiber is convoluted to start with, but there appear to be more convolutions in the torsionally ruptured fiber than in the untested one. The ability of nylon to shed its twist when it breaks perhaps explains why such a large constant tension is necessary to prevent snarling for this type of fiber, as it shows that the energy due to twisting remains stored in the fiber.

Examination of the actual breaking points seems to indicate that, for pure tensile breakage, there is

a clean break, typical of brittle metals, usually at right angles to the fiber axis while, when the twisted fibers break, a V-shaped break reminiscent of that for ductile metals is seen.

Variability of the Results and Estimate of Errors

From considerations of the individual results used in obtaining the mean tenacity and breaking extension at any one twist, for example by plotting scatter diagrams of the individual readings as in Figure 5a, an idea of the variability in the results can be obtained. The variation was very great for cotton, less for wool and the man-made staple fibers, and less again for the filament fibers, depending generally on the number of filaments in the original yarn. These differences are reflected in all the properties of fibers in these different sample forms.

Though quite a lot of the variation found in the results for one fiber sample is due to randomness and variability between fibers and their properties, due to either natural causes or process errors, there may be errors of up to 5% due to the experimental method.

By use of the means of groups of individual results the variance is much reduced. Probably the error in any one mean will be less than 5%, except at high twists. Thus the errors in the curve drawn through several of these means should be quite accurate, except perhaps for cotton, which showed a very great variability in fiber properties. Wool showed a large difference in fineness among fibers, but less in their properties.

Conclusion

Summary and Comparison of Results

The results show that both the tenacity and the extension at break decrease with the increase of twist and that all fibers respond in a similar manner.

The most notable deviations from the general trend are those of the nylon and Terylene fibers for constant-tension twisting, which show a slight increase in breaking extension up to quite high twists.

The results for breakage by pure tension and pure torsion are compared in Table XII. In this table, the fibers are ranked in order, based on the mean ranking for tenacity, reciprocal of breaking extension, contraction or contractive stress, and the difference between breaking twist factors for the two methods of twisting.

It can be seen that in general the highly oriented fibers are stronger and extend less in pure tension; in pure torsion they contract more or develop greater contractive stresses. They break at lower twist factors for constant length, but there is no direct relation with breaking twist factor for constant-tension twisting.

The results obtained for the two methods of twisting are closely related. Thus the breaking twist factors for constant-length twisting are approximately equal to the twist factors used in constant-tension twisting when break occurs at the original specimen length (i.e., the extension due to the tension equals the contraction due to the twist); the tenacities at this latter factor equal the contractive stresses at the breaking-point for constant-length twisting. There is also fairly close correlation between contraction in constant-tension twisting and contractive stress in constant-length twisting for the different types of fibers.

Structural Explanations

Torsional properties can be explained on a molecular basis, in the same way as other mechanical properties. When twisting commences the intermolecular bonds take all the strain and the molecular structure tightens. Further twisting spirals the molecules themselves at an angle to the fiber axis and begins to break the cross links. The twisting angle increases till the structure locks and breakdown occurs due to molecular slippage as more and more bonds are fractured. Very little molecular breakage will occur.

When the fiber has been twisted a small amount and is then subjected to a tensile extension, the cross links are in a restrained position and will render the fiber less extensible, but this will be offset by increased coherence and lateral forces within the fiber. Thus there will be little decrease in tenacity and breaking extension at low twists. At higher twists, rapid breakage of bonds and the increased helical inclination of the molecules to the fiber axis will cause breakage at much lower tenacities and extensions.

Nylon and Terylene contain highly disordered amorphous regions with few cross links, so breakage of intermolecular bonds will be less important, and the structure will uncoil like a spring. Thus these fibers will have large breaking extensions, even at high twists. This also applies in a lesser degree to cotton, with its naturally spiraled micellar structure.

For constant-length twisting, twist will lock the structure much more rapidly for highly crystallized or highly oriented high-tenacity fibers, as little twist is absorbed in the initial local orientation of the structure. Thus these strong fibers break at lower twists than the more amorphous wool, acetate, and Acrilan staple fibers.

For constant-tension twisting, the fibers are free to contract, so the coiling properties of nylon, Terylene, and cotton can act and absorb a large quantity of twist. Thus a much larger amount of twist is needed to break these fibers (which were brittlest for constant-length twisting) by constant-tension twisting; consequently these fibers show a large difference in breaking twist factors.

Criteria for Breakage

Values of the maximum principal strains and maximum shear strains at rupture have been calculated, but neither proves very satisfactory as a constant criterion for the breaking point. In fact it is quite probable that no one criterion can give a true guide to the breaking stresses or strains over the whole twist range.

This is to be expected for textile fibers, which are anisotropic. Thus the value of the parameter deciding breakage would be expected to differ depending on the direction considered within the fiber, i.e., it will be different in a direction transverse to the fiber axis from that in a direction along the fiber axis itself.

Also under one set of combined strains the strain distribution can be considered as an ellipse; hence breakage will occur when the resultant strain in one direction reaches the breaking criterion in that direction. This is not necessarily the maximum strain, due to the uneven distributions of both the strain and the criteria.

Comparison with Previous Work

There is good agreement with the results of former workers. The results of Husung [9] show complete agreement. Similarly, the tenacity results of Nakval and Ahmed [20] and Conrad and Berkley [4] agree very well, although the former found a slight initial increase in strength for cotton at low twists. The results of Kaswell and Platt [10] show quite a sudden decrease in tenacity with twist, especially for Abaca. This is as expected, as these are highly oriented natural leaf fibers. Alexander and Sturley

TABLE XII

Fiber	Constant-tension twisting			Breaking twist factor, tex[1] turns/cm.	Breaking twist angle	Constant-length twisting		Contractive stress, g./tex	Breaking twist factor, tex[1] turns/cm.	Breaking twist angle	Difference in breaking twist factor	Mean ranking
	Tenacity, g./tex	Breaking extension, %	Contraction, %			Tenacity, g./tex	Breaking extension, %					
Nylon, extra high tenacity	80.0(1)*	16.0(2)	21.8(2)	117.0	50.0°	78.2(1)	16.3(3)	38.6(2)	65.0	34.5°	(4)	1 =
Terylene high tenacity	61.0(2)	17.0(3)	21.5(3)	128.5	51.0	58.5(2)	15.6(2)	39.4(1)	67.9	33.0	(2)	1 =
Cotton, Sudan	35.1(5)	7.6(1)	24.0(1)	121.6	47.5	41.3(5)	8.9(1)	25.0(3)	52.8	25.5	(1)	3
Cotton, Sea Island	23.7	5.7	27.2	135.2	50.5	34.1	7.0	29.3	35.7	18.0		
Nylon filament B	54.5(3)	32.0(9)	19.9(4)	135.0	55.0	54.0(3)	33.5(9)	27.2(4)	87.0	42.5	(5)	4
Nylon filament A	—	—	—	—	—	46.5	36.0	23.0	94.0	42.5		
Viscose high tenacity	23.5(6)	23.6(4.5)	12.9(6)	105.0	43.5	21.2(6)	23.5(5)	9.0(6)	77.2	35.0	(7)	5
Terylene filament 1	40.2(4)	34.3(10)	18.0(5)	156.1	56.0	43.5(14)	35.7(10)	23.1(5)	95.7	42.5	(3)	6
Terylene filament 2	39.1	35.8	16.8	155.0	46.0	42.2	37.5	23.0	102.8	44.5		
Viscose filament	15.0(7)	29.3(7)	11.7(7)	101.2	42.5	14.9(7)	27.4(7)	6.3(7)	75.2	34.5	(8)	7
Viscose staple	14.6(8)	25.0(6)	10.4(8)	94.0	40.5	14.5(8)	24.6(6)	5.7(8)	71.4	33.0	(11)	8
Triacetate filament	9.8(13)	23.6(4.5)	9.4(10.5)	95.0	43.0	9.7(12)	23.8(4)	4.5(10)	64.0	32.0	(6)	9
Acetate filament	10.7(11)	31.1(8)	9.7(9)	105.0	46.0	10.4(11)	33.5(8)	3.8(11)	81.9	38.5	(10)	10
Acrilan staple	14.5(9)	43.8(12)	6.7(12)	103.0	47.0	14.4(9)	49.0(13)	5.2(9)	87.0	42.5	(12)	11
Acetate staple	10.0(12)	42.5(11)	9.4(10.5)	107.0	46.5	9.2(13)	41.7(11)	3.2(12)	91.1	41.5	(9)	12
Wool crossbred	13.8(10)	45.3(13)	3.2(13)	114.8	48.5	12.9(10)	48.0(12)	2.3(13)	113.3	48.0	(13)	13
Wool Merino	7.6	19.6	1.4	90.6	41.5	6.8	23.8	1.1	98.1	44.0		

* Figures in brackets are orders of ranking.

[1] and Thakur [26] have shown an initial increase in breaking extension for nylon, which is again in agreement with the results of this investigation.

There is agreement with the results on contraction obtained by Nakval and Ahmed [20], Husung [9], and Breuer [3]. They all show a constant increase in contraction over the ranges they tested, while the results for contractive stress by Fuchino, Matsuda, and Nakazato [8] show the typical lessening of the increase for nylon at high twists.

The results of Koch [12] and Husung [9] on breaking twist angle θ_B have been found to be lower than the present values, being intermediate in value between the results of the constant-length and constant-tension twisting.

Strength of Twisted Fibers in Yarns

It appears that for fiber twist factors up to 40 or 50 tex$^{\frac{1}{2}}$ turns/cm., there can be little effect on the yarn strength and extension due to twist in the fibers themselves. There may be some slight effects due to twist smoothing out the elastic limit.

In general, yarn twists are less than this, even if the fibers are twisted as much as the yarn. This is very far from the case where the yarn contains many fibers, as the twist factor in the individual fiber will be $1/(\sqrt{n}) \times$ yarn twist factor, where n is the number of fibers in the yarn cross section.

The notable exceptions where the effect of twist on the fibers will probably affect the yarn are crepes and voiles. Here the hard twist will tend to ensure that the fibers themselves are highly twisted. Cotton voiles can have twist factors up to 49–53 and cotton crepes up to 57–77, while rayon crepes regularly have twist factors up to 96–102 for 200-den. yarns.

It has been shown for viscose yarns, up to the twists when snarling starts, that little change in breaking extension occurs, while acetate yarns have smaller breaking extensions and nylon and Terylene yarns have larger elongations at rupture. Various explanations of yarn structure help to explain these points, but the effect of twist on the breaking extension of nylon and Terylene fibers perhaps throws light on the effect with yarns. For the filaments there is an increase in the nominal breaking extension similar to that shown by the yarns up to twist factors of 100. The increase with yarns is greater; again this is no doubt due to the composite form of the specimen. The mutual support among the fibers will help the weaker points and so increase the breaking extension still more. This is a further effect superimposed on the over-all increase in the fiber breaking extension due to the filament properties.

Acknowledgment

The research reported in this paper has been made possible through the support and sponsorship of the U. S. Department of Army through its European Research Office.

Literature Cited

1. Alexander, F. J. and Sturley, C. H., *J. Textile Inst.* **43**, P1 (1952).
2. Anderson, S. L. and Cox, D. R., *J. Textile Inst.* **41**, T481 (1950).
3. Breuer, K., *Kunstseide u. Zellwolle* **21**, 202, 242 (1939).
4. Conrad, C. M. and Berkley, TEXTILE RESEARCH **8**, 341 (1938).
5. Das, D. B., Guha, S. R. D., and Wareham, J. F., *J. Sci. Ind. Res.* **11**, 449 (1952).
6. Deppe, B., *Z. Tierzücht. Züchtungsbiol.* **29**, 27 (1926).
7. Frezel, W. and Perner, H., *Faserforsch. u. Textiltech.* **4**, 1, 63 (1953).
8. Fuchino, K., Matsuda, K., and Nakazato, K., *J. Soc. Text. & Cell. Ind. Japan* **8**, 532 (1958).
9. Husung, E., *Monatsch. Seide u. Kunstseide Zellwolle* **42**, 215, 273 (1937).
10. Kaswell, E. R. and Platt, M. M., TEXTILE RESEARCH JOURNAL **21**, 5 (1951).
11. Krais, P., *Textil-Forsch.* **3**, 86 (1921); **4**, 4 (1922).
12. Koch, P. A., *Textil-Rundschau* **4**, 199 (1949); **6**, 111, 281 (1951).
13. Lord, E., *J. Textile Inst.* **38**, T84 (1947).
14. Meredith, R., *J. Textile Inst.* **36**, T107 (1945).
15. Meredith, R., *J. Textile Inst.* **41**, T481 (1950).
16. Meredith, R., "Mechanical Properties of Textile Fibres," Amsterdam, North Holland Publishing Company (1956).
17. Meredith, R., "Mechanical Properties of Textile Fibres," Amsterdam, North Holland Publishing Company, 85 (1958).
18. Morton, W. E. and Permanyer, F., *J. Textile Inst.* **40**, T371 (1949).
19. Nakazato, K., *J. Soc. Text. & Cell. Ind. Japan* **8**, 537 (1958).
20. Nakval, H. and Ahmad, N., *J. Textile Ind.* **28**, T307 (1937).
21. Peirce, F. T., *J. Textile Inst.* **17**, T355 (1926).
22. Schwab, R., *Klepzig's Textil-Z.* **42**, 397 (1939).
23. Semple, W. L., unpublished work.
24. Tänzer, E., *Melliand Textilber.* **8**, 1017 (1927); **11**, 667, 747 (1930).
25. Timoshenko, S., "Theory of Elastic Stability," New York, McGraw-Hill, 169 (1936).
26. Thakur, V. M., Ph.D. Thesis, Manchester University (1959).
27. Vinckers, J. B., *De Textielindustrie* **3**, 253 (1922).

Manuscript received March 28, 1960.

A Computer for the Automatic Processing of Fiber, Yarn, and Fabric Stress-Strain Data

W. J. Thorsen

Western Regional Research Laboratory,[1] Albany, California

Abstract

During single-fiber tensile tests, major transitions in rheological behavior occur at the Young's modulus and yield-point regions. In the former region there is a transition from uncrimping (nonlinear spring) to approximate spring-like or Hookean behavior, and then to viscoelastic or plastic flow. In the latter region the transition is from Hookean extension to maximum plastic flow. The center of each transition region provides the basis of a new and better definition of the Young's modulus and yield points since these points are directly determined by the molecular-flow properties of the fiber. The uncrimping point is also defined on the basis that it is at or near the center of a transition from pure helical spring to nonlinear spring and then to approximate Hookean behavior. An advantage of defining the parameters in this way is that they may be located through the use of the second and third stress derivatives as obtained by electronic analog computer techniques. Such techniques involve the use of inexpensive standard laboratory-type computer components. Thirty percent stretch and the ultimate tensile points may also be obtained. Voltage analogs of stress, strain, slope, and energy are stored in the computer's memory section at any of these points, or at any other selected stress or strain points. Twenty-one or more parameters may be computed and stored. Adaptations to yarn and fabric tensile tests and a modification to automatically dial in initial fiber length and reverse elongation are also described. Through the use of analog-to-digital converters, these data may be automatically punched on cards or tape for storage or further analysis on a digital computer.

Introduction

D-C analog computers are relatively simple and inexpensive electronic devices now commonly used to solve, with slide-rule accuracy, a variety of problems in applied mathematics and engineering design. Such computers represent the variables of a given problem by corresponding voltages which vary continuously with time; time is generally used as the independent variable in problems involving differential equations. The principal computing elements are d-c amplifiers with resistive and capacitive feedback networks. With the computer connected to solve a given problem, the variables (voltages) are set to the correct initial conditions. The computing elements are then made operative and force the voltages to vary in a manner prescribed by the differential equations. Voltage variations with time are then recorded and constitute solutions of the given problem.

In textile research and processing control the stress–strain properties of fibers, yarns, and fabrics are routinely used to evaluate the effectiveness of many treatments and processes [3, 6]. Such tests are usually not excessively time-consuming, but the subsequent data-reduction process is quite tedious. Moreover, a more serious difficulty is that many of the most important stress–strain parameters have not yet been defined. For example, in the case of the stress–strain curve of single fibers, standards for the exact location of the uncrimping point,[2] Young's modulus, and yield stress have not yet been agreed upon. As a consequence, data of various observers are not comparable. In practice Young's modulus is usually taken as the slope of the tangent to the stress–strain curve in the initial linear region. Unfortunately, with all organic fibers no "linear" region exists since the curve is actually sigmoidal [2]. This is seen in Figure 1 for wool. Location of the yield stress point is also highly subjective in that it is

[1] A laboratory of the Western Utilization Research and Development Division, Agricultural Research Service, U. S. Department of Agriculture.

[2] ASTM Committee D-13 is presently formulating tentative standards for the uncrimping energy, initial length l_0, and uncrimping force of single fibers.

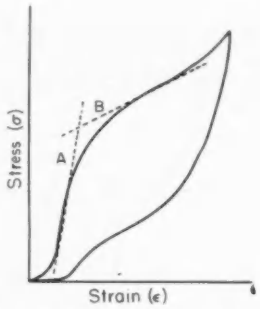

Fig. 1. Stress–strain curve of a single wool fiber.

usually determined [5] by the intersection of the above-mentioned tangent (Line A, Figure 1) with another line which passes through the linear portion of the post-yield region (Line B, Figure 1), this "linear" portion also being nonexistent.

It is the purpose of this paper to propose a quantitative definition of the uncrimping, Young's modulus, and yield points, based on the mathematics of the stress–strain curve. This would appear to be a more logical approach since each of these points is at or near the center of a physical or rheological flow-transition region of the fiber.

A computer will be described which, based on the above approach, automatically processes the stress–strain data obtained during tensile tests. Circuits are described for the simultaneous evaluation and storage of 21 or more parameters of the single wool fiber stress–strain curve with an accuracy which is limited primarily by the characteristics of the tensile tester used. Measurements of yarn and fabric tensile properties are also described.

Definition of the Major Stress–Strain Curve Parameters

The stress–strain curve of wool, along with the first, second, and third derivative curves, are shown in Figures 2a, 2b, 2c, and 2d.[3] No "linear" region occurs in the Young's modulus region; the curve is actually sigmoidal [2] with a point of inflection at *b* (Figure 2a). At this point the slope or first derivative of the curve is at a maximum (see Figure 2b). From a rheological standpoint, inflection point *b* is highly significant in that it is located at or near the center of a major transition region. In this region the stress in the fiber builds up sufficiently to cause internal flow; e.g., there is a transition from uncrimping (nonlinear spring) to momentary approximate springlike or Hookean and then to viscoelastic or plastic behavior. As seen in Figure 2c, at this transition point the value of the second derivative passes through zero. Therefore the second derivative voltage in the computer can be used to initiate a switching action at this point which will store the first derivative (now at a maximum) in the memory section.

[3] The derivative curves shown are only approximations.

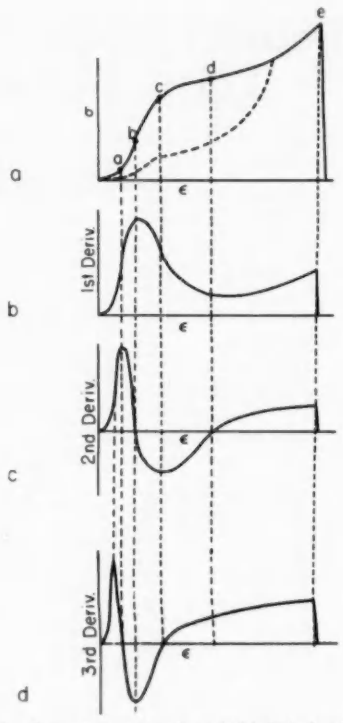

Fig. 2. Zero, first, second, and third derivatives of stress–strain curve of single wool fiber.

The uncrimping and yield stress regions also have transition points *a* and *c* respectively (Figure 2a) which can be located by observing when the value of the third derivative passes through zero (Figure 2d). At these points the second derivative is either at a maximum or a minimum (Figure 2c) and, since the second derivative is the acceleration of the stress (or recorder pen), it may be said that the acceleration or deceleration of the stress is at a maximum at these points. This also indicates that points *a* and *c* are located where the radius of curvature of the stress–strain curve is at a minimum.

Uncrimping point *a* represents the central point of a broad transition region in which fiber stress–strain behavior shifts from pure helical spring to

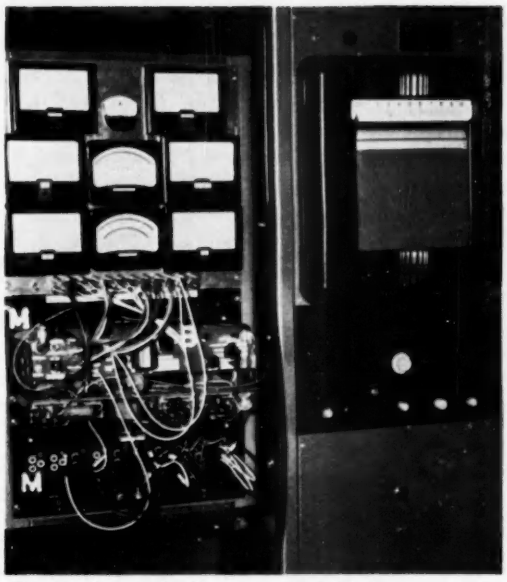

Fig. 3. Automatic fiber, yarn, and fabric stress–strain curve computer connected to a tensile tester.

nonlinear helical spring behavior, and then to approximate Hookean behavior. Actually fiber elongation at point a nearly coincides with the value l_o, obtained by the above-mentioned proposed ASTM method of extrapolating the Young's modulus line to zero stress.

Yield point c (Figure 2a) represents the center of a transition from approximate Hookean behavior to full viscoelastic flow.

Equipment Used

Two inexpensive, self-powered computer manifolds are used. They are shown in Figure 3, mounted in the lower portion of the left relay rack (compenents M). Each manifold accommodates ten plug-in operational amplifiers which may be interconnected as desired by means of front-panel banana jacks. Other type amplifiers may be plugged in to operate in conjunction with the operational amplifiers; e.g., chopper stabilizers (for integration), cathode followers (for power amplification), high-gain or low-noise amplifiers, etc. Connections are made through the front-panel banana jacks.

A large plug-in board was constructed (see Figure 3, component B) to facilitate interconnecting the amplifiers in one of the manifolds and to support the various relays, switches, control cable jacks, and other hardware. The lower manifold is used primarily to perform the three differentiations required; here only individual plug-in elements were used in order to facilitate modification of the differentiation circuit. This was found quite convenient, since a large amount of trial-and-error work was required to find the best way to filter out signal noises originating in the tensile tester [2]. An advantage to the plug-in technique is that the computer may be quickly freed for the solution of other problems.

One-percent panel meters are mounted in the upper half of the rack, along with a sensitive null-meter for precision zero balancing of the integrator. If measurement accuracies higher than 1% are required a D-C potentiometer may be used to read out all voltages.

Circuit Description

General

Since tensile testers operate at a constant rate of loading or a constant rate of elongation, the electronic analog computer is readily adapted to their operation. This may be explained as follows with the example of the constant-rate-of-elongation tester used in this study.[4] In such testers elongation is the independent variable and, of course, it varies linearly (on the average) with time. Force is the dependent variable. With electronic analog computers, time is generally taken as the independent variable, so any mathematical operations performed on the force analog voltage with respect to time automatically result in operations with respect to fiber elongation. For example, differentiation of the force analog voltage results in a voltage which is directly proportional to ∂ force/∂ length or, if the force and length are converted to stress, σ, and strain, ϵ, $\partial\sigma/\partial\epsilon$. Also, an integration can be timed so that the energy or work to stretch at the corresponding elongation will be known.

As the theory of the use of operational amplifiers [4] is well known, the following discussion will include only descriptions of the functions of the various circuit elements employed. All resistors are precision and ½-watt unless otherwise specified. Mylar dielectric capacitors with a 10% tolerance are used.

Force-to-Stress Converter

One of the first operations performed by the computer is the conversion of the force analog voltage to a stress analog voltage (Figure 6). Since the

[4] Instron Model No. TT-B.

force signal potentiometer is mounted on the pen mechanism of the recorder in the Instron Tensile Tester in such a way that its armature does not rotate completely to zero voltage output when zero force is indicated on the recorder, some method is needed to subtract out the residual voltage. This is accomplished by the zero force adjust section which is a voltage-subtracting circuit connected to the input of amplifier 4.[5] The + and − 300 V potentials required for both of these circuits are available from banana jacks on the front panels of the computer manifolds. The force-to-stress converter circuit is simply a voltage multiplier which multiplies the force analog voltage by factor R_f/R_i or $E_o = (R_f)/(R_i)E_i$ where E_o is the output (or stress) voltage, E_i the input (or force) voltage, R_f the feedback resistor (500 K), and R_i the input (denier or cross-sectional area) potential (500 K). The latter pot. is a 0.1% linear, 10-turn precision helical potentiometer. If the denier pot. dial is set to 10.00 or 500 K the multiplication factor (or gain) is 1.0. With it set to 5.0, the factor is 2.0. If a certain tex (or denier) fiber is being tested, the full-scale stress range (g./tex.) can be maintained by setting the denier pot. to the correct tex (or denier). A small loading error is introduced in the signal pot. by the denier pot.; the amount is no larger than 0.25% of full scale [4].

Strain Circuit

This circuit converts the voltage obtained from the elongation pot. (helical, precision) to percent elongation. The elongation pot. is connected to the Instron's elongation mechanism cross-arm screw by a timing belt drive and gear box as shown in Figure 4. The gear box is mounted inside the Instron top cover and has three helical pots. and three sets of speed-changing gears. For textile specimen 1-in., 3-in., and 10-in. long, gear ratios are 10:1, 3:1, and 1:1 respectively. Since the Instron cross-arm drive screw turns exactly one revolution per inch of cross-arm travel, the elongation pot. shaft (see Figure 4) will rotate ten times for 100% elongation of each of the above specimen lengths. If the specimen is longer than 1 in., 3 in., etc., this amount is dialed and locked into the gauge length (l_0) pot. A and the gear mechanism subtracts the same rotation from the elongation pot. The gauge length pots. are maintained locked during the test. In this manner the voltage output of the strain circuit (Figure 6) will always be one volt for each 2% elongation. The turns per extra inch of the l_0 pot. are 10 for a 1-in. specimen length, 3.33 for a 3-in. specimen, and 1.00 for a 10-in. specimen. If desired, with the single fiber test l_0 may be rapidly estimated and set in just after the uncrimping region (see "Additional

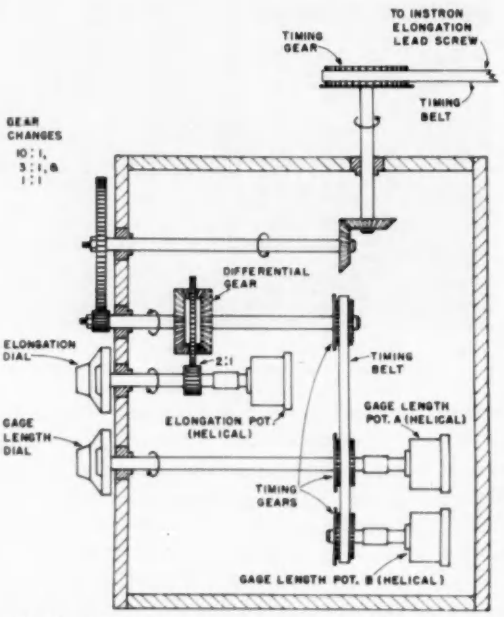

Fig. 4. Arrangement of gears in a gauge-length compensator which converts elongation to percent elongation and first derivative to true Young's modulus.

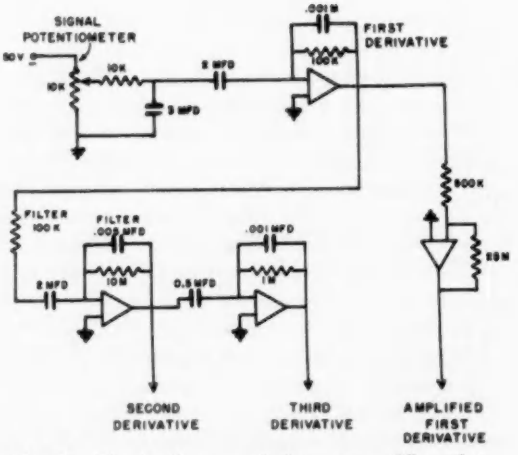

Fig. 5. Circuit diagram of three-stage differentiator.

[5] Amplifiers 1–10 are in the upper manifold and A–J in the lower manifold.

Features" section for method wherein the gauge length pots. are set automatically).

Differentiation Circuit

The use of differentiators is avoided if at all possible in computing circuits because their frequency-response characteristics tend to produce noisy and unstable setups. However, there is no alternative but to use differentiators here, first to obtain Young's modulus and, second, to obtain the control circuits desired. As expected, noise increases with each succeeding stage of differentiation. To counteract this, RC filters may be added.[6] However, filtering alters the frequency-response characteristics of the differentiator and differentiation error increases with frequency. The solution is to make no better a differentiator than actually required [1]. A differentiation circuit which has a good signal-to-noise ratio in each stage is shown in Figure 5. By impressing a high voltage (50 V DC) across the signal pot. little filtering is required in the second stage and the noise level is 0.1 V or less in all stages. Signal outputs as high as 40 V are obtained with voltage changes from the signal pot. of the same order as that expected from the stress circuit during single-fiber stress–strain (10%/min.) tests. A sine wave generator is easily assembled [4] and may be used as input in place of the pot. for testing purposes.

Adaptation of the Differentiation Circuit to Tensile Tester Characteristics

The extension mechanisms of most tensile testers elongate the textile specimen at a rate which is, on the average, fairly constant. However, short-term vibrations and oscillations, with periods from 1 to 3 sec., cause the extension rate (as measured by the first derivative voltage) to vary as much as 100% [2]. This means that at times the specimen is not being elongated at all and is stress-relaxing, while at other times elongation is double the average rate. What effect such variations have on ordinary stress–strain measurements is not known, but the results of certain tests are affected [2]. Variations of the above type were also observed with the tensile tester used in this study. Such variations are, of course, converted to random electrical noise by the signal pot. and cause extreme fluctuations in the derivative voltages, particularly the third derivative. Such variations make any evaluation of Young's modulus (first derivative) and the use of the second and third derivative voltages as control voltages quite impossible without filtering. The first step taken was to find the minimum amount of filtering required to stabilize the first derivative for accurate Young's modulus measurement. With this filtering, the second stage requires practically no filtering, but the third (most sensitive) stage requires considerable filtering.

All three stages are shown in Figure 6 with the stress voltage as input. Wiring of the remainder of the computer elements is also shown.

The first derivative voltage is fed into the Young's modulus compensator (Amplifier C) which corrects the voltage according to the initial length of the textile specimen. The gauge length l_o is dialed into the gauge length pot. B automatically as gauge length pot. A is set. This operation multiplies the first derivative voltage by a factor proportional to fiber length so that the output of Amplifier C is proportional to true Young's modulus ($\partial\sigma/\partial\epsilon$).

The error in Young's modulus introduced by the filter is 1% for stress changes corresponding to a sine wave frequency of about one cycle every 1.5 min. The Young's modulus analog voltage is connected to the memory section, which will store the voltage when triggered by the second derivative voltage.

The error produced by filtering of the third derivative voltage is such that the highest frequency which may be passed with 1% error is approximately one cycle every two minutes. Since the error is proportional to frequency squared, a 4% error will occur at twice this frequency. The above errors will cause delays in the switching actions described below.

Integration Circuit

The stress analog voltage is fed into the integration section (see Figure 6). A chopper stabilizer plug-in (Type P) is used in conjunction with the operational amplifier in order to reduce drift errors to negligible levels over the period of integration (3 min.). At point *d* (Figure 2a) the elongation is reversed and the energy to stretch analog voltage is stored in the memory section (described below) and the integration for the energy of retraction (area under dotted line in Figure 2a) is begun. This storage action is initiated by a voltage pulse which the control chassis on the tensile tester generates at the instant the Up button is pushed to reverse the elongation. A few

[6] No additional filtering is required for the computer supplies, since they are regulated to 0.1% or better.

milliseconds after this storage action, the integrator condenser is momentarily shorted and discharged. Then integration for energy of retraction begins and when the stress returns to zero the integration condenser will maintain its charge and the voltage output of Amplifier 2 may be read.

The output of the integrator is also fed into another readout circuit of the memory section so that the energy to uncrimp may be obtained. A "Young's modulus check" switch connects the integrator output to the first stage of the differentiation circuit. By rotating the signal pot. to various fixed voltages, various continuously rising voltages may be generated (ramp functions) and the rate of rise is proportional to the fixed input voltage. Thus the first-stage differentiation circuit may be checked as its output should be directly proportional to the signal pot. voltage.

A precision null-meter is mounted on the computer meter panel (Figure 3) to accurately null the output of the integrator before each test. This is done by the zero force adjust pot.

Memory Section

The memory section consists of a number of readout circuits built as shown in Figure 6. The readout circuit is based on the fact that an integrator in the "hold" position constitutes an analog storage device which "remembers" its last-computed output voltage [4]. In these circuits a condenser is connected across the output voltage to be stored and, at the instant storage is desired, a latching relay connects

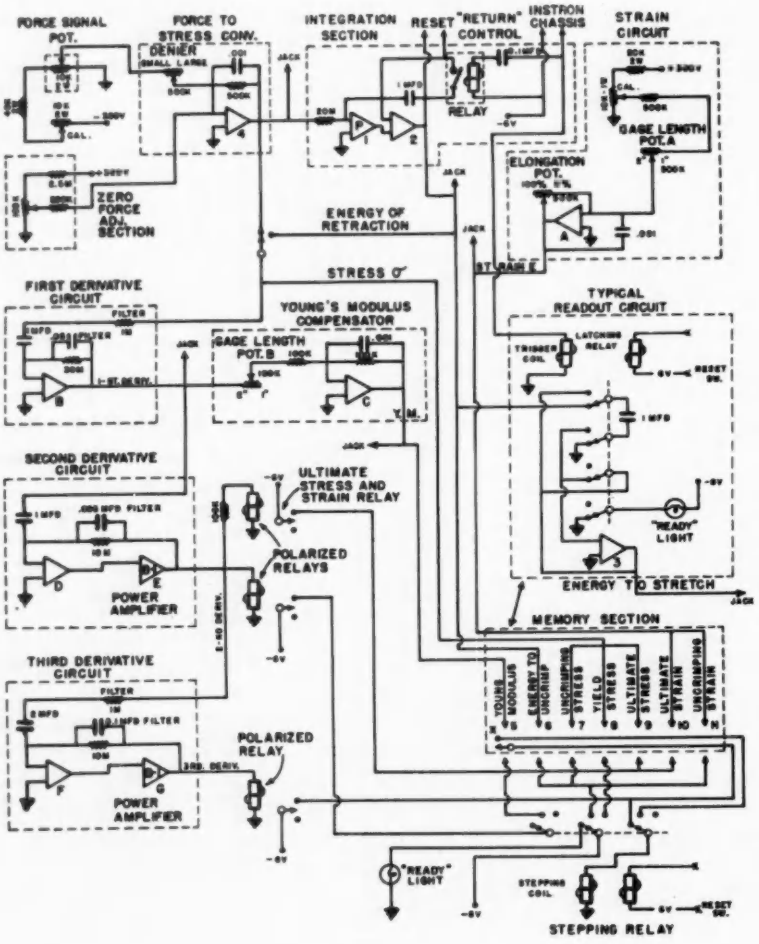

Fig. 6. Final circuit diagram of eighteen-amplifier stress–strain curve computer with a memory of eight parameters. ▷ designates an operational amplifier, [P]▷ a chopper stabilizer, and [B-1]▷ a cathode follower power amplifier.

the condenser in feedback to an operational amplifier. The output of the amplifier then becomes equal to the voltage on the condenser. Due to the small leakage in the capacitor, it will lose its charge at an initial rate of 100/RC%/sec. In the present circuit where $C = 10^{-6}$ farads and R (leakage resistance) $= 50 \times 10^{9}$ ohms, the initial leakage rate is 0.002%/sec. In 100 sec. the drop will be 0.27% so there is ample time to read out all of the voltages after a test.

All of the latching relays are reset to their initial condition and the capacitors shorted by flipping a multiple rotary lever switch.

If desired the "pipping" circuit may be energized by the latching relays at the time they fire so that the exact location of each stress point will be marked on the stress–strain curve.

The output of each operational amplifier may be tapped by a rotary selector switch for initial zeroing, and the output of each readout circuit is connected to an individual meter for rapid observation of test results. The selector switch is double-pole since signal polarity of the amplifiers may be either plus or minus.

Switching Circuits

To obtain sufficient power to drive a relay, the second and third derivative circuits are each connected to a plug-in, cathode-follower power amplifier.[7] Each follower amplifier drives one or more highly sensitive, fast-response polarized relays. The armature of these relays will switch from one contact to the other when coil polarity is reversed. Due to their high coil resistance, coil voltages as high as 50 volts will not overload these relays. Contact reversal occurs on a voltage change of less than one volt. As seen in Figure 2, the first of the derivative voltages to pass through zero and initiate a switching action is the third derivative voltage. By our definition (see above) this is the uncrimping point (point *a*, Figure 2a). At this time the third derivative polarized relay reverses contact and steps the stepping relay to its second set of contacts. As indicated schematically by the arrows pointing to the memory section from the stepping relay, a voltage pulse is thereby fed into the uncrimping readout circuits, causing the uncrimping stress, uncrimping strain, and uncrimping energy analog voltages to be stored in the memory section. When the relay armature is at the first set of contacts, an interlock connection prevents any other type of switching action from taking place. At the second set of contacts the second derivative relay is tapped, which is appropriate since the next voltage to pass through zero is the second derivative voltage (Figure 2c). At this instant (point *b*, Figure 2a) the Young's modulus analog voltage is stored in the memory section, and, if desired, the stress, strain, or energy could also be stored if other readout circuits were available. The interlock circuit on the Young's modulus latching relay in the memory section now reactivates the third derivative relay by the closure of contacts X (Figure 6); when its voltage again passes through zero (Figure 2d) the yield point (point *c*, Figure 2a) has been reached and the yield stress is stored in the memory. Again, any of the other parameters could also be stored. After this switching action, all further switching by the above relays is locked out. Of course the elongation may be reversed at any selected stress or strain value and the energy to stretch and energy of retraction will be stored as described above.

In ultimate tensile-strength measurements at the instant of fiber or yarn breakage (point *e*, Figure 2a), the value of the second derivative voltage very rapidly drops (Figure 2c) to its maximum negative value of 50 V DC. This voltage is dropped sufficiently by a 100-K resister so that the voltage impressed across the coil of the ultimate stress and strain relay is kept small and the relay "fires" only at breakage points (when recorder-pen-speed acceleration is at a maximum and the second derivative voltage approaches its maximum negative value of 50 volts). Thus the ultimate tensile strength and elongation analog voltages are stored at this time.

Performance

Wet Single Wool Fiber Tests

Table I is a tabulation of four wet stress–strain parameters of a single wool fiber as obtained both by hand (from the strip chart) and with the computer. The fiber was tested a number of times and allowed to relax no more than a few minutes between tests. In each test the fiber was elongated 20% at a rate of 10%/min. It is seen that there is a slight downward drifting of most of the parameters. Variability of measurement is generally higher in the hand measurements. Calibration for Young's modulus was performed by using several springs between the jaws of the Instron, and the Young's modulus

[7] Stock computer item.

values were found to be a precisely linear function of the strip chart slopes. The parameters obtained by the two methods are quite comparable in magnitude, with the exception of the return energy, in which case the hand values are about 5.5% low. This is due to the fact that the return curve was obtained by reversing the direction of chart motion when the cross-arm direction was reversed. When the chart motor is reversed, a large error is introduced in the chart motion due to motor armature inertia and chart gear-train back-lash.

Table II is a tabulation of a number of parameters obtained from the first, and then the repeat 30% wet stress–strain loop of four single wool fibers. The fibers were allowed to relax more than 24 hr. between tests. All parameters were obtained as described above, with the exception of the uncrimping parameter. Due to considerable noise in the third derivative voltage, good switching accuracy could not be obtained. To overcome this, a polarized relay was connected (through a cathode-follower amplifier) across the stress analog voltage and adjusted to switch the uncrimping parameters at approximately 1.0 g./tex. It is seen from the data in Table II that good reproducibility is obtained with all parameters.

In order to better compare the computer vs. hand methods of taking data, estimates were made of the variance of the Young's modulus and yield stress data. Table III shows the results of repeated hand evaluations of these parameters on a single stress–strain curve. From these data, and the data in Table II, the standard deviation of Young's modulus as obtained by the computer is estimated to be 1.31, whereas for the hand method it is 2.91, which is a significant difference at the 90% probability level. However, there is no significant difference in the variances of the yield stress data—they were 0.01 and 0.012 for the computer and hand methods, respectively. The comparisons above, although not conclusive, seem to indicate that the computer method is as good as, and possibly better than, the hand method of taking data. A primary advantage in the computer method is in its speed of acquiring the desired data.

Dry Single Fiber Tests

Accuracy at about the 1% level was obtained, but variations in force due to slippages in the fiber mounts, atmospheric turbulences, and humidity variations can cause premature switching of the ultimate tensile strength properties. This may be overcome by resetting after each premature relay "firing."

Yarns and Fabrics

A great deal less filtering (first and third stages) is required since the "shocks" from variations in cross-arm speed are mostly absorbed by the yarn or fabric under test. Adjustments in the filtering produce parameter-measuring circuits again operating within a 1% accuracy level.

Additional Features

If desired, the stress, first derivative, strain, or energy may be determined at any selected stress or elongation by manually triggering the appropriate readout latching relays. Each relay would have to be individually connected to a 6 V power source. Also, by the attachment of a solenoid brake to the gauge length shaft (see Figure 4), this shaft, which initially moves with the cross-arm lead screw, can be stopped from moving at the time the uncrimping parameters are switched by the switching voltage. In this manner fiber length at 1.0 g./tex (see "Performance" above) is automatically determined and dialed in. At this instant the elongation shaft, at rest previously due to a greater frictional force, commences its rotation and the strain circuit now

TABLE I. A Single Wool Fiber Repeatedly Elongated 20% in Water, Without Appreciable Rest. Comparison of Computer and Hand Methods of Evaluating the Parameters. T = 70° F., tex = 0.812, Elongation Rate 10%/min.

	Young's modulus, g./tex		Yield stress, g./tex		Outgoing energy, g. cm./tex		Return energy, g. cm./tex	
Cycle	Computer	Hand	Computer	Hand	Computer	Hand	Computer	Hand
1	86.4	85.4	2.48	2.50	1.53	1.54	.706	.655
2	85.8	84.4	2.50	2.50	1.52	1.53	.705	.670
3	85.8	81.4	2.48	2.46	1.51	1.51	.705	.658
4	85.8	82.6	2.48	2.43	1.50	1.53	.703	.679
5	85.8	86.2	2.48	2.43	1.49	1.52	.700	.673

TABLE II. Repeat Elongation of Single Wool Fibers in Water after 24 Hours of Relaxation, as a Test of Computer Reproducibility. T = 70° F., Elongation Rate 10%/min.

Fiber	Fineness, tex	Uncrimping energy, g. cm./tex	Young's modulus, g./tex	Yield stress, g./tex	Outgoing energy, g. cm./tex	Return energy, g. cm./tex
#1	.621	.00962	89.8	2.32	1.49	.721
Repeat #1		.00962	88.7	2.32	1.48	.705
#2	1.021	.0107	101.6	2.47	1.53	.673
Repeat #2		.0112	103.8	2.45	1.54	.683
#3	1.06	.00423	108.4	2.34	1.69	.761
Repeat #3		.00423	109.6	2.34	1.69	.761
#4	.931	.0144	82.9	2.02	1.52	.706
Repeat #4		.0123	85.4	2.00	1.51	.706

indicates percent elongation based on the dialed-in fiber length. Automatic reversal of the elongation mechanism at any predetermined percentage elongation may be accomplished through the use of a contact meter relay in place of the strain meter. This type of meter has an adjustable pointer with a contact on it which can be set to close a circuit at any selected voltage. By setting the pointer at, for example, 15 volts (30% elongation) and with a suitable connection to the Instron elongation reversal circuit, elongation will be automatically reversed at this point.

Cost of Components

The cost of components totals approximately $1800, including $1200 for the two computer manifolds and $160 for the meters.

Adaptation To Further Data Processing With a Digital Computer

In order to make a permanent record of the analog voltages and to facilitate further data processing (statistical analyses etc.), it is best to store the computed data on punch tape or cards. Equipment can be attached which will, on command, automatically punch the data on tape or cards.

TABLE III. Repeated Hand Evaluations of the Stress–Strain Parameters of a Single Wool Fiber Stress–Strain Curve. T = 70° F., Tex = 1.021, Elongation Rate = 10%/min.

Young's modulus, g./tex	Yield stress, g./tex
110.1	2.54
106.7	2.52
103.3	2.55
106.7	2.52
109.0	2.54
102.1	2.52
107.9	2.53

Literature Cited

1. "Analog Computer Techniques Applied to Industrial Instrumentation and Control, Part II," IRE-PGEC Notes, G. A. Philbrick Researches, Inc.
2. Grignet, J. and Monfort, F., TEXTILE RESEARCH JOURNAL **28**, 47 (1958).
3. Harris, M., Mizell, L. R., and Fourt, L., *J. Research Nat. Bur. Standards* **29**, 73 (1942).
4. Korn, F. A. and Korn, T. M., "Electronic Analog Computers," 2nd Ed. (1956).
5. O'Connell, R. A. and Lundgren, H. P., TEXTILE RESEARCH JOURNAL **24**, 677 (1954).
6. von Bergen, W. and Wakelin, J. H., TEXTILE RESEARCH JOURNAL **22**, 123 (1952).

Manuscript received April 5, 1960.

The Relation between Crystallite Orientation and Mechanical Properties of Mercerized Cottons

B. R. Shelat, T. Radhakrishnan, and B. V. Iyer

The Ahmedabad Textile Industry's Research Association, Ahmedabad-9, India

Abstract

Bundles of cotton fibers have been mercerized at various controlled stretches. The x-ray orientation factor, static elastic modulus, and load-extension behavior of these fibers have been determined. The effect of changes in fine structure on changes in mechanical properties is discussed in terms of the above data.

Introduction

Other things remaining constant, the elastic moduli of fibers are expected to increase and creep to become less prominent with increasing degree of molecular orientation. Well oriented cellulosic fibers such as flax and Fortisan have a much higher Young's modulus than fibers with medium orientation, such as cotton or medium tenacity viscose [9]. In raw cotton itself, a linear dependence of static Young's modulus on the optical orientation factor [4] as well as on the x-ray angle [7] is known to exist. Young's modulus for viscose rayon is known to increase linearly with optical orientation factor [3, 8]. The present paper is an attempt to extend this type of quantitative information to mercerized cottons. It has been shown in an earlier paper [5] that, depending upon the stretch exerted during mercerization, fibers with controlled crystallite orientation (always higher than raw cotton) and, surprisingly enough, nearly constant crystallinity, can be obtained. The earlier paper was concerned with the relation between crystallite orientation and rupture properties such as tensile strength and extension at break. The present work deals primarily with static Young's modulus and the load–extension curve. It also contains some observations on creep properties, as inferred from cyclic extension data.

TABLE I. Some Properties of Raw Cottons Studied

Fiber property	Cotton name and initials: CO2–134 C	Karnak K	Andrews Sea-Island S	Jarila J
X-ray orientation factor, f_x	0.70_8	0.71_3	0.74_4	0.79_7
Static elastic mod. (10^{10} dynes/cm.^{2})	4.8	6.3	7.6	7.3

Experimental Techniques and Results

Sample Selection and Preparation

The cottons selected for this purpose were Karnak, Andrews Sea-Island (a variety grown in India), and two Indian cottons, CO2-134 and Jarila. The first two samples belong to the species of *G. barbadense*, the third is a *G. hirsutum*, and the fourth, *G. herbaceum*. Some relevant properties of the raw cottons, as measured by techniques to be described subsequently, are shown in Table I.

The fiber bundle mercerizing technique (using the Instron tensile tester to control stretch) has been fully described in the earlier paper. The stretched fiber lengths ranged from 15% below the original cotton length (for slack mercerization), in steps of 2.5%, to about 10% in excess of the original length. Some incidental observations were made on the force required to stretch the alkali-swollen cotton bundles. It was noted that these bundles had very low resistance to stretching as compared with raw cotton bundles. Typical stress–extension curves are shown in Figure 1 for three swollen cottons and one raw control. For the former, the extension is calculated on the basis of the "swollen" length. These curves will be commented upon in a later section.

Measurement of Orientation Factor

The definition of the x-ray orientation factor f_x of Hermans [2] and a description of a method of measurement by using Geiger counter diffractometry have already been discussed in detail in the earlier paper [5]. Here it will only be recorded that f_x is evaluated from azimuthal intensity

distributions of the (10$\bar{1}$) and (101) equatorial interferences. The x-ray orientation factor is calculated from the well-known relation

$$f_x = 1 - \tfrac{3}{2}(\overline{\sin^2 \gamma} + \overline{\sin^2 \beta}) \qquad (1)$$

The reader is referred to the earlier paper [5] or to Herman's well-known work [2] for definitions of $\overline{\sin^2 \beta}$ and $\overline{\sin^2 \gamma}$.

One interesting point about orientation of mercerized cottons, which escaped mention in the earlier paper, will be dwelt upon in detail. In raw cotton, there is no great difference in the distribution of intensities along the arcs of the three equatorial interferences (002), (10$\bar{1}$), and (101). This fact has been used to advantage in calculating the orientation factor of raw cotton from the single intense interference (002). In the case of mercerized cottons, it has been found that the (002) and (10$\bar{1}$) interferences, which are not fully resolved from each other, have much the same intensity-distribution curve. The (101) plane is less perfectly oriented and has a greater average orientation angle than the other two. This situation is shown in Figure 2. The relative trends in orientation of the (10$\bar{1}$) and (101) planes are similar to what has been reported in the case of viscose rayon spun at various stretches [2].

On account of the fairly good correlation (0.94) between the orientations of the (10$\bar{1}$) and (101) planes (see Figure 2) there is some promise that the x-ray orientation factor of mercerized cotton can be determined without much loss of accuracy from measurements on a single arc, such as the intense (10$\bar{1}$, 002) doublet. A suggested formula for this purpose, which is applicable to the present data, is

$$f_x \approx 1 - \tfrac{7}{2}\overline{\sin^2 \beta} \qquad (2)$$

However, all orientation factors reported in this paper are based on independent measurements of both interferences.

The orientation factors of the various mercerized samples are plotted in Figure 3 against the mercer-

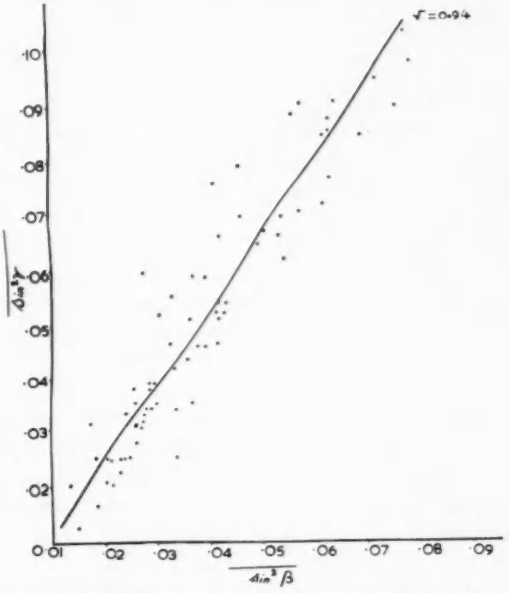

Fig. 2. Relation between orientation angles of (101) and (101) planes in mercerized cotton.

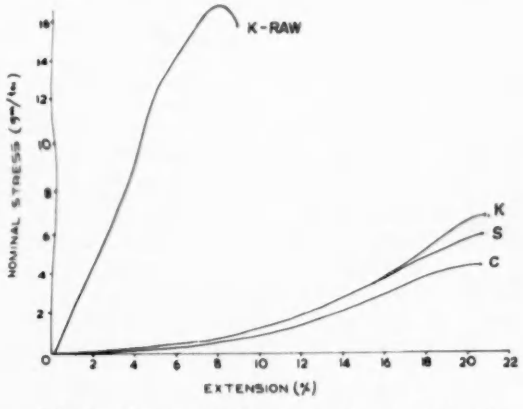

Fig. 1. Stress–extension curves of untreated and alkali-swollen cotton bundles.

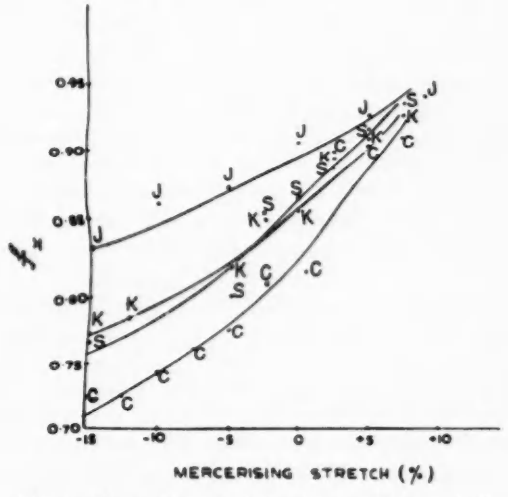

Fig. 3. Crystallite orientation factor of mercerized cottons versus mercerizing stretch.

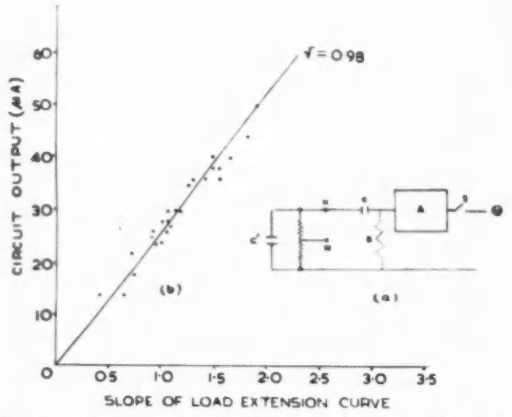

Fig. 4. (a) Differentiator circuit and (b) its performance.

izing stretch, each cotton being identifiable by the use of the initials given in Table I. It is seen that separate curves are applicable to the different cottons, as already reported in the earlier paper [5].

Elastic Modulus Determination

From load–extension curves. Values of "quasi-static" Young's modulus were measured at 27° C. and 65% RH for about 100 single fibers picked at random from bundles mercerized at each stretch. The Instron tensile tester was used for modulus determinations, with a nominal specimen test length of 1 cm., a rate of extension of 5%/min., and a full-scale sensitivity of 2 g. The slope of the initial straight portion of each load–extension curve was measured in terms of grams per percent extension, taking into account the initial gauge length, slack length, and also crimp of the fiber, if any. The average value of this slope was divided by the average tex value of the fiber (obtained by cutting, counting, and weighing 1-cm. lengths). In the initial experiments, each individual fiber was vibroscoped for getting fiber fineness and the individual elastic moduli ascertained. But this procedure was found to be without much merit, since, somewhat surprisingly, it did not in any way decrease the observed coefficient of variation of the elastic modulus. Theoretically, it can be proved that vibroscopy is not essential when we are interested only in the *mean* value of Young's modulus. Let f and μ respectively be the load per unit extension and the fineness of a single fiber. Let v_f and v_μ be the fractional coefficients of variations of these quantities and r the correlation coefficient between them. There is a well-known statistical relation [6] which states that when μ and f are normally distributed

$$E\left(\frac{f}{\mu}\right) = \frac{E(f)}{E(\mu)}[1 - rv_f v_\mu + v_\mu^2] \qquad (3)$$

Typical values of these parameters (obtained in the laboratory) are $r = 0.6$, $v_f = 0.4$, $v_\mu = 0.25$. In this case

$$E\left(\frac{f}{\mu}\right) = 1.0025\,\frac{E(f)}{E(\mu)} \qquad (4)$$

and near equality is maintained even for substantial changes in r, v_f, and v_μ. In such circumstances vibroscopy does not sensibly improve the precision of results, which is already limited by fixing the number of fibers at 100.

By differentiator. A method of shortening the time factor for these tests was tried out whereby the recording and processing of individual load–extension diagrams could be dispensed with. A suitable electrical differentiator, attached to the final output of the Instron amplifier, can directly record the slope of the linear portion of the load–extension curve. If we write the equation for this portion of the curve as

$$f = ke$$

we have

$$df/dt = k\,de/dt \qquad (5)$$

whence

$$k = (1/\rho)\,df/dt \qquad (6)$$

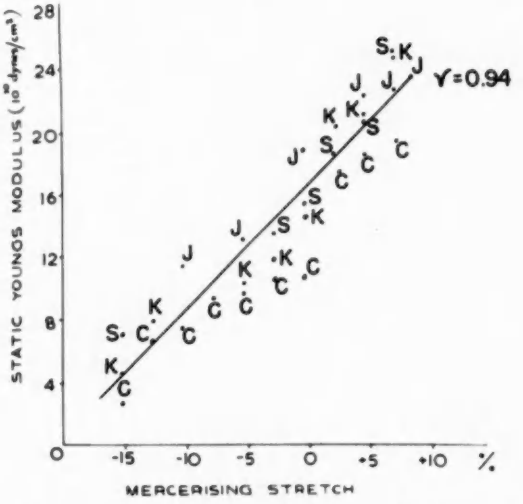

Fig. 5. Static Young's modulus of mercerized cottons versus mercerizing stretch.

where ρ is the constant-time rate of extension. A simple (RC) differentiator circuit was adopted. It is shown in Figure 4a. The Instron amplifier output is connected through a condenser C to the high-gain input terminal of a Brush DC Amplifier (shown as A in the diagram), which has an input impedance R (shown in dotted lines) of 1 megohm. The double-ended output is measured with an ordinary voltmeter. Switch S is opened to avoid kick-back of the meter during reverse differentiation. Capacitor C has a value of 0.25 μf, giving a satisfactory time constant as well as adequate input into the Brush amplifier. The condenser C^1 (0.05 μf) was used to smooth out ripples in the Instron amplifier output. As the fiber was stretched, the reading of meter V would rise and remain steady before falling. The steady reading was noted in each case. The differentiator readings could be calibrated by direct comparison with the slopes obtained from load–extension curves. Such a calibration is illustrated in Figure 4b.

The differentiator described above was adequate for the purpose, but suffered from the inherent defect of requiring a high time constant for sensitivity and a low constant for fidelity. With a faster rate of loading and a more limited gain in the output amplifier, a feed-back type of differentiator could be used, with a high-speed recorder for output.

The measured Young's moduli for the various mercerized samples are plotted in Figure 5 against the stretch used in mercerization. As before, different cotton names are identified by their initials. One common line appears to fit all the data; this line has been drawn by inspection. The over-all correlation coefficient between mercerizing stretch and Young's modulus is 0.94.

Stress–Strain Curve

Typical single fiber stress–strain curves were obtained as follows. Load–extension diagrams were plotted on the Instron tensile tester for 50 fibers belonging to selected orientation groups. Out of these, one diagram was chosen for which the fiber breaking strength and elongation came nearest to the average values of these properties for the 50 fibers studied. The forces corresponding to various values of percent extension were measured off from this diagram of a "typical fiber" and divided by the *average* tex value of the fibers mercerized with that particular stretch. These values of "nominal stress" in grams per tex were converted to dynes per square centimeter (using an assumed constant specific gravity of 1.52 for cellulose). The stress–strain curves of three typical single fibers, corresponding to three mercerizing stretches, are shown in Figure 6. These fibers were from the same cotton (Karnak), but it is believed on the basis of some preliminary data as well as by analogy with Young's modulus and rupture strength [5] that serious intercotton differences may be minimized by mercerization.

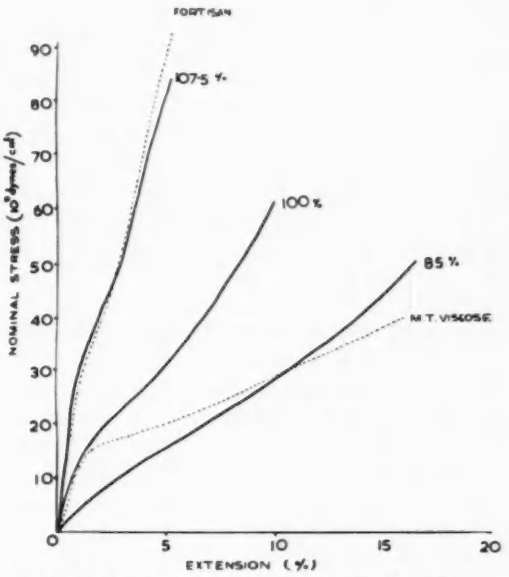

Fig. 6. Stress–strain curves of single fibers from mercerized cotton, Fortisan, and M.T. viscose.

Observations on Cyclic Extension

A complete specification of creep behavior requires very detailed investigation. For cotton, there is the complicating factor of interfiber variability, which necessitates the collection of data from a hundred or so single fibers. Rather than provide such exhaustive data, it was thought worth while to limit the present study to an observation of how certain components of creep were affected by orientation. The experimental technique adopted was to cycle single fibers at a constant rate of extension between fixed load points, according to a method suggested by Hamburger [1]. The Instron tensile tester, equipped with a "load cycling" device, was ideal for this purpose. Energies of loading and unloading were also recorded with the Instron Integrator. Only 15 fibers were selected from each orientation group. The

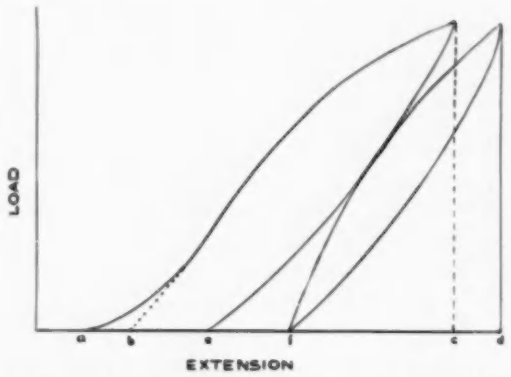

Fig. 7. Cyclic load–extension diagram showing quantities measured. ab = Slack and crimp of fiber (to calculate true initial test length), be = initial set, bc = initial extension, bd = total extension, bf = total set, and fd = extension for conditioned cycles.

fixed load points were 0 g. and 2.5 g. The quantities which were evaluated from the load–extension diagrams are shown in Figure 7.

In addition, energies of loading and unloading during the first cycle and the conditioned cycles were measured on the Instron integrator. The data pertaining to the 15 fibers in each orientation group were unexpectedly uniform. They were therefore averaged out.

By use of the above technique, the creep properties of fibers mercerized under three stretches (slack, 100%, and 107.5%) were studied. The results are shown in Figures 8a and b. The significance of these results will be taken up in the discussion which follows.

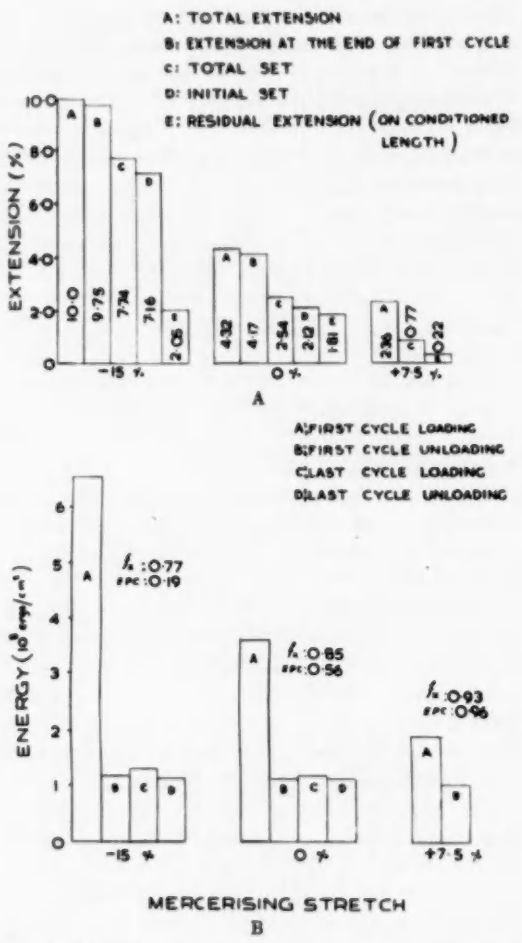

Fig. 8. Creep properties of single fibers from cotton mercerized at different stretches: (a) extension (b) energy.

Discussion

The purpose of the present studies is to highlight the effect of orientation *per se* on mechanical properties. As mentioned earlier, fiber mercerization at controlled stretch provides fibers with the cellulose II lattice, substantially constant crystallinity (of about 50%), and a range of crystallite orientation factors from 0.70 to 0.95 (i.e., high medium to very high orientation). Changes in mechanical properties can be attributed almost exclusively to changes in orientation. There is an obvious flaw in correlating mechanical properties like static Young's modulus with crystallite orientation factor, rather than over-all longitudinal orientation. However, it is assumed, by analogy to earlier reported work on viscose [2], that trends in over-all longitudinal order are duplicated by trends in x-ray orientation factor. Having granted such a dependence, it only remains to examine the load–extension and creep data as functions of f_x. Figure 9 shows the pooled data on static elastic moduli for all cottons, plotted against the corresponding values of f_x. A strong dependence (sensibly linear) is obvious. There is some extra scatter in the lower left-hand part of the plot, but it will be seen shortly that the moduli determinations are least precise in this region. The over-all correlation coefficient is 0.96. It is known that, in raw cotton, the relation between Young's modulus and orientation is much weaker. Correlation coefficients of -0.82 with 40% x-ray angle [7] and $+0.92$ with optical orientation factor [4] have been reported. It appears, therefore, that a strong swelling and

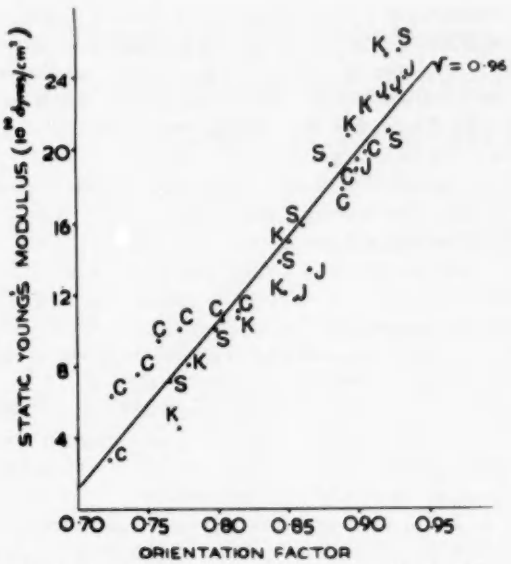

Fig. 9. Static Young's modulus of mercerized cotton versus x-ray orientation factor.

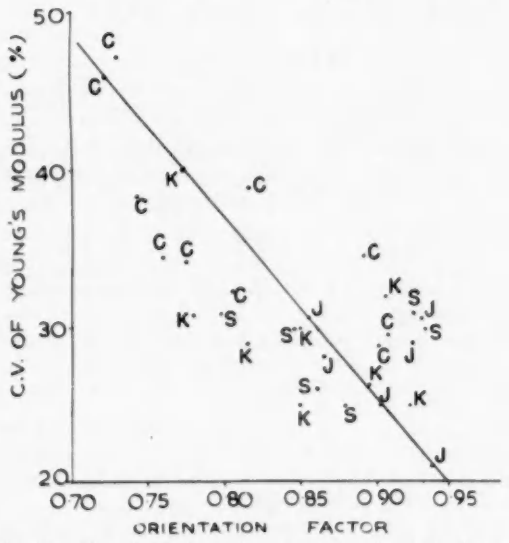

Fig. 10. CV of elastic modulus versus orientation factor.

stretching treatment like mercerization serves to minimize intercotton differences in mechanical properties. This conclusion would be more forceful if based on a large number of varieties of raw cotton, as against only four in the present case. But even in these four varieties, it can be seen that the relation between f_x and Young's modulus before mercerizing is rather poor (Table I).

The reason for the somewhat higher scatter of data in the lower part of the regression line of Figure 9 becomes clear when the data on coefficient of variation of the moduli of individual fiber are examined. Figure 10 shows the CV of slope of the initial parts of the single fiber load–extension curves. These CV's have been plotted against the average orientation factor. The trend towards fall of CV with higher values of f_x is unmistakable. This is the reason for higher scatter of points in the lower part of Figure 9. It should be remembered that Figure 9 is based on a kind of synthetic elastic modulus, namely, $\overline{(\text{force}/\text{area})}$, rather than $(\overline{\text{force}/\text{area}})$. Nevertheless, even if this second and true Young's modulus were to be obtained by vibroscopy, it is clear that while there may be some over-all drop in CV (on account of having accounted for differences between individual fiber cross sections), the same trend would persist. In other words, it seems reasonable to assume that mercerizing stretch reduces interfiber differences in mechanical properties (probably by reducing interfiber differences in orientation).

The change in Young's modulus secured over a span of orientation from 0.70 to 0.95 is more than tenfold. At the lowest orientation, mercerized cotton has a static Young's modulus of the order of 2×10^{10} dynes/cm.^{2}, comparable to a low tenacity viscose. At the highest orientation, this rises to above 20×10^{10} dynes/cm.^{2}, comparable to ramie or Fortisan, which are fibers with similar orientations, too. In fact, the entire stress–strain curve of the fiber with highest orientation factor closely resembles that of ramie or Fortisan (see Figure 6). At the lower orientations, it has not been possible to find other cellulosic fibers with comparable orientation as well as stress–strain behavior. Nevertheless, the curve for a M.T. viscose is given for comparison in Figure 6 (see also [10]).

Turning finally to the data on cyclic load–extension curves, it will be seen from Figure 8a that, in addition to becoming stiffer, the fiber starts losing secondary creep with increasing orientation. Secondary creep has practically vanished at the highest orientation factor. Moreover, the approach to mechanical conditioning by the end of the first cycle becomes better with higher orientation. These trends are illustrated more graphically in Figure 8b, which shows the energies absorbed and recovered for the first as well as for the conditioned cycle. It will be

seen that, with increasing orientation, there is a perceptible trend towards less hysteresis in the conditioned cycles. But, on the whole, orientation has no marked effect on the absolute energies absorbed and recovered from the first *unloading* cycle onwards. There is a very sizable drop in the energy of loading in the first cycle, caused largely by progressive disappearance of secondary creep with increasing orientation.

By combining the data on energies absorbed and recovered with those on extensibility and creep into a single number, as proposed by Hamburger [1], the elastic performance coefficients of the fibers have been computed. These e.p.c. values are entered against orientation factor in Figure 8b. They show a steep rise from 0.19 to 0.96 over a relatively low span of orientation (0.77–0.93).

To round off this discussion, it is clear that the effect of free swelling in caustic soda (with its attendant contraction) is to leave the fiber with its internal cohesive forces greatly loosened and to build up a number of "free dashpots" or irreversible flow mechanisms. Increasing stretch (and thereby molecular orientation) of the swollen cotton progressively removes these dashpots and stiffens "spring" mechanisms in general. This structure gets partially "frozen in" and probably reinforced when the fibers are washed and dried. The subsequent data on mechanical behavior are qualitatively in line with what one should expect. In addition, quantitative data of this kind can be used as tests of any proposed theory of the mechanism of re-orientation and its influence on rheological behavior. Studies of stress relaxation as well as of dynamic elastic properties are now being undertaken to provide supplementary data.

Conclusions

1. Alkali-swollen cotton shows far less resistance to stretching (even near rupture point) than raw cotton.

2. In mercerized cotton, the orientations of the equatorial planes are highly correlated, so that measurements on a single plane can suffice to determine fairly well the crystallite orientation factor.

3. The differentiation of load–extension curves (by electrical or other means) is a promising means of simplifying the determination of average Young's modulus of a large number of fibers.

4. Irrespective of the cotton used, the correlation between the average single fiber static Young's modulus and the average x-ray orientation factor of mercerized cotton is as high as 0.96. The elastic modulus increases more than tenfold over a range of x-ray orientation factor from 0.70 to 0.95. The CV of elastic modulus of single fibers tends to decrease with increasing average orientation.

5. Stress–strain curves of mercerized cotton fibers are broadly similar in trend to those obtained with other cellulosic fibers of comparable orientation (such as viscoses of different tenacity).

6. Cyclic load–extension curves of mercerized fibers show progressive removal of permanent set with increasing orientation factor. Increasing stretch in mercerization appears to remove "free dashpots" and to stiffen "spring" mechanisms in the fiber.

Literature Cited

1. Hamburger, W. J., TEXTILE RESEARCH JOURNAL **18**, 102 (1948).
2. Hermans, P. H., "Physics and Chemistry of Cellulose Fibres," New York, Elsevier, 255–260 (1949).
3. Horio, M. and Onogi, S., *J. Appl. Phys.* **22**, 977 (1951).
4. Meredith, R., *J. Textile Inst.* **37**, T205 (1946).
5. Radhakrishnan, T., Iyer, B. V., Viswanathan, G. S., and Wakeham, H., TEXTILE RESEARCH JOURNAL **29**, 322 (1959).
6. Rao, C. R., "Advanced Statistical Methods in Biometric Research," New York, Wiley, 154 (1952).
7. Rebenfeld, L. and Virgin, H. P., TEXTILE RESEARCH JOURNAL **27**, 286 (1957).
8. Rose, L. and Griffiths, D., *J. Textile Inst.* **39**, 265 (1948).
9. Wakeham, H., "Cellulose," New York, Interscience, Part III, 1253 (1955).
10. Work, R. W., TEXTILE RESEARCH JOURNAL **29**, 381 (1949).

Manuscript received April 21, 1960.

A Measure of the Variation in Blend Proportions Along Blended Yarns and its Relation to the Number of Doublings Used in Processing

P. G. Walker[1]

Shirley Institute, Manchester, England

Abstract

Measurements of short-term variations in blend proportions along the length of a yarn are compared with the variations predicted theoretically. For few doublings the observed variation is found to be greater than the theoretical variation. The results are used to express, as an equivalent number of doublings, the action of the card on this variation in blend proportion.

Introduction

Recent papers by Coplan and Klein [1, 2] give a measure of the degree of fiber mixing in blended yarns. This measure, known as the Index of Blend Irregularity (IBI), was shown by Walker [10] to be related to the χ^2 test of statistical theory and is put to use in the present paper in an attempt to relate short-term variations in blend proportions to the number of doublings used in processing.

De Barr and Walker [6] have discussed elsewhere the effect of departure from ideal blending, on such cloth properties as color and strength, in terms of the two main types of problem associated with blending. One of these is the effect of fiber properties and processing conditions on the arrangement of fibers within the yarn, and in this connection De Barr and Walker [5] have derived a relation between the intimacy of mixing of blended fibers when in a flat ribbon-like arrangement and the number of doublings.[2]

Associated with this problem is that of the relation between processing conditions and variations in blend proportions. In particular it is of interest to know how the number of doublings used in processing is related to short-term variations in blend proportions; in the present paper an attempt is made to throw light on this problem.

The variation in blend proportions is expressed in terms of a modified form of Coplan and Klein's Index of Blend Irregularity and an attempt is made to relate it theoretically to the number of doublings. The observed variation in blend proportions is then compared with this theoretical relation and also with another relation proposed by Cox [4]. In addition an attempt is made to interpret the action of the card on this type of blend variation in terms of an equivalent number of doublings.

A Measure of Variation in Blend Proportions

Yarns were prepared, with different numbers of doublings, from spun-dyed black Fibro and bright (i.e. white) Fibro mixed in different proportions. Observations have been made of the number of black and white fibers at many places in the yarns. It is desirable to reduce the many observations for each different yarn to a mathematically simple form. Three methods [2, 4, 8] of dealing with results of this kind have been proposed in the literature. The tests proposed by Hampson and Onions [8] for application to the variation in blend proportions are applicable only to single sections and are therefore less valuable in the present work than other methods.

Cox [4] considers a yarn cross section containing groups of white and colored fibers corresponding to the original white and colored slivers from which the yarn was formed. The number, Ω, of groups is equal to the total number of doublings as defined above. He gives (p. T119) the formula

$$\text{var}\ (\log_e R) = \frac{1}{\bar{f}\bar{p}(1-\bar{p})} + \frac{A_w}{\Omega_w} + \frac{A_c}{\Omega_c}$$

[1] Present address: Turner Brothers Asbestos Co. Ltd., Rochdale, England.

[2] In this paper the term "number of doublings" has its usual meaning of the total number of individual assemblies going to make up the yarn, sliver, or other product under consideration.

where $R = f_w/f_c$; f_w, f_c are functions of x, giving respectively the numbers of white and colored fibers in the yarn cross section at a distance x from some fixed point in the yarn; $\bar{f}$ = mean number of fibers per section in the yarn; p = mean proportion of white fibers; A_w, $A_c = V_w^2 \times 10^{-4}$, $V_c^2 \times 10^{-4}$; V_w, V_c are the coefficients of variation of the numbers of fibers in the white and colored slivers; and Ω_w, Ω_c are the numbers of doublings of the white and colored fibers respectively.

If we assume the mean number of fibers in and the irregularity of each of the original slivers to be the same, then

$$A_w = A_c = V^2 \times 10^{-4}$$
$$\Omega_w = p\Omega$$
$$\Omega_c = q\Omega$$

The mean proportion of colored fibers, q, is $(1 - p)$. Then Cox's formula, after multiplication by $\bar{f}pq$, becomes

$$\bar{f}pq \text{ var } (\log_e R) \doteq 1 + \frac{V^2\bar{f}}{\Omega} \times 10^{-4} \qquad (1)$$

The expression is used in this form later in the paper.

Coplan and Klein [2] use their Index of Blend Irregularity to reduce a large number of observations to a single figure and claim that the Index is a "measure of the extent to which the blend deviates from expected randomness." The Index has been shown [10] to be identical with $\sqrt{\frac{\chi^2}{n}}$ where

$$\chi^2 = \sum_{\text{sections}} \left\{ \frac{(f_w - pf)^2}{pf} + \frac{(f_c - qf)^2}{qf} \right\}$$
$$= \sum_{\text{sections}} \frac{(f_w - pf)^2}{pqf}$$

The square of this index, or more precisely $\frac{\chi^2}{n-1}$, is an approximate measure of the ratio of the observed variance of the numbers of black (or white) fibers to the expected random variance.

It is shown in the Appendix that

$$\frac{\chi^2}{n-1} \doteq 1 + \frac{V^2\bar{f}}{\Omega} \cdot 10^{-4} \qquad (2)$$

This relation is only approximate (see Appendix) but is more convenient for our purpose than the modified form—Equation 1—of Cox's equation. (It may be noted in passing that Equations 1 and 2 together imply that $\frac{\chi^2}{n-1} \doteq \bar{f}pq \text{ var } (\log_e R)$.)

Results and Discussion

Spun-dyed black Fibro ($1\frac{1}{2}$ den., $1\frac{7}{16}$ in.) and bright Fibro were carded separately on a revolving flat card of recent manufacture. The resulting black slivers and white slivers were combined at the first drawframe in different proportions and were given different numbers of doublings before being spun into yarn of 30's cotton count (approximately 20 tex). One half-lea of yarn from each of four spindles was wrapped on a reel. Each half-lea was cut, giving 40 ends of yarn each 54 in. apart; every cut end was teased out into a "fan" and the numbers of black and white fibers in each fan were counted with the aid of a microscope. Thus there were 160 observations of the number of black and white fibers at cross sections along the length of each yarn. As explained earlier, the value of $\frac{\chi^2}{n-1}$ determined for each set of 160 observations provides a useful estimate of the variation in blend proportion. Values of $\frac{\chi^2}{n-1}$ so determined are plotted against $\log_{10} \frac{V^2\bar{f}}{\Omega}$ in Figure 1. For this purpose it is assumed that $V = 10\%$. Although a greater value of V gives better agreement with the experimental results, experience shows that V is very unlikely to be greater than 10%. Also shown on this figure is the relation given by Equation 2; i.e., the curve

$$y = 1 + 10^{-(4+x)}$$

where

$$y = \chi^2/n - 1$$
$$x = \log_{10} \frac{V^2\bar{f}}{\Omega}$$

As expected, for a large number of doublings $\frac{\chi^2}{n-1}$ tends to unity. In other words, the observed variance of the numbers of black or white fibers tends to the value predicted for a random arrangement as the number of doublings is increased. For a small number of doublings the variance of the number of black and white fibers is much larger than is the case when only chance determines the variation. It is interesting that the observed values lie well above the theoretical curve. This is discussed elsewhere [11].

The numbers of black and white fibers observed can be used to test Cox's theory. The value of $\bar{f}pq$ var ($\log_e R$) is calculated for each set of 160 observations and plotted in Figure 2 against $\log_{10} \frac{V^2\bar{f}}{\Omega}$ together with the curve derived from Equation 1. These points are more widely scattered than values of $\frac{\chi^2}{n-1}$; possibly this is because the standard error of points in Figure 2 can be as much as three times that of points in Figure 1. This is seen from the following values: the standard error of $\bar{f}pq$ var ($\log_e R$), when $\log_e R$ is normally distributed, is $\bar{f}pq$ var ($\log_e R$) $\sqrt{\frac{2}{n}}$, the highest and lowest values of which from these observations were approximately 0.34 and 0.11, and the standard error of $\frac{\chi^2}{n-1}$ is $\sqrt{\frac{2}{n-1}}$, which for $n = 160$ is 0.11.

Another interesting feature of the results is that the values of $\bar{f}pq$ var ($\log_e R$), like those of $\frac{\chi^2}{n-1}$, lie much above the predicted curve. This is in agreement with the findings of Ingham [9], and the explanation given [11] is that the contribution of sliver irregularity to yarn irregularity is underestimated.

The Action of the Card on the Variation in Blend Proportions

Laps of spun-dyed black Fibro and bright Fibro were fed to the card in each of the four ways shown diagrammatically in Figure 3. (a) represents full-width black and white Fibro laps superimposed. (b) represents half-width black and white Fibro laps side-by-side. (c) and (d) represent quarter-width black and white Fibro laps side-by-side.

These laps were carded and some of the sliver from each was spun direct into yarn with no further doublings. In addition, some of the sliver was given one drawframe passage, feeding six ends, before being spun into yarn. In this way, these yarns had six doublings after carding. (All the yarns were spun from single roving.)

The yarns were examined by the method described above and the values of $\frac{\chi^2}{n-1}$ were evaluated. Now from the curve drawn through the points of Figure 1 it is possible to determine the corresponding values of $\frac{V^2\bar{f}}{\Omega} \times 10^{-4}$, and by substitution of appropriate values of V and $\bar{f}$ a value can be obtained for the value of Ω. This is the total number of doublings, which is equal to the number of doublings in the feed to the card multiplied by the equivalent number of doublings within the card and further multiplied by the number of subsequent doublings. Thus a value can be obtained for the equivalent number of doublings within the

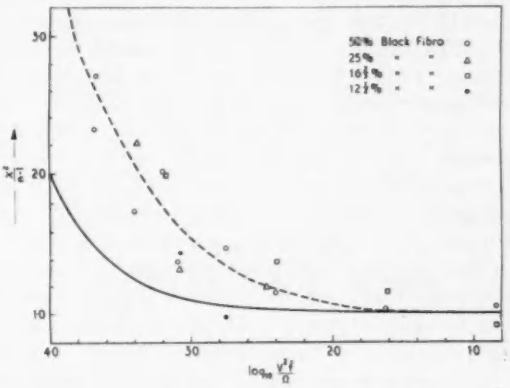

Fig. 1. Variation in blend proportions, measured by $\frac{\chi^2}{n-1}$ as a function of $\log_{10} \frac{V^2\bar{f}}{\Omega}$. The full line shows the relation given by Equation 2.

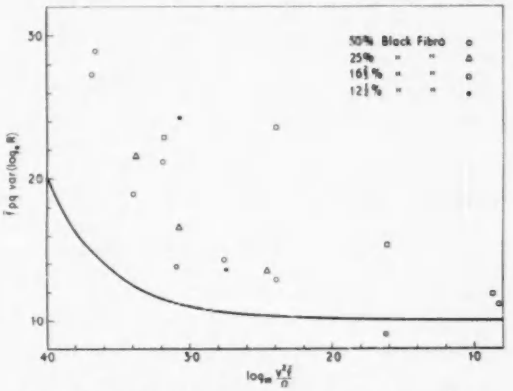

Fig. 2. Variation of blend proportions measured by $\bar{f}pq$ vary ($\log_e R$) as a function of $\log_{10} \frac{V^2\bar{f}}{\Omega}$. The full line shows the relation given by Equation 1.

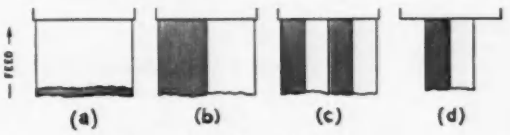

Fig. 3. Plan view of blended laps.

card from the nose of the feed plate to the doffer comb.

The mean number of fibers per section, $\bar{f}$, is known from the observations but it is possible to estimate the value of V only approximately. General experience of scutcher laps suggests that a reasonable value for a full-width lap is 20%, and the values for half-width and quarter-width laps will depend upon the variation of thickness across the width of the lap. If there is no such variation, V will be 20% for half- and quarter-width laps also. If there is much variation, the values of V for half- and quarter-width laps will be up to $\sqrt{2}$ times 20% and up to 2 times 20% respectively. In practice, the value of V for a half-width lap is probably between 20% and $\sqrt{2}$ times 20%, and the value for a quarter-width lap is probably between 20% and 2 times 20%. With these assumptions it is possible to estimate the equivalent number of doublings within the card, and this is done in Tables I and II. The values of Ω given in the tables are based upon assumed values of V, as described above.

For a completely random arrangement the value of $\frac{\chi^2}{n-1}$ is unity. If the actual fiber arrangement is more ordered than a random arrangement the observed variance of the number of black (or white) fibers will be less than the random variance and the value of $\frac{\chi^2}{n-1}$ will be less than unity. In practice, such values are unlikely but may occasionally be obtained on some sections of yarn where, by chance, the fiber arrangement is more ordered than random. In Tables I and II those values of $\frac{\chi^2}{n-1}$ less than unity have, however, been taken as unity for the purpose of deducing the number of equivalent doublings within the card.

For conditions (b), (c), and (d) the equivalent number of doublings within the card is between 1 and 10. No significance can be attributed to the apparently greater numbers of equivalent doublings within the card when doubling has also been carried out after carding. The number is much higher with condition (a) and, because of the nature of the method of feeding the laps to the card, it is probable that a much higher value than 2 should be assumed for the number of doublings in the feed.

An explanation of this can be given as follows. In condition (a), when the fringe of fibers presented to the taker-in is examined, it is seen to consist of alternate groups of black and white fibers, the groups of each color varying widely in size. An approximation to this type of feed can be made by assuming that the black and white Fibro laps are each divided parallel to the direction of the feed,

TABLE I. No Doublings After Carding

Doubling technique	$\frac{\chi^2}{n-1}$	$\frac{V^2\bar{f}}{\Omega} \times 10^{-4}$	$\bar{f}$	Total number of equivalent doublings, Ω	Number of doublings in the feed, Ω'	Number of equivalent doublings within the card, Ω/Ω'
(a)	0.85	<0.01	86.8	>350	2	>175
(b)	6.6	1.9	96.7	Between 2 and 4.1	2	Between 1 and 2
(c)	3.4	0.8	93.5	Between 4.7 and 18.7	4	Between 1.2 and 4.7
(d)	5.6	1.5	98.4	Between 2.6 and 10.5	2	Between 1.2 and 5.3

* These values are predicted by extrapolating the curve through the points in Figure 1.

TABLE II. Six Doublings After Carding

Doubling technique	$\frac{\chi^2}{n-1}$	$\frac{V^2\bar{f}}{\Omega} \times 10^{-4}$	$\bar{f}$	Total number of equivalent doublings, Ω	Number of doublings in the feed, Ω'	Number of equivalent doublings within the card, $\Omega/6\Omega'$
(a)	0.92	<0.01	88.5	>350	2	>30
(b)	1.54	0.100	93.5	Between 38 and 95	2	Between 3.1 and 7.9
(c)	1.43	0.0723	92.5	Between 54 and 214	4	Between 2.2 and 9.0
(d)	1.62	0.115	93.0	Between 32 and 130	2	Between 2.7 and 10.8

into m strips, the strips being arranged in order black, white, black, white . . . across the width of the card. In this case the coefficient of variation of thickness along each strip might be between 20% and $\sqrt{m}$ times 20% depending on the variation in thickness across the lap. The number of doublings in the feed would be $2m$ instead of 2. Thus, in condition (a) with no doublings after carding, the equivalent number of doublings within the card would not be smaller than $175/m$. To be consistent with conditions (b), (c), and (d), the value of m required is greater than 30. With a 45-in. lap-width the strips would then be narrower than 1.5 in.; this seems quite reasonable from the appearance of the fringe presented to the taker-in.

These results suggest that the action of the card itself is to reduce the variation in blend proportion of a lap to an extent equivalent to between one and ten doublings. A further interesting conclusion is that, by feeding two superimposed laps to the card, the total equivalent number of doublings in processing is increased far more than is possible at any subsequent stage.

Acknowledgment

The author wishes to acknowledge, with thanks, the help of Mr. B. Griffiths of these laboratories with the statistical theory.

Appendix

The Relation Between $\frac{\chi^2}{n-1}$ *and* Ω

For reasons given elsewhere [10] $\frac{\chi^2}{n-1}$ is a convenient measure of variation in blend proportions. In order to make use of this quantity, however, it is necessary to be able to relate it to the total number of doublings used in processing, and such a relation is derived here. (The symbols have the meaning given in the text of the paper.)

If the deviation of the number of fibers at any point in the yarn, f, from the mean number of fibers, $\bar{f}$, is small compared to $\bar{f}$, then $\frac{f-\bar{f}}{f} = \Delta f/\bar{f}$ is small. The expected value of $(\Delta f)^2$ is var (f). $E(\Delta f)^2$ may not tend to zero, but $\frac{E(\Delta f)^2}{\bar{f}^2}$ is assumed to do so since $\Delta f/\bar{f}$ is small. Then, as $f_w = pf$

$$\text{var } (f_w) = p^2 \text{ var } f + \bar{f}^2 \text{ var } P \qquad \text{A1}$$

where $P = \frac{f_w}{f_{(w+c)}}$ is the actual proportion of white fibers at any cross section of the yarn. Then

$$V^2(P) = \frac{10^4 \text{ var } P}{p^2} = 10^4 \left[\frac{\text{var } f_w}{p^2\bar{f}^2} - \frac{\text{var } f}{\bar{f}^2} \right] \qquad \text{A2}$$

But, as $\frac{\text{var } f}{\bar{f}^2}$ tends to zero

$$V^2(P) \doteq 10^4 \frac{\text{var } f_w}{p^2\bar{f}^2} \qquad \text{A3}$$

Now

$$\begin{aligned} \chi^2 &= \sum \frac{(f_w - pf)^2}{pqf} \\ &= \sum \frac{(f_w - pf)^2}{pq(\bar{f} + \Delta f)} \\ &= \sum \frac{(f_w - pf)^2}{pq\bar{f}} \left(1 - \frac{\Delta f}{\bar{f}} + \frac{(\Delta f)^2}{\bar{f}^2} + 0(\Delta f)^3 \cdots\right) \end{aligned}$$

As $\Delta f/\bar{f}$ is small, terms in Δf and all higher orders may be neglected, so that

$$\begin{aligned} \chi^2 &\doteq \frac{\sum (f_w - pf)^2}{pq\bar{f}} \\ &\doteq \frac{(n-1) \text{ var } f_w}{pq\bar{f}} \end{aligned} \qquad \text{A4}$$

Thus, from A3 and A4

$$V^2(P) \doteq 10^4 \frac{pq\bar{f}}{p^2\bar{f}^2} \frac{\chi^2}{n-1} \qquad \text{A5}$$

In the work of Cox and Ingham [3] and Foster [7], the following relation is implied [see Cox [4] (p. T115)]:

$$V^2(f_{(w+c)}) = \frac{k}{\bar{f}} \cdot 10^4 + \frac{V^2}{\Omega} \qquad \text{A6}$$

and from this it follows [4] that

$$V^2(f_w) = \frac{1 + (k-1)p}{p\bar{f}} \cdot 10^4 + \frac{V^2}{p\Omega} \qquad \text{A7}$$

where k is a constant ($\doteq 1.3$).

The required relation can now be obtained as follows.

From A1, A6, and A7

$$V^2(P) = \frac{q}{p\bar{f}} \cdot 10^4 + \frac{qV^2}{p\Omega} \qquad \text{A8}$$

From A5 and A8

$$\frac{\chi^2}{n-1} \doteq 1 + \frac{V^2\bar{f}}{\Omega} \cdot 10^{-4} \qquad 2$$

Literature Cited

1. Coplan, M. J. and Klein, W. G., TEXTILE RESEARCH JOURNAL **29**, 632 (1959).
2. Coplan, M. J. and Klein, W. G., TEXTILE RESEARCH JOURNAL **25**, 743 (1955).
3. Cox, D. R. and Ingham, J., *J. Textile Inst.* **41**, P376 (1950).
4. Cox, D. R., *J. Textile Inst.* **45**, T113 (1954).
5. De Barr, A. E. and Walker, P. G., *Shirley Inst. Mem.*, **30**, 63 (1957); *J. Textile Inst.* **48**, T405 (1957).
6. De Barr, A. E. and Walker, P. G., *J. Textile Inst.* **49**, P353 (1958).
7. Foster, G. A. R., *J. Textile Inst.* **41**, P376 (1950).
8. Hampson, A. G. and Onions, W. J., *J. Textile Inst.* **46**, T377 (1955).
9. Ingham, J., *J. Textile Inst.* **49**, P353 (1958).
10. Walker, P. G., *J. Textile Inst.* **48**, T133 (1957).
11. Walker, P. G., *J. Textile Inst.* **49**, P353 (1958).

Manuscript received March 28, 1960.

The Stabilizer in Hydrogen Peroxide Bleaching

David M. Cates and Winnifred H. Cranor

The Textile Research Center, School of Textiles, North Carolina State College, Raleigh, North Carolina

Abstract

Stabilized hydrogen peroxide decomposed at a slower rate than unstabilized peroxide and, for a given amount of decomposition in the presence of cellulose fabric, was more effective in raising reflectance and causing chemical damage. The ratio of reflectance to reduction of viscosity, however, was the same, suggesting that damage to cellulose is unavoidable and related to the amount of colored impurities destroyed. This ratio is dependent on the history of the fiber.

THE STABILIZER is an important component of the alkaline solutions of hydrogen peroxide that are used to bleach cellulose. It is possible that the stabilizer is intimately involved in the mechanisms through which bleaching is accomplished. Because present knowledge does not extend to the basic mechanisms, our understanding of the effect of the stabilizer is based primarily upon the differences observed between experiments carried out in the presence and absence of stabilizer. The chief effect of the stabilizer, which is invariably observed, is to reduce the rate of peroxide decomposition, allowing a degree of control that would otherwise be difficult to achieve. The effect of the stabilizer on such properties of the bleached fabric as reflectance and fluidity is more difficult to ascertain, because the results of comparative experiments may be attributed to the intrinsic nature of the stabilizer, to the altered rate of decomposition, or to other possible variations between experiments.

The stabilizer used in the present work was the system of $CaCl_2$ and Na_2HPO_4 [1, 2]. Previous work, carried out in the absence of fabric [1], showed that the stability of the peroxide in solution is a function of the composition of the bath.

In Figures 1 and 2 are shown recent results that were obtained on cotton huck toweling when the concentration of the calcium and phosphate components of the bath was varied. While the effect of composition of the bath on the stability of the peroxide is pronounced, the effect on reflectance and viscosity of the bath is less obvious. The effect of pH of the bleaching solution on reflectance and viscosity is apparently very important. There is a suggestion that this is so in Figure 2, where the drop in pH is caused by the removal of hydroxyl ions from solution by calcium. Variation in concentration of NaOH, however, produces a wide range of pH values (Figure 3), and the effect on reflectance and viscosity is immediately apparent.

In this paper the results are given for a series of experiments in which the kinetics of hydrogen peroxide decomposition was studied in bleaching solutions maintained at pH 10.5. Stabilized and unstabilized baths were used, with and without cellulose fabric. The rate of decomposition was varied by varying

the temperature. Fabric from the bleaching experiments was examined for reflectance (under a blue filter) and chemical damage. Thus it was possible to compare kinetic results obtained with and without stabilization, to determine the effect of rate of peroxide decomposition on the properties of the bleached fabric both for stabilized and unstabilized systems, and to compare the properties of fabric bleached with and without stabilization In a later series of experiments a study was made of the effect of de-ashing the fabric on the kinetics of peroxide decomposition and on the properties of the bleached fabric.

The decomposition of hydrogen peroxide is complex, involving homogeneous reaction in solution and heterogeneous reaction at surfaces, e.g., the surfaces of the vessel, cellulose fabric, and any colloidal material or precipitate that may be present. It must be recognized, therefore, that the kinetic results described below apply specifically to the particular system that was used and that their extrapolation to other systems must be handled with caution.

Materials and Methods

The fabric used in the rate experiments was a desized cotton huck toweling that had been scoured on a beck for 1½ hr. at the boil, using (on the weight of the fabric) 2% sodium carbonate, 2% soap, and 0.5% phosphate sequestering agent. The scoured fabric contained many seed husks. A portion of this fabric was used directly and is identified below as scoured fabric.

Part of the fabric was given additional purification treatment. The scoured fabric was bleached for 90 min. at 90°–100° C. in a kettle of tap water containing (mmol./ml.): Na_2HPO_4, 3×10^{-3}; $CaCl_2$, 4×10^{-3}; NaOH, 20×10^{-3}; H_2O_2, 150×10^{-3}. The bleached fabric was rinsed first with water, then with 0.1 *N* HCl to remove any phosphate precipitate, and neutralized with ammonium hydroxide. Finally, the fabric was rinsed with several changes of distilled water, dried, and stored for future use. Because an insufficient quantity of fabric was purified by this treatment the first time, additional fabric was purified later in the course of the experiments, following approximately the same procedure. The treated fabrics are identified below as purified fabrics I and II.

Reagent grade chemicals ($Na_2HPO_4 \cdot 12H_2O$, $CaCl_2$, NaOH, and H_2O_2) were used without additional purification.

The stabilizer used throughout was the system of $CaCl_2$ and Na_2HPO_4 [1, 2]. The compositions of the stabilized and unstabilized solutions, given in

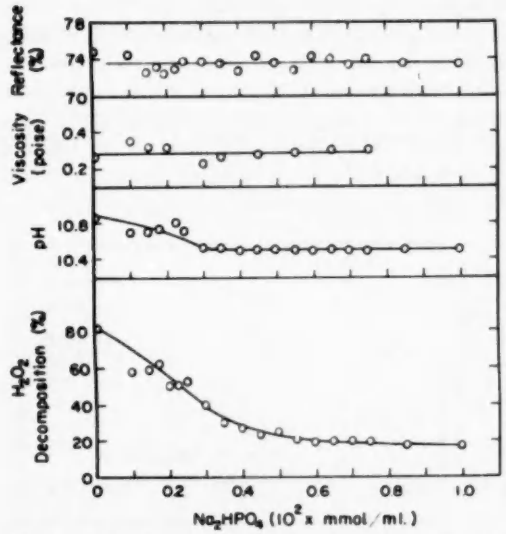

Fig. 1. Effect of variation of Na_2HPO_4 concentration on bleaching results at 90° C. Reaction time 30 min.; concentrations in solution (mmol./ml.): Na_2HPO_4, varied; $CaCl_2$, 0.00386; NaOH, 0.0202; H_2O_2, 0.148.

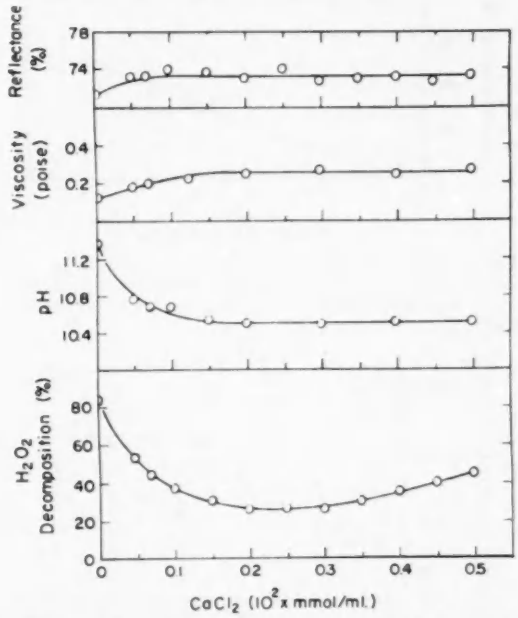

Fig. 2. Effect of variation of $CaCl_2$ concentration on bleaching results at 90° C. Reaction time 30 min.; concentrations in solution (mmol./ml.): $CaCl_2$, varied; Na_2HPO_4, 0.00325; NaOH, 0.0202, H_2O_2, 0.148.

Table I, were chosen to give a pH of 10.5 because satisfactory bleaching of normal fabrics can usually be obtained in the pH range of 10.0–11.0.

The reaction solution was made up with the chemicals, with the exception of peroxide, and brought to the desired temperature on a bath controlled to ±0.2° C. The peroxide was then added and the timing of the experiment begun. The volume of the solution was always 100 ml. After the desired interval of time the solution was removed from the bath. An aliquot was quickly cooled, and the concentration of H_2O_2 was determined by titration. The pH of the reaction solution, cooled to room temperature, was measured. The longest reaction time was 90 min.

TABLE I. Composition of Reaction Solutions

	Stabilized (mmol./ml.) × 10^2	Unstabilized mmol./ml.) × 10^2
Na_2HPO_4	3.25	0
$CaCl_2$	3.86	0
NaOH	20.2	10.1
H_2O_2	147.8	147.8

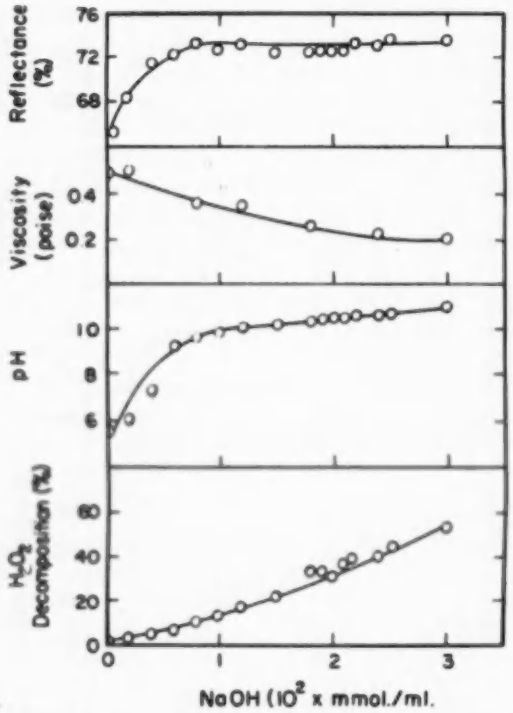

Fig. 3. Effect of variation of NaOH concentration on bleaching results at 90° C. Reaction time 30 min.; concentrations in solution (mmol./ml.): NaOH, varied; Na_2HPO_4, 0.00325; $CaCl_2$, 0.00386; H_2O_2, 0.148.

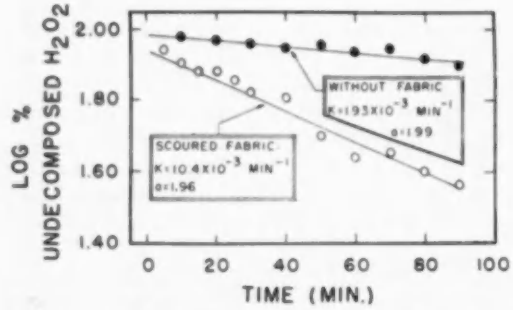

Fig. 4. Decomposition of H_2O_2 at 90° C. as a function of time; stabilizer present.

Two round-bottom flasks were used interchangeably to contain the reaction solutions. A rubber stopper containing a thermometer dipping into the solution was kept loosely in place throughout the reaction to reduce evaporation. After each experiment the flask was washed with 1 *N* HNO_3 before cleaning with distilled water. This procedure was followed to make certain that traces of precipitate, soluble in nitric acid, did not influence subsequent reactions carried out in the same flask.

Approximately 3 g. of fabric was used in each of the bleaching experiments. The fabric, which was kept beneath the surface of the solution throughout reaction, was quickly removed at the end of the experiment, washed in running tap water 30 min., and dried.

The reflectances of the bleached samples were determined on a Hunter reflectometer under a blue filter against MgO as a standard. It is realized there are properties of the bleached fabric other than reflectance that are important. The property of re-

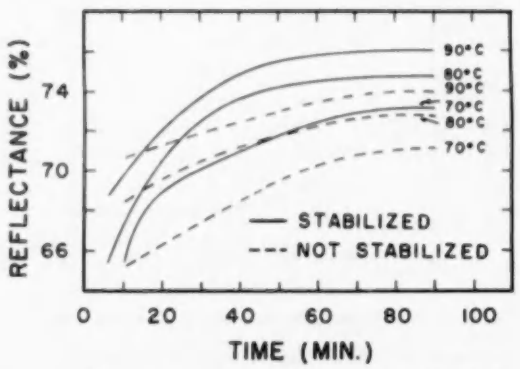

Fig. 5. Reflectance of scoured fabric as a function of time.

flectance, however, is believed to be sufficient to give valid insight into the effect of the particular variables under study.

For viscosity determinations, fabrics were available that had been bleached at a given temperature for varying periods of time; the amount of peroxide decomposed in bleaching the fabrics at a particular temperature was dependent on the bleaching time. For each of the temperatures, therefore, fabric was selected for viscosity measurements to cover a wide range of peroxide decomposition. The viscosity measurements were made on 0.5% solutions in Ostwald-Fenske viscometers at 25.2° C. ± 0.1° C. Cupriethylene diamine (0.5 *M*) was used as the solvent.

Results and Discussion

The pH values of the reaction solutions, determined at room temperatures at the end of each experiment, were usually 10.5 ± 0.1, but in a few instances ranged as low as 10.3 and as high as 10.8.

Kinetics of H_2O_2 Decomposition

The decomposition of H_2O_2 was found to follow first order reaction kinetics: log (% undecomposed H_2O_2) = $(-kt/2.303) + a$, where k is the specific rate constant, t is the time, and a is a constant. A plot of this equation for a typical experiment is shown in Figure 4. Since a is equal to the logarithm of percent of undecomposed H_2O_2 at zero time, its theoretical value is 2. When k is determined at two or more temperatures, the frequency factor, A, and activation energy, E_a, can be obtained from the Arrhenius equation $k = Ae^{-E_a/RT}$.

The kinetic results are summarized in Table II.

The value of the constant a from the rate equation is close to the theoretical value of 2 for the stabilized systems but is appreciably less than 2 for the unstabilized systems (Table II). This is interpreted to mean that in the unstabilized baths a relatively large portion of the peroxide decomposes in "zero" time. Probably much of this decomposed peroxide is unavailable either as bleaching agent or as degrading agent.

By viewing the data in Table II, it is seen, for otherwise the same conditions, that k (scoured fabric) > k (purified fabrics) > k (without fabric). Thus it is evident that the fabric contains materials that contribute to the instability of the peroxide and that a portion of these materials was removed by the purification treatment.

The kinetic results for purified fabrics I and II are appreciably different, presumably because of differences originating in the purification treatments.

Table II also shows, for otherwise the same conditions, that k (unstabilized) > k (stabilized), as expected. By comparison of the data for the scoured fabric, it is seen that the decomposition rate in the stabilized baths is from $\frac{1}{4}$ to $\frac{1}{2}$ as great as that in the unstabilized baths. Although the frequency factor is larger by several orders of magnitude in the stabilized system, stabilization reduces the activation en-

TABLE II. Kinetic Results for Stabilized and Unstabilized Bleaching Systems

		Stabilized				Unstabilized			
	Temp., °C.	a	Specific rate constant, (min.$^{-1}$) $\times 10^3$	Frequency factor	Activation energy, kcal./mol.	a	Specific rate constant, (min.$^{-1}$) $\times 10^3$	Frequency factor	Activation energy, kcal./mol.
Without fabric	70	2.00	0.44			1.90	3.6		
	80	2.00	0.76			—	—		
	90	1.99	1.93	1.0×10^9	19.4	—	—	—	—
With scoured fabric	70	1.98	3.02			1.98	11.4		
	80	1.99	5.79			1.81	16.3		
	90	1.96	10.44	2.1×10^8	16.9	1.84	21.3	3.6×10^8	7.0
With purified fabric I	70	1.96	0.69			1.90	6.0		
	80	1.99	2.30			1.90	11.4		
	90	—	—	1.6×10^{15}	28.7	—	—	1.3×10^{17}	30.4
With purified fabric II	70	1.99	2.01			1.96	7.0		
	80	1.98	1.66			1.88	7.9		
	90	1.98	3.22	8.9×10^9	5.8	1.91	18.5	2.5×10^5	11.9

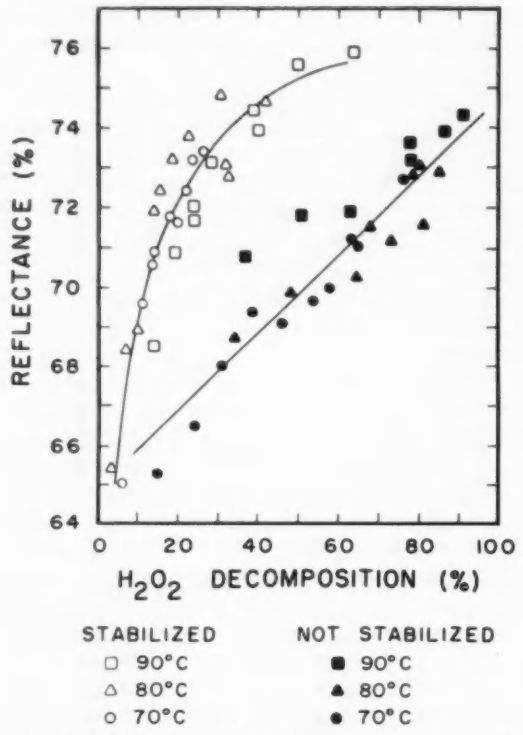

Fig. 6. Reflectance of scoured fabric as a function of amount of decomposition; initial reflectance, 53.0.

ergy sufficiently to bring about a diminution in rate. The values for the frequency factor and activation energy obtained in the case of the two purified fabrics are peculiar and cannot be explained.

Reflectance and Chemical Damage

The reflectance values obtained for the scoured fabric after bleaching are shown in Figure 5 as a function of time for the various temperatures. The variables of time and temperature are obviously important in their effect on reflectance. These variables determine more directly the amount of peroxide that is decomposed, however, and it is this latter quantity that is the more fundamental variable.

This can be seen in Figure 6, where the dependence of reflectance on the relative amount of H_2O_2 decomposed is clearly demonstrated.

Since the relationship in Figure 6 between reflectance and amount decomposed is roughly the same at all three temperatures, within a given system (i.e., stabilized or unstabilized), it appears that the rate of decomposition *per se* has little effect on the degree of reflectance achieved. Data are presented (Figure 8) indicating that rate of decomposition within a given system also has little effect on damage to the fiber.

In the case of the purified fabrics, higher reflectances were obtained than with the scoured fabric (see Figure 7); again, reflectance was dependent on the amount of decomposed peroxide, time and temperature exerting a comparatively small perturbing effect except with respect to the amount of decomposition. The relationship between reflectance

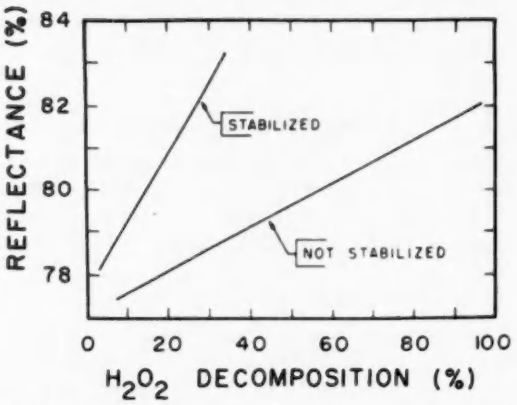

Fig. 7. Reflectance of purified fabrics as a function of amount of decomposition in the temperature range 70°–90° C.; initial reflectance, 76.8.

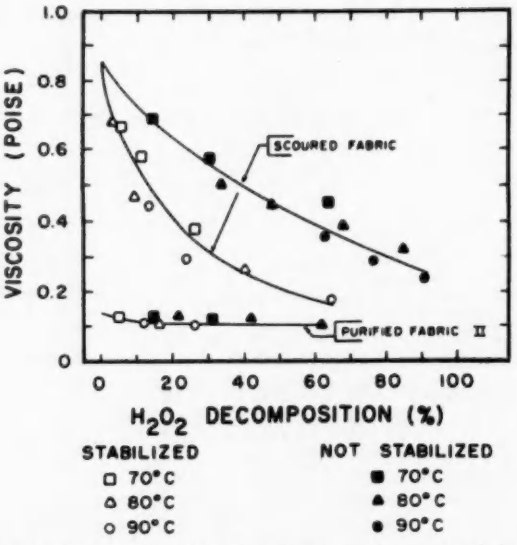

Fig. 8. Viscosity (Cuen) as function of amount of decomposition. Initial viscosity (poise): scoured fabric, 0.85; purified fabric II, 0.14.

and amount of decomposition was essentially the same for purified fabrics I and II and is best described by the least mean square plots of Figure 7, where experimental points were omitted to avoid confusion.

Chemical attack on the scoured fabric, as measured by reduction of viscosity, is shown in Figure 8 also to be a function of the relative amount of peroxide decomposed. The relationship appears to be roughly the same for all three temperatures, indicating that chemical attack is not much affected by the rate of decomposition within a given system (i.e., stabilized or unstabilized). No effort was made, however, to characterize the nature of the oxidized celluloses formed at the various temperatures.

It is clear from Figures 6 and 8 that, for a given amount of decomposition, the "efficiency" of unstabilized peroxide in destroying colored impurities and in damaging the cellulose is much less than that of the stabilized peroxide. Evidently much of the decomposed peroxide from the unstabilized bath is unavailable for either purpose and is evolved to the atmosphere as free oxygen. It is probable that most of the peroxide decomposed in zero time is "wasted" in this way. Thus the frequently-made statement that unstabilized solutions will damage cellulose excessively is not necessarily true.

The reflectance achieved per unit reduction of viscosity was the same, within experimental error, for both stabilized and unstabilized systems (Figure 9). This suggests that the destruction of colored impurities cannot be accomplished by the peroxide without concomitant damage to the neighboring regions of cellulose and perhaps is indicative that the bleaching mechanism is the same in stabilized and unstabilized baths.

The attack on purified fabric II was the same with stabilization as without (Figure 8). Bleaching, however, apparently caused little measurable damage (i.e., measurable in terms of a change in viscosity) beyond that attributable to the purification treatment. Figure 9 shows that reflectance was gained at the expense of a very small additional reduction of viscosity. What this reduction of viscosity means in terms of the degree of polymerization of the cellulose was not established.

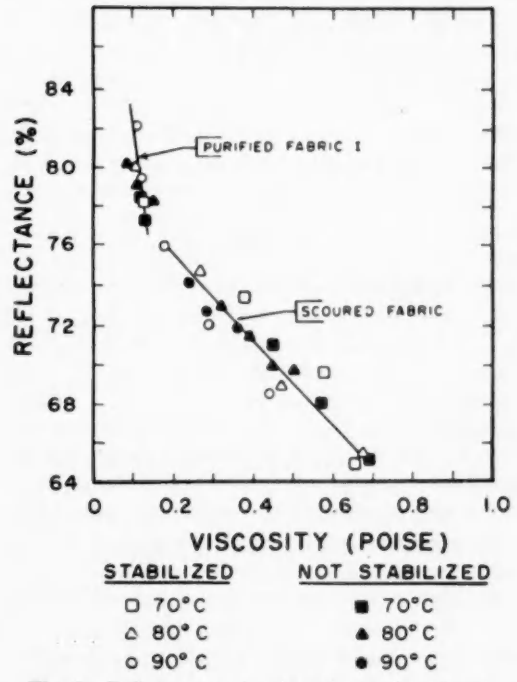

Fig. 9. Reflectance as function of viscosity (Cuen).

De-Ashed Cellulose

Bleaching and chemical damage can take place only when the active agent in peroxide solutions, presumably molecular oxygen [3], comes into rather close contact with the fiber. The data of Figure 9

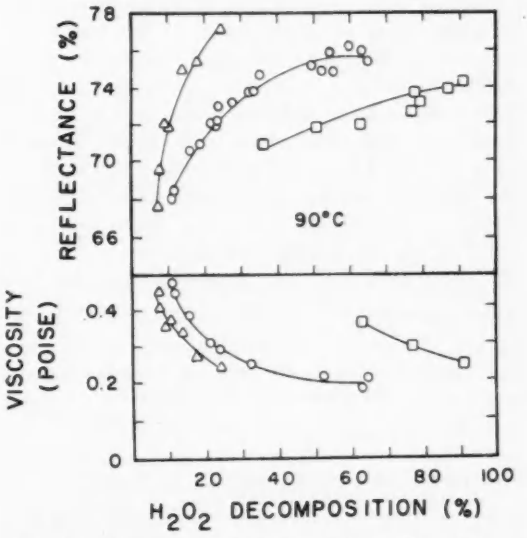

Fig. 10. Properties of the bleached fabrics (de-ashed and untreated) as a function of amount of decomposition. △ de-ashed, stabilized bleach; ○ untreated, stabilized bleach; □ untreated, unstabilized bleach.

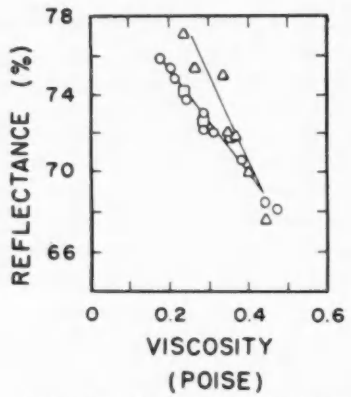

Fig. 11. Reflectance as a function of viscosity (Cuen). △ de-ashed, stabilized bleach; ○ untreated, stabilized bleach; □ untreated, unstabilized bleach.

suggest that bleaching cannot be achieved without accompanying chemical damage. Potential sources for damage are found in sites on the cellulose occupied by catalytically active substances. Cellulose frequently contains metal catalysts or has the possibility of absorbing them from solution. Decomposition at these "active centers" is ideal for building up large concentrations of molecular oxygen in the intimate contact presumed to be necessary before damage can occur.

A series of experiments was carried out to determine what effect the removal of these active centers from the cellulose would have on the kinetics of peroxide decomposition and on the properties of the bleached fabric.

The same scoured fabric that was used in the previous work was de-ashed by tumbling the fabric in 0.1 *N* HCl for 1 hr. The fabric was then neutralized and washed in several changes of distilled water and dried. Following this the fabric was bleached at 90° C. in the way already described.

Table III compares the kinetic results with those previously obtained on the scoured fabric in stabilized and unstabilized solutions. The rate of peroxide decomposition in stabilized solution was in the case of the de-ashed fabric only about one-fourth as large as that in the case of the untreated fabric.

TABLE III. Kinetic Results at 90° C. for Scoured and De-Ashed Scoured Fabric

	a	$k \times 10^3$ (min.$^{-1}$)
Unstabilized solution; scoured fabric with no pretreatment (untreated)	1.84	21.3
Stabilized solution; scoured fabric with no pretreatment (untreated)	1.96	10.4
Stabilized solution; scoured fabric treated 1 hr. in 0.1 *N* HCl prior to bleaching (de-ashed)	1.97	2.42

Figure 10 shows the effect of de-ashing on the properties of the bleached fabric. It is clear that a given amount of peroxide decomposition produces a higher reflectance in the de-ashed fabric than in the untreated fabric, but also causes more damage. Still, if the reflectance achieved per unit of viscosity is considered, the de-ashed fabric gives somewhat better results (Figure 11).

It is possible that the mechanism of bleaching in stabilized and unstabilized solutions is the same, the difference being that in unstabilized solution a smaller proportion of the hydrogen peroxide is "active." The nonactive portion is evolved to the atmosphere; the active portion raises reflectance and causes damage. Ideally the objective in bleaching, of raising reflectance with little or no drop in viscosity, can be accomplished by making the bleaching reaction specific to the colored impurities; in this case a plot of reflectance against viscosity would be a vertical line. It seems, however, that some limit will be reached before this state can exist, because the mechanism of bleaching appears to involve a certain amount of damage as a necessary by-product in obtaining a particular level of reflectance. The data in Figure 11 indicate, however, that the price the fiber pays, in terms of chemical damage, to obtain higher reflectance is dependent on the history of the fiber. Thus, the importance of properly preparing the fiber for bleaching should not be underestimated.

Summary

The kinetics of hydrogen peroxide decomposition was studied in bleaching solutions controlled at pH 10.5. Stabilized and unstabilized baths were used, with and without cellulose fabric. The stabilizing system consisted of Na_2HPO_4 and $CaCl_2$. The rate of decomposition was varied by varying the temperature. Fabric from the bleaching experiments was examined for reflectance and chemical damage.

The rate of peroxide decomposition was substantially reduced when the fabric was purified or when stabilizer was used. In unstabilized baths a relatively large amount of peroxide decomposed in a very short time ("zero" time) and presumably was responsible for comparatively little bleaching or chemical damage to the cellulose.

The reflectance and chemical attack on fabric bleached for various times and temperatures were found to be a function of the amount of H_2O_2 decomposed. Both reflectance and viscosity of the bleached fabric were relatively unaffected by the rate of decomposition in the particular system (i.e., stabilized or unstabilized) under study.

For a given amount of decomposition, the stabilized peroxide was more effective than the unstabilized in raising reflectance, but also caused more damage. There was no difference, however, in reflectance achieved per unit reduction of viscosity.

When scoured fabric was treated to remove traces of metal and then bleached with stabilized peroxide, the rate of decomposition was appreciably reduced. For a given amount of peroxide decomposed, the de-ashed fabric was more effectively bleached than the untreated scoured fabric, but it was also damaged to a greater extent. In terms of reflectance achieved per unit reduction of viscosity, however, better results were obtained with the de-ashed fabric.

Literature Cited

1. Cates, D. M. and Cranor, W. H., TEXTILE RESEARCH JOURNAL **28**, 708 (1958).
2. Easton, B. K. and Feldman, P., *Textile Bull.* **82**, 77 (1956).
3. Scheller, E., *Milliand Textilber.* **25**, 234 (1944).

Manuscript received April 13, 1960.

The Kinetics of Wool Dyeing—Some Effects of Alcohols on Wool Dyeing Rates

J. A. Medley

Physics Department, Wool Industries Research Association, Torridon, Headingley, Leeds, England

M. W. Andrews

C.S.I.R.O. Wool Research Laboratories, Division of Textile Physics, Ryde, N.S.W., Australia

Abstract

The action of alcohols in the "solvent dyeing" of wool is considered and, from an analysis based on the diffusion characteristics of the fiber, the increased dyeing rates obtained are attributed largely to faster movement of the dye *within* the fiber. The reduced resistance to dye diffusion within the fiber is associated with the presence of the alcohol during the diffusion process and also with the removal of greasy material from the interior of the fiber by the alcohol–water phase.

Introduction

Peters and Stevens [13] and Karrholm and Lindberg [5] have shown that the rate of wool dyeing may be greatly increased, particularly at low temperatures, by the addition of small amounts of certain alcohols (e.g., n-butanol, amyl alcohol) to the dyebath. No single theory of the effect is universally accepted and there is still some doubt whether it is essentially a phenomenon associated with the surface of the fiber or its interior [6].

The cleaning action of one alcohol in particular on wool is well known. Ethanol will extract further material from wool which has been previously extracted with petroleum ether or diethyl ether; the extraction is slow [4]; some of the material is believed to come from the interior of the fiber. In particular, ethanol-extracted wool will dye faster than wool extracted with ether alone [8]. Similar effects were considered possible with other alcohols; hence the pretreatment of the wool has been given particular attention in this investigation.

The occurrence of a surface barrier to dye penetration, and the consequent possibility of distinguishing experimentally between surface and bulk effects

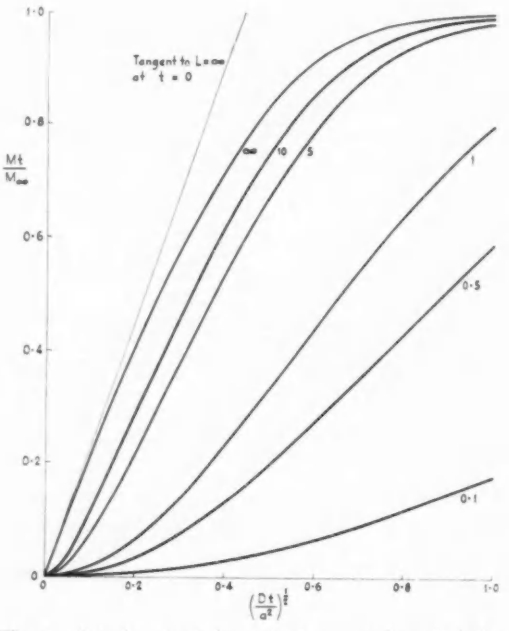

Fig. 1. Sorption (and desorption) curves from Relation 3. Numbers on the curves are values of $L = a\alpha/D$.

in the diffusion of dyes into wool fibers, was discussed in a recent paper [9]. In the present work the theory of a surface barrier has been extended, for, as will be shown below, the method of analysis used previously has limited application. The aim has been to see whether this extended theory can explain in detail the experimental relationship between uptake and time, and, if so, to separate and evaluate the surface and bulk factors controlling penetration during "solvent dyeing."

The Theory of Wool-Dyeing Kinetics

Several workers [7, 9, 14, 16] have used the rate of dye uptake into wool fibers from a dyebath of constant concentration to determine D, the diffusion coefficient of the dye, assuming semi-infinite diffusion. The ratio of the dye uptake (M_t) to the uptake at saturation (M_∞) is plotted against time$^{\frac{1}{2}}$; D may be obtained from the slope, S, of the linear portion of this curve by the relation

$$S = \frac{4}{\pi^{\frac{1}{2}}}\left(\frac{D}{a^2}\right)^{\frac{1}{2}} \tag{1}$$

where a is the fiber radius. For the case of the free acid of Orange II diffusing from aqueous solution into virgin wool, the occurrence of an initial concave-upwards portion for this curve has been demonstrated and attributed to a surface barrier, perhaps the epicuticle [9]. The linear portion for the above system lies between 0.1 and 0.4 saturation. Thus the assumption of semi-infinite diffusion, implicit in the use of Equation 1, has been made for conditions where the dye has penetrated considerably into a cylindrical medium. However, when polyamide and polyester fibers are dyed under similar conditions [15, 17], the dye uptake conforms closely to that expected theoretically for a homogeneous cylinder with no barrier [3]. This theoretical uptake is illustrated graphically by Crank [2] and is shown in Figure 1 (the curve $L = \infty$). At no stage can the (M_t/M_∞)–time$^{\frac{1}{2}}$ curve be considered linear, but at small times its slope changes only slowly from the initial value of $4/\pi^{\frac{1}{2}}\,(D/a^2)^{\frac{1}{2}}$ at $t = 0$.

These considerations call for an examination of the validity of the assumption that wool–dye systems show semi-infinite behavior over the range of uptake for which the (M_t/M_∞)–time$^{\frac{1}{2}}$ curve is a straight line. Accordingly the theory of a surface barrier has been extended to take into account the finite nature of the medium. Medley and Andrews [9] have shown that the theoretical equation for the dye uptake of a medium with a surface barrier is formally that given by Newman [12] and Crank [1] for the drying of porous solids. The case considered was a semi-infinite medium; the development for a cylindrical medium follows below.

For a uniform, homogeneous cylinder of infinite length and radius a, the "surface admittance," α, due to the presence of a thin surface barrier of thickness δ is given by [9]

$$\alpha = \frac{D_b C_b}{\delta C_m} \tag{2}$$

where C_b and C_m represent the equilibrium concentration in the barrier and bulk respectively and D_b is the diffusion coefficient in the barrier. Then, from Newman [12]

$$\frac{M_t}{M_\infty} = 1 - \sum_{n=1}^{\infty} \frac{4L^2 e^{-\beta_n^2 \frac{Dt}{a^2}}}{\beta_n^2(\beta_n^2 + L^2)} \tag{3}$$

where the β_n's are the roots of $\beta J_1(\beta) - LJ_0(\beta) = 0$, D is the diffusion coefficient in the bulk, and $L = a\alpha/D$.

Newman [12] has calculated M_t/M_∞ for various values of L and Crank [1] has presented a selection of these results graphically, as in Figure 1. (For the present work we have supplemented Newman's results with our own calculations for additional val-

ues of L, particularly for values of $L > 10$.) From the shapes of the curves in Figure 1 the influence of the barrier is seen to be maintained during the whole period of dyeing; it prevents the bulk of the fiber from completely controlling the rate at any stage. The linear portion of the curve now appears as an inflexion caused when the increase in the rate, due to the waning effects of the surface barrier, "balances out" the decrease due to the approaching saturation of the finite medium.

Determination of the Diffusion Parameters from Experiment

The value of L is a measure of the ratio of the surface and bulk diffusion characteristics and may vary considerably, particularly with the dye and the dyeing conditions. For higher values of L the surface influence is comparatively small once the initial curved portion of the plot is over, and little error is introduced into the analysis of experimental results by using the semi-infinite approach [9]. However, if L is small, the surface influence is severe, so that the slope of the linear portion of the (M_t/M_∞)–time$^{\frac{1}{2}}$ curve is considerably less than $4/\pi^{\frac{1}{2}}(D/a^2)^{\frac{1}{2}}$ and is not determined by D alone. Under these conditions the calculations of the parameters of the sample must be modified to consider a cylinder rather than a semi-infinite medium. In practice this is difficult because, even if an experimental curve conformed exactly to the relevant theoretical curve for a homogeneous cylinder with barrier, the family of curves (Figure 1) do not vary sufficiently in shape with L to enable it to be determined easily from the given curve. Moreover, variations in a, α, and D within the sample, together with departures from circular cross section among the fibers, will aggravate this problem.

The following method has been found satisfactory for determining the value of L from an experimental curve. For small times Equation 3 becomes

$$\frac{M_t}{M_\infty} = \frac{2\alpha t}{a} - \frac{8}{3a}\frac{\alpha^2 t^{\frac{1}{2}}}{(\pi D)^{\frac{1}{2}}} + 0(t^2) + \cdots \qquad (4)$$

Thus the initial uptake varies linearly with time and may be determined by the relationship

$$\left[\frac{d}{dt}\left(\frac{M_t}{M_\infty}\right)\right]_{t=0} = \frac{2\alpha}{a}$$

Let S_1 be the maximum slope of an *experimental* (M_t/M_∞)–time$^{\frac{1}{2}}$ curve associated with the model outlined above; i.e.,

$$S_1 = \left[\frac{d}{d\sqrt{t}}\left(\frac{M_t}{M_\infty}\right)\right]_{max}$$

Let the function of L, $K(L)$ be the maximum slope of the *theoretical* curves plotted with axes $Mt/M\infty$ and $(Dt/a^2)^{\frac{1}{2}}$ (see Figure 1); i.e.,

$$K(L) = \left[\frac{d}{d\sqrt{\frac{Dt}{a^2}}}\left(\frac{M_t}{M_\infty}\right)\right]_{max}$$

Now $S_1 = K(L_1)\left(\frac{D_1}{a_1^2}\right)^{\frac{1}{2}}$ where L_1, a_1, etc. are the values appropriate to the experimental case. Then

$$\frac{S_1^2 a_1}{\alpha_1} = \frac{K(L_1)^2 D_1}{a_1^2} \times \frac{a_1}{\alpha_1} = \frac{K(L_1)^2}{L_1}$$

A graph of $K(L)^2/L$ against L is shown in Figure 2. As $S_1^2 a_1/\alpha_1$ is known from experiment (S_1 and α_1 by graphical methods from the respective slopes of M_t/M_∞ vs. $t^{\frac{1}{2}}$ and t), L_1 may be read from Figure 2; therefore $D_1 = a_1\alpha_1/L_1$ can be evaluated.

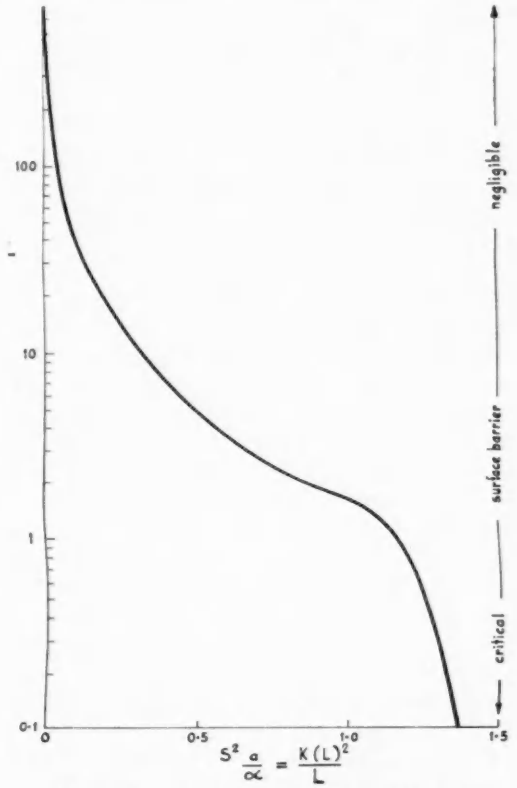

Fig. 2. Graph for finding the surface–bulk ratio from experimental data.

The general method for finding $K(L)$ for a given value of L was to obtain the value of Dt/a^2 at the point of inflexion by equating the second derivative of the expression for M_t/M_∞ in Equation 3 to zero, and solving numerically. This value of Dt/a^2 was then substituted in the first derivative of Equation 3 to give $K(L)$. For small values of L, $K(L)$ could be obtained graphically with sufficient accuracy for the present purpose. The limiting value of $K(L)^2/L$ as L approaches zero is $4/e$.

Experimental

Dye uptake measurements were made, as described in detail earlier [9], by following the change of conductance of the dyebath, which consisted of a $M/2000$ solution of the free acid of Orange II in the appropriate dyeing medium. Solutions of butanol in water were prepared from Analar n-butanol; they gave adequately low background conductance to enable the conductance method of measuring dye uptake to be used. Density has been used as a convenient index of butanol concentration, changes in density being sufficiently proportional to concentration changes for this to be applicable. The concentration of dye in the dyebath was maintained approximately constant by the addition of concentrated dye acid as required.

Orange II free acid was prepared from Naphthalene Orange G (I.C.I.), C.I. Acid Orange 7, by the method given elsewhere [9]. Lissapol N (I.C.I.) was used as supplied by the manufacturers; the diethyl ether was of "solvent ether" quality.

The fiber samples used were root ends of pen-grown Merino wool, mean diameter 21 μ, of the same origin as that used previously [9]. They were all given preliminary cleaning by Soxhlet extraction with petroleum ether (boiling point fraction 60–80° C.) for approximately 50 changes, followed by thorough washing in distilled water.

Results

The details relating to the pretreatments and dyeing conditions for the series of experiments are given below; the calculations from them are summarized in Table I. In Figure 3, the experimental points for Experiments 1, 3, and 5 are shown. The curves associated with the experimental points show the theoretical uptake, evaluated from Equation 3, using the radius of the wool fibers and the appropriate diffusion parameters in Table I.

The uptake rates in Experiments 2, 3, and 5 were sufficiently rapid to allow the wool to proceed to its equilibrium uptake. Spectrophotometric observations indicated that the pretreatments with butanol and Lissapol N solutions extracted material from the fibers. The presence of butanol does not markedly alter the final concentration of dye in the fibers.

Experiment 1

The wool was given no pretreatment (i.e., it was given only the initial cleaning outlined above). The results of this experiment have been reported in earlier work [9], where, by use of the simplifying assumption of semi-infinite diffusion behavior, D was calculated to be 4×10^{-12} cm.^{2} min^{-1}.

Experiment 1a

The pretreatment was Soxhlet extraction for 2 hr. with diethyl ether. The results were so close to Experiment 1 that the calculations are identical.

Experiment 2

The wool was Soxhlet extracted for several hours in ethanol. This is a representative result, but there

TABLE I. Dye Uptake Rates at 30° C. of Merino Wool Soxhlet-Extracted with Petroleum Ether

Experiment	Additional pretreatment	Dyeing solvent	$\alpha \times 10^7$, cm./min.	$S \times 10^3$, min.$^{\frac{1}{2}}$	$\frac{S^2a}{\alpha}$	L	D, cm.^{2} min.$^{-1}$
1	None	Water	1.6	4.3	0.12	35	4.8×10^{-12}
2	Ethanol soxhlet	Water	10.7	18.4	0.35	9.5	1.2×10^{-10}
3	Butanol solution, ether	Water	14	22	0.32	9.6	1.53×10^{-10}
4	Lissapol N solution, approx. 2%	Water	2.7	10.9	0.47	5.6	5.0×10^{-11}
5	Butanol solution, ether	Butanol solution	35	61	1.15	1.1	3.4×10^{-9}
6	Prolonged butanol solution, no ether	Butanol solution	8.7	34	1.39	<0.1	—

are variations and, in particular, pure dry ethanol seems to produce smaller alterations in diffusion rates.

Experiment 3

The wool was soaked for 48 hr. at 35° C. in water saturated with butanol, rinsed in acetone, Soxhlet extracted for 30 min. in diethyl ether, and then soaked for 12 hr. in water.

Experiment 4

The wool was dyed from an approximately 2% solution of Lissapol N in water. The calculated parameters are of value only for rough comparisons of dyeing rates because the wool was not initially equilibrated with the detergent solution.

Experiment 5

After pretreatment as for Experiment 3, the wool was equilibrated with butanol solution and dyed from a butanol solution dyebath. The density of the butanol solutions was 0.9886 g./cc. at 25° C., which is approximately a 7½% solution.

Experiment 6

The wool was soaked for several weeks in butanol solution, including 1 week at 45° C., and then introduced directly to a butanol solution dyebath. The density of the butanol solutions was as in Experiment 5.

Discussion

It cannot be claimed that α and D have been determined with any great accuracy; the results depend upon measurements of the slopes of curves, and values of D derived from small values of L must be treated with particular caution. Nevertheless, the results are significant in view of the magnitude of the changes brought about by the various treatments. The close correlation of the theoretical curves with experiment (Figure 3), over a wide range of surface and bulk parameters, leads to the conclusion that wool fibers behave as homogeneous, infinitely long cylinders with a surface barrier for the rate of dyeing with the free acid of Orange II. (Further investigations have shown that wool behaves similarly with the free acids of other simple acid dyes [10].) It is thus possible to evaluate both dyeing assistants and also pretreatments in terms of surface and bulk effects and, in particular, to isolate the accelerating action observed in solvent dyeing.

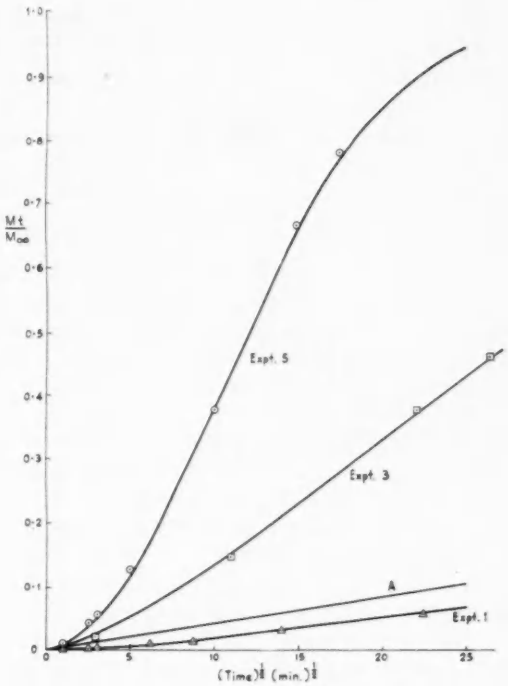

Fig. 3. Experimental dye uptake for various surface–bulk ratios. The curves associated with the experimental points show the theoretical uptake for the appropriate parameters which are shown in Table I. Curve A shows the theoretical uptake of a semi-infinite medium with no barrier, with D the same as for Experiment 1.

Wool given only the preliminary cleaning and wool subsequently extracted with diethyl ether show very little difference in the rate of uptake of Orange II from aqueous solution (Experiments 1 and 1a). However, if the wool is extracted with ethanol (Experiment 2) or pretreated with butanol (Experiment 3) the dyeing characteristics are markedly increased.

Wool pretreated with butanol should be subsequently extracted with diethyl ether; otherwise dyeing from an aqueous dyebath may be even slower than in Experiment 1. A similar effect on the dyeing rate occurs with a dyebath of butanol solution (compare the rates in Experiments 5 and 6).

Although butanol penetrates very slowly into dry wool, it is rapidly absorbed by keratin from aqueous solution. (Some preliminary experiments indicate a diffusion coefficient of 5×10^{-7} cm.^{2} min.$^{-1}$ for butanol in water-saturated horn keratin at 25° C.) Under these conditions it might be expected to extract material from wool in a way similar to ethanol [4], but we have concluded that unless the butanol-

treated wool is subsequently extracted with diethyl ether, some material removed by the butanol remains deposited at the fiber surface, insulating it from the dye. (Residual grease from incomplete soap and soda scouring has been observed to leave a surface barrier to Orange II in the same way [10].) It could be inferred that the increase of the bulk diffusion coefficient in Experiment 4 is also due to the removal of material from the interior of the fiber.

As the result of pretreatments with alcohols, the value of D from a water dyebath approaches the value of 3.2×10^{-10} cm.^{2} min.$^{-1}$ previously observed [9] for horn keratin treated with hot water. It has been noticed that alcohol pretreatments of horn keratin affect the self-diffusion rates of the amylbenzene sulfonate ion very little [11]; hence wool grease may be mainly responsible for the discrepancy originally noted between virgin wool and horn keratin.

If, as is the practice in solvent dyeing, the wool is directly introduced into a solution of both butanol and dye in water (that is, the wool has no alcohol pretreatment) the effect of any cleaning action which the butanol may have during the course of the dyeing is superimposed on the contribution from another process. The magnitude of the latter is illustrated by the difference between the rates in Experiments 3 and 5 (Figure 3). This difference indicates that the rate is increased due to the participation of the butanol in the dyeing itself (as reported above, the butanol penetrates much more rapidly than the dye).

If we compare the values of α and D for Experiments 3 and 5 we see that D is increased by over 20 times while α is increased only by a factor of 2.5; a comparison of Experiments 1 and 3 shows that D is increased by over 30 times while α is increased by a factor of only 9 times. For both cases the increase in the bulk diffusion coefficient is the predominant factor. Thus in a practical case of solvent dyeing, the surface barrier, although reduced in absolute value (α slightly increased), will exert a considerable retarding influence on the dyeing rate by virtue of the much greater promotion of dye movement within the fiber (D considerably increased).

Conclusion

Wool fibers behave as homogeneous, infinitely long cylinders with a surface barrier when dyed with the free acid of Orange II. The accelerating action of aqueous butanol on the rate of wool dyeing is connected with a modification of the dyeing process which has its major effect in the interior of the fiber. Butanol solutions increase diffusion rates reversibly by this modification of the dyeing process, and also irreversibly, probably by removing material from the interior of the fibers (this irreversible effect is also produced by ethanol). The over-all effect is to make the surface barrier, or surface resistance to dyeing, more significant than when dyeing from an aqueous dyebath.

Acknowledgments

This work was carried out as the result of cooperation between the C.S.I.R.O. Wool Research Laboratories, Australia, and the Wool Industries Research Association, England. We are grateful to Mrs. P. A. McCormick for the computations of $K(L)$.

Literature Cited

1. Crank, J., "The Mathematics of Diffusion," Oxford, Clarendon Press, 57, 73 (1956).
2. Crank, J., "The Mathematics of Diffusion," Oxford, Clarendon Press, 72 (1956).
3. Hill, A. V., *Proc. Roy. Soc.* **B104**, 39 (1928).
4. Human, J. P. E. and Speakman, J. B., *J. Textile Inst.* **45**, T162 (1954).
5. Karrholm, M. and Lindberg, J., TEXTILE RESEARCH JOURNAL **26**, 528 (1956).
6. Landerl, H. P. et al., *Am. Dyestuff Reptr.* **47**, 789 (1958).
7. Lemin, D. R. and Vickerstaff, T., Symposium on Fibrous Proteins (Soc. Dyers and Colourists) 129 (1946).
8. Lindberg, J., TEXTILE RESEARCH JOURNAL **23**, 573 (1953).
9. Medley, J. A. and Andrews, M. W., TEXTILE RESEARCH JOURNAL **29**, 398 (1959).
10. Medley, J. A. and Andrews, M. W., unpublished work.
11. Medley, J. A. and Ramsden, D. K., to be published.
12. Newman, A. B., *Trans. Am. Inst. Chem. Eng.* **27**, 203 (1931).
13. Peters, L. and Stevens, C. B., *The Dyer* **115**, 327 (1956); *J. Soc. Dyers Colourists* **72**, 100 (1956).
14. Speakman, J. B. and Smith, S. G., *J. Soc. Dyers Colourists* **52**, 121 (1936).
15. Vickerstaff, T., *J. Soc. Dyers Colourists* **59**, 92 (1943).
16. Vickerstaff, T., "The Physical Chemistry of Dyeing," London, Oliver and Boyd, 134 (1954).
17. Waters, E., *J. Soc. Dyers Colourists* **66**, 609 (1950).

Manuscript received March 3, 1960.

Sodium Chlorite Bleaching

Heinz Hefti[2]

The Textile Research Center, School of Textiles, North Carolina State College, Raleigh, North Carolina

Part I: Decomposition Studies[1]

IN THE last few years, especially in Europe, much attention has been given to the bleaching of textile goods with sodium chlorite.[3] In the field of bleaching on an industrial scale, acid-chlorite bleaching and ester-activated chlorite bleaching have been the most successful from the point of view of bleaching effect and fiber protection. However, both methods have some disadvantages, e.g., long bleaching time, high costs, etc. The purpose of the present work was to undertake studies with other "activators." Reaction mechanisms as well as bleaching effects were investigated.

In an earlier study [3] it was shown that sodium chlorite in acid solution in the absence and the presence of cotton undergoes decomposition which proceeds in three different directions:

$$5ClO_2^- + 2H^+ \rightarrow 4ClO_2 + Cl^- + 2OH^- \quad (I)$$

$$3ClO_2^- \rightarrow 2ClO_3^- + Cl^- \quad (II)$$

$$ClO_2^- \rightarrow Cl^- + 2O \quad (III)$$

It was also shown that the bleaching is done, in the case of acetic acid-activation in the pH range of 2–5 by the liberated oxygen or by intermediate products of the reactions which are responsible for the oxygen formation. Thus, for effective bleaching it may be of interest to speed up Reaction III and to stop or minimize Reactions I and II.

In the present work the activation action on chlorite solutions of esters and hydrolyzable salts was investigated.

Experimental Procedure

For the complete examination of the decomposition of chlorite solutions it is necessary to determine the following in presence of one another: ClO_2, O_2, Cl^-, ClO^-, ClO_2^-, ClO_3^-. The same analytical methods as described earlier [3] were used.

The experimental procedure used in all decomposition studies was as follows: to chlorite solutions of 1 g./l. (99.7% sodium chlorite, 0.34% sodium chlorate) kept at 95° C. (±0.25° C.), different amounts of "activators" were added. After 1 hr. the reaction products were analyzed and the pH of the reaction solution was measured at room temperature.

The reaction was carried out in the dark and under nitrogen, in absence of air, although earlier tests [3] showed that the same results are obtained in the presence and absence of air. During the reaction a nitrogen stream (0.001% oxygen) of 15 l./hr. was passed through the bleaching solution. The chlorine dioxide in the nitrogen was absorbed in 1 *N* sodium hydroxide solution and the oxygen was determined in a special apparatus [3]. A photograph of the entire apparatus is shown in Figure 1.

Results and Discussion

Acetic Acid–Sodium Acetate Buffer

Tests in 0.2 *M* acetic acid–sodium acetate buffer solutions were made to study the influence of pH, at the chosen test conditions, on the decomposition of sodium chlorite. The results, shown in Figures 2 and 8, indicate that the velocity of sodium chlorite decomposition is very much influenced by the pH of the solution. In the pH range 7–5 the decomposition is slow, but it is rapid below pH 5. The formation of chlorine dioxide is the main reaction over the entire pH range, but it becomes less important as the pH decreases. No chlorate was found above pH 5; below this pH its formation becomes increasingly important. Over the whole range tested the relative amount of oxygen is small and, at the reaction temperature of 95° C., changes very little with pH.

If the present results obtained at a temperature of 95° C. are compared with those obtained in earlier work [3] under similar conditions at a temperature

[1] This work was sponsored by Olin Mathieson Chemical Corporation (1957–58).

[2] Present address: Gellertpark 6, Basel, Switzerland.

[3] Sodium chlorite was introduced by the Mathieson Alkali Works in 1940 under the trade name of Textone.

of 60° C., it is found, as expected, that the rate of chlorite decomposition and the rate of formation of reaction products is greater at the higher temperature. In the case of the oxygen, the relative amounts formed in 1 hr. of reaction time are less important at the higher temperature, although the absolute amounts are about the same. Thus, at pH 2.4, about 9% at 60° C. and about 3% at 95° C. of the decomposed chlorite is converted to oxygen.

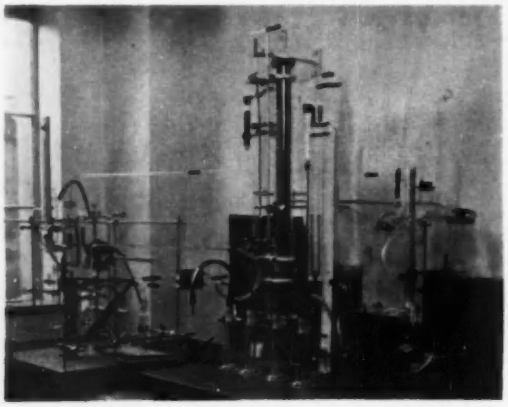

Fig. 1

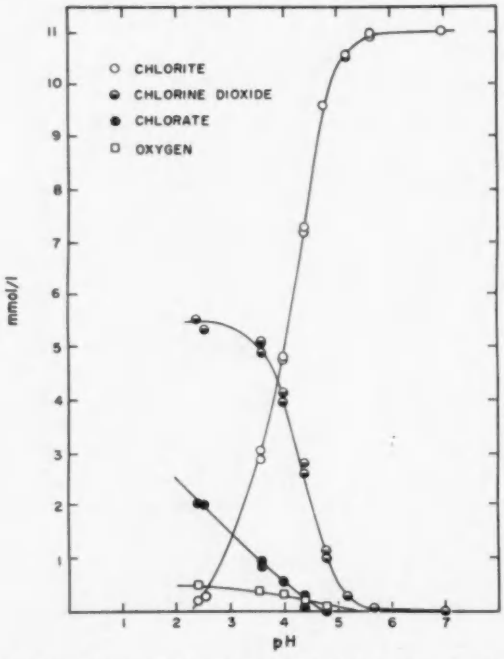

Fig. 2. Decomposition of sodium chlorite as a function of pH; undecomposed chlorite and chlorine dioxide, chlorate, and oxygen formed.

Organic Esters

The activation of chlorite with esters has become of some interest, especially in Europe [1, 2, 5, 6]. The influence of three different esters (diacetin, diethyl *d*-tartrate, ethyl lactate) on chlorite decomposition was studied. The results obtained (see Table I) show a linear relationship between ester concentration and chlorite decomposed and the oxygen and chlorine dioxide evolution. The reaction velocity of the chlorite decomposition, however, is different in all three cases. Diethyl *d*-tartrate shows the highest reaction velocity, followed by diacetin and ethyl lactate. Thus 23% chlorite in the case of diethyl *d*-tartrate, 19% chlorite in the case of diacetin, and 7% chlorite in the case of ethyl lactate, all with 0.05 ml./l. of activator, decomposes during the 1-hr. reaction period.

The amounts of chlorite which were used for the chlorine dioxide, chlorate, and oxygen formation, following Reactions I, II, and III, are expressed in Table I in percent of chlorite decomposed.

It has been stated in the literature [7] that esters

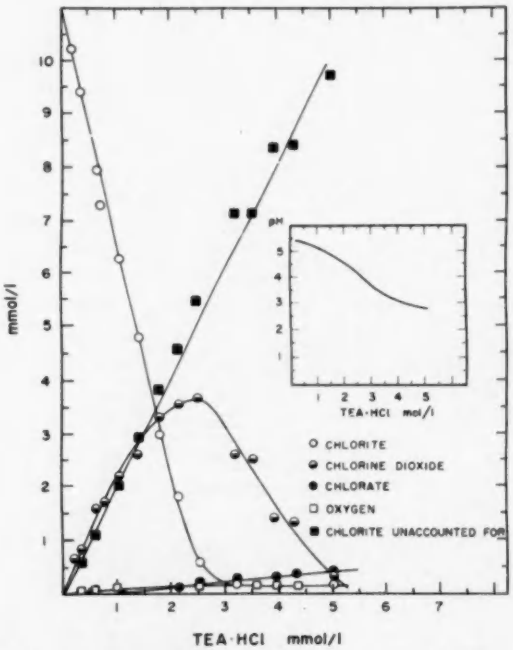

Fig. 3. Decomposition of sodium chlorite as a function of TEA·HCl concentration.

or their saponification products are oxidized by chlorite solutions. However, in the case of diacetin, the decomposition of sodium chlorite could not be fully explained by Reactions I, II, or III, indicating that some of the chlorite was decomposed in another way. The loss of oxidizing power can possibly be explained by the oxidation of the alcohol group on the ester. It could not be determined which of the reaction products was responsible for the oxidation.

The chlorine dioxide evolution is always the main reaction. With ethyl lactate almost the full amount of chlorite decomposed is used for the chlorine dioxide formation. The results show that the ester activation of chlorite solutions forms practically no chlorate. Even with diethyl *d*-tartrate only small amounts were found. In all three cases small amounts of oxygen are formed. Ethyl lactate gives the lowest oxygen values.

Ammonium Salts

Ammonium salts were proposed as corrosion inhibitors [4] in chlorite-bleaching processes and more recently as activators [7] of chlorite-bleaching liquors.

With ammonium acetate, even at a concentration of 27 g./l. (0.35 mole/l.), almost no decomposition was observed. The influence of ammonium chloride, nitrate, and sulfate on the decomposition of chlorite can be seen from Table II. The amounts of chlorite which were used by Reactions I, II, and III are expressed in percent of chlorite decomposed. The decomposition of sodium chlorite solutions in the presence of ammonium salts is relatively slow. The ammonium salt most effective in promoting decomposition of sodium chlorite in terms of grams per liter was the chloride, followed by nitrate, sulfate, and acetate. In the case of the chloride, nitrate, and sulfate salts, however, there is almost no difference if the salt concentrations are expressed in moles per liter instead of grams per liter.

Ammonium chloride and nitrate showed a linear relationship between salt concentration and chlorite decomposed. With ammonium sulfate no such relationship was found. Here, the increase in reaction velocity as the salt concentration was raised became relatively less.

In the case of the ammonium salts of chloride, nitrate, and sulfate, the formation of chlorine dioxide and oxygen were the main reactions. Only with ammonium chloride was a small amount of chlorate formed. The main reaction, however, in all three cases is the formation of chlorine dioxide. With respect to oxygen evolution the chloride is a little more effective than nitrate or sulfate.

Triethanol Amine Hydrochloride

The effect of triethanol amine hydrochloride (TEA·HCl) on chlorite solutions in the absence

TABLE I

Ester	Diacetin		Diethyl *d*-tartrate		Ethyl lactate	
Ester concentration, g./l.	5	15	5	15	5	15
Chlorite decomposed, mmol./l.	11.8	35.0	15.0	36.0	7.0	13.8
Reaction I—%	66	66	93	86	98	96
Reaction II—%	—	—	—	6.0	—	—
Reaction III—%	8.3	5.3	6.8	7.0	2.0	4.0
pH	5.1	5.2	5.1	5.2	4.9	4.7
Remarks	linear		linear		linear	

TABLE II

Ammonium salt	Chloride			Nitrate			Sulfate		
Salt concentration, g./l.	10	20	30	10	20	30	10	20	30
Chlorite decomposed, mmol./l.	11.0		32.6	6.5		17.5	7.5	12.4	15.5
Reaction I—%	90.6	88	87	95	95	95	95	95	95
Reaction II—%	1.3	2.4	2.5	—	—	—	—	—	—
Reaction III—%	8.0	7.5	7.5	6.0	7.0	7.0	6.0	5.0	5.0
pH	6.2	6.2	6.1	6.4	6.4	6.4	6.6	6.5	6.5
Remarks	linear			linear			curved		

and the presence of scoured cotton cloth (huck toweling) was studied. In the bleaching experiments the cloth:liquor ratio was 1:50. The results in Figure 3 indicate that the velocity of the decomposition of sodium chlorite solutions in the presence of TEA·HCl is high. Practically no change in velocity was observed in the presence of cloth (Figure 4). In the decomposition (Figure 3) and bleaching (Figure 4) experiments, the chlorine dioxide evolution goes through a maximum at 2.6 mmol./l. TEA·HCl. The chlorine dioxide values are considerably lower in the bleaching experiments than in the decomposition studies. In both test series the chlorate formation increases slightly and at practically the same rate. The chlorate values, however, are small, and the amount of detectable oxygen is in both cases very small over the full range studied. With increasing TEA·HCl concentrations the pH values decrease.

In the decomposition experiments the decrease of chlorite cannot be explained completely by Reactions I, II, and III. Part of the decomposed chlorite must have been used up by another path. If the values of chlorite unaccounted for by Reactions I, II,

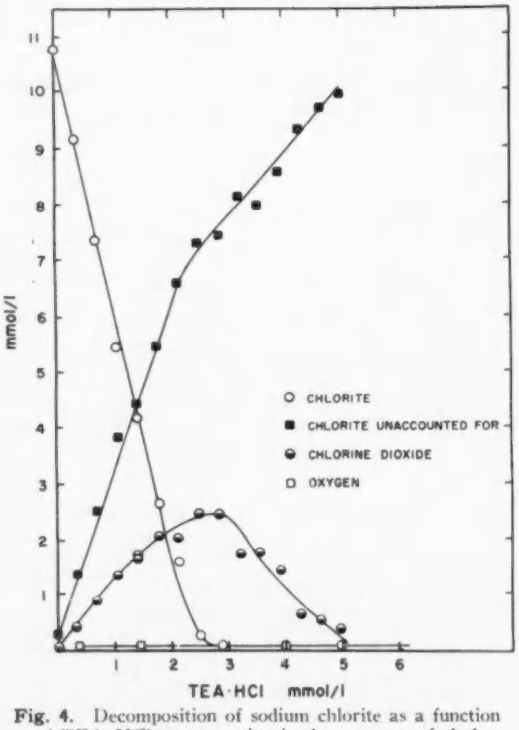

Fig. 4. Decomposition of sodium chlorite as a function of TEA·HCl concentration in the presence of cloth.

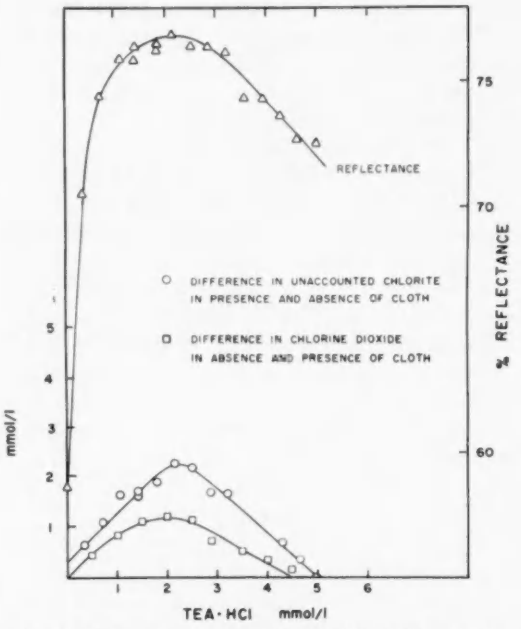
REFLECTANCE
%
mmol/l
TEA·HCl mmol/l
DIFFERENCE IN UNACCOUNTED CHLORITE IN PRESENCE AND ABSENCE OF CLOTH
DIFFERENCE IN CHLORINE DIOXIDE IN ABSENCE AND PRESENCE OF CLOTH

Fig. 5. Reflectance as a function of TEA·HCl concentration; difference in unaccounted-for chlorite and difference in chlorine dioxide in the presence and absence of cloth as a function of TEA·HCl concentration.

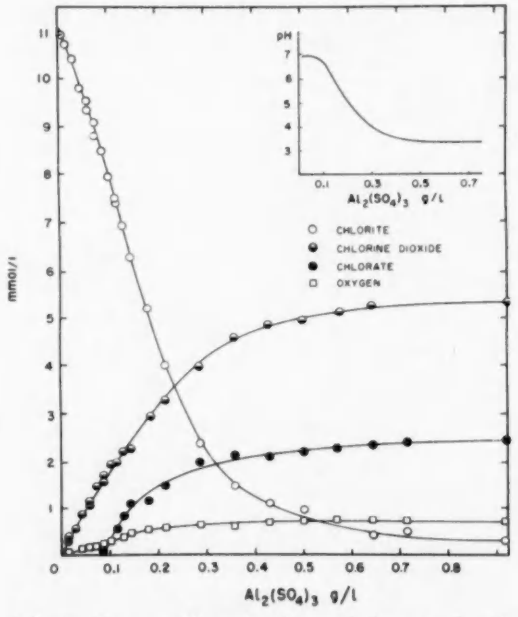

Fig. 6. Decomposition of sodium chlorite as a function of aluminum sulfate concentration; undecomposed chlorite, chlorine dioxide, chlorate, and oxygen formed.

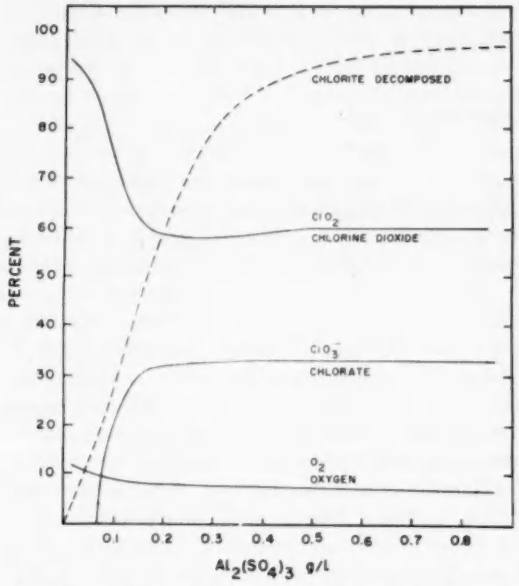

Fig. 7. Percent of decomposed chlorite used for reaction products as a function of aluminum sulfate concentration.

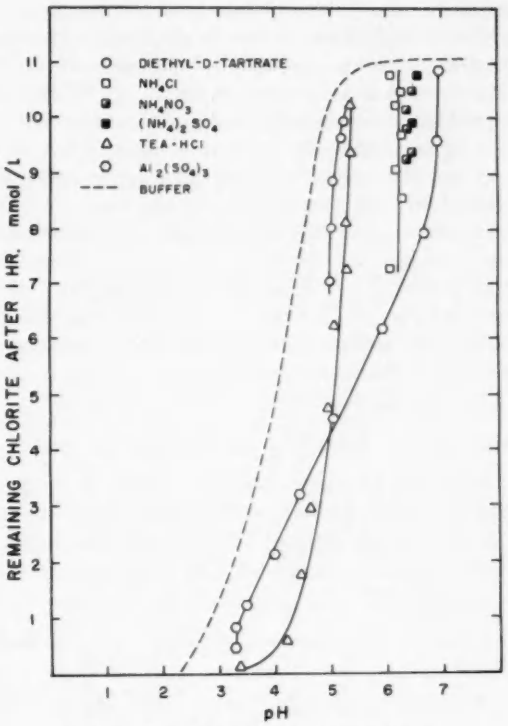

Fig. 8. Remaining chlorite after 1 hr. as a function of pH.

and III are plotted against the concentration of TEA·HCl, a linear relationship is obtained, which shows that for 1 mmol. of TEA·HCl, 2.00 mmol. of chlorite are missing. This observation could be accounted for by assuming that two of the three alcohol groups of TEA·HCl are oxidized to carboxyl groups. The velocity of this oxidation reaction is greater than the velocity of the chlorine dioxide formation. The maximum in the chlorine dioxide curve can, therefore, be explained by this difference in reaction velocity, since with increasing TEA·HCl concentration the chlorite available for the chlorine dioxide formation decreases more and more. It therefore appears that the oxidation of TEA·HCl is responsible for the depressing action of TEA·HCl on the chlorine dioxide evolution.

In the presence of cloth, the amount of chlorite unaccounted for by Reactions I, II, and III was considerably higher than that found in the absence of cloth. In the latter studies it was found that 2 mmol. of chlorite were used for 1 mmol. of TEA·HCl. It is logical to assume that the same relative amount was also used, at least at lower TEA·HCl concentrations, by TEA·HCl in the bleaching experiments. If the difference in chlorite unaccounted for by Reactions I, II, and III in the bleaching and decomposition studies is plotted against TEA·HCl concentration (Figure 5) it is found that this difference, which must be an indication of the least possible amount of chlorite used for bleaching, goes through a maximum at 2.2 mmol./l. TEA·HCl. This maximum coincides with the maximum of reflectance obtained on the bleached cloth (Figure 5).

The curve for the difference in chlorine dioxide evolution in the bleaching and decomposition studies has the same shape as the curve for the difference in unaccounted-for chlorite. It may be thought that the bleaching was done by chlorine dioxide since the amounts of chlorine dioxide found in the bleaching experiments were lower than in the decomposition studies. However, a closer study of the results shows that not all the bleaching could have been done by missing chlorine dioxide. Chlorine dioxide is formed following Equation I. This means that four chlorine dioxide molecules are generated from five chlorite molecules. At least the difference in unaccounted-for chlorite must have been used for bleaching. This amount is in all cases higher than 5/4 of the chlorine dioxide difference. Thus, at least some of the bleaching must have been done by

an agent other than chlorine dioxide. In the case of the decomposition studies the shape of the chlorine dioxide curve was explained by the difference in the reaction velocity between oxidation of TEA·HCl and chlorine dioxide formation. From those studies it was concluded that with increasing TEA·HCl concentration the chlorite available for chlorine dioxide formation decreases more and more. In the bleaching experiments an additional amount of chlorite was used for the bleaching reaction, a reaction with a velocity of the same magnitude as the oxidation reaction of TEA·HCl. Therefore, the amount of chlorite available for chlorine dioxide formation was, in the case of the bleaching experiments, smaller than in the decomposition studies.

Zinc Nitrate and Magnesium Chloride

With zinc nitrate concentrations between 0.6 g./l. and 13.5 g./l., a constant small amount of chlorite (4.5%) was decomposed. The chlorine dioxide evolution consumed about 95% and the oxygen formation about 5% of the decomposed chlorite. With magnesium chloride at a concentration of 15 g./l., only 0.5% of the available chlorite was decomposed. No chlorate formation was found with either salt.

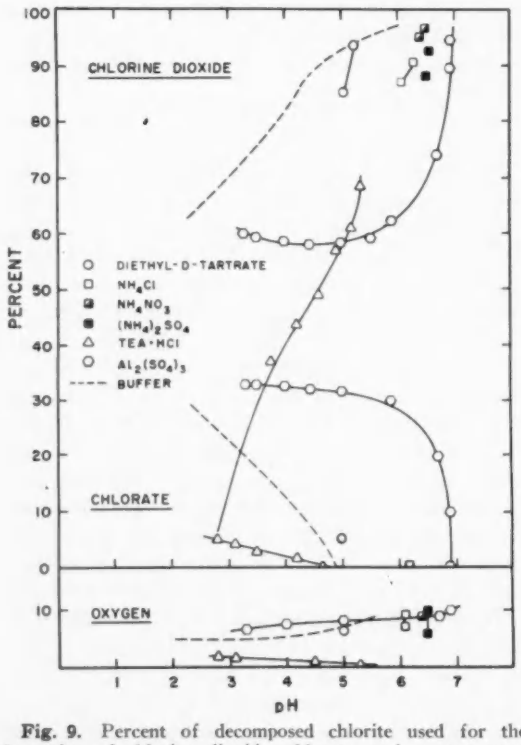

Fig. 9. Percent of decomposed chlorite used for the formation of chlorine dioxide, chlorate, and oxygen as a function of pH.

Aluminum Sulfate

The results, which are shown in Figures 6 and 7, indicate that the decomposition velocity of sodium chlorite increases rapidly with increasing aluminum sulfate concentration. The chlorine dioxide formation is always the main reaction. However, this reaction rapidly becomes less important with increasing aluminum sulfate concentration and reaches a steady state about 200 mg./l. aluminum sulfate [$Al_2(SO_4)_3$] (Figure 7). The chlorate formation starts about 70 mg./l. aluminum sulfate, increases first rapidly with increasing aluminum sulfate concentration, and then levels off. The absolute values of the liberated oxygen lie above those obtained with the other activators studied. The oxygen formation loses some of its importance with increasing aluminum sulfate concentration (Figure 7).

The final pH of the reaction solutions shows the following changes with increasing aluminum sulfate concentration: up to 50 mg./l. a constant value of pH 6.9 is obtained; from 50 mg./l. to about 500 mg./l. the pH decreases steadily; it levels off above 500 mg./l. at pH 3.3. Above an aluminum sulfate concentration of 50 mg./l., flakes of aluminum hydroxide were observed in the test solution.

Influence of pH

In Figures 8 and 9 the results obtained with all activators tested are shown as a function of end-pH. In general the velocity of the chlorite decomposition increases rapidly with decreasing pH. Figure 8 shows, however, that the decomposition is directed not only by the pH but also by the chemical nature of the activator.

Conclusion

In all cases tested the chlorite decomposition in the absence of any oxidizable substances could be fully explained with the equations

$$5ClO_2^- + 2H^+ \rightarrow 4ClO_2 + Cl^- + 2OH^- \quad (I)$$

$$3ClO_2^- \rightarrow 2ClO_3^- + Cl^- \quad (II)$$

$$ClO_2^- \rightarrow Cl^- + 2O \quad (III)$$

Reaction I was always the main reaction; Reaction II consumed small amounts of chlorite in three cases and reached some importance in the case of alumi-

num sulfate; Reaction III occurred in all tests but never consumed over 10% of the chlorite decomposed.

Following Equation I the chlorine dioxide formation has to be directed by the hydrogen ion activity of the test solution. Figure 9 shows that the chlorine dioxide formation is greatly affected by a decrease in pH. Unfortunately, the relationship between pH and hydrogen ion activity of the different activators is not known, and no general rule could be found. The relative amounts of chlorite used for the chlorine dioxide formation decreases with decreasing pH (see Figure 9).

Chlorate formation was found only in the case of diethyl *d*-tartrate, ammonium chloride, TEA·HCl, and aluminum sulfate. With the exception of aluminum sulfate, measurable amounts of chlorate were found only at pH values lower than pH 5. The chlorate formation generally increases with decreasing pH.

All activators tested gave small amounts of oxygen. The amounts of decomposed chlorite used for oxygen formation generally lie between 6% and 9% of the decomposed chlorite and are only slightly affected by pH. On the other hand, decreasing pH values increase the chlorite decomposition velocity; therefore, under the chosen test conditions, lowering of pH should call for shorter bleaching times.

Literature Cited

1. Baier, H., *Melliand Textilber.* **38**, 53 (1957).
2. French Patent No. 1,100,066; British Patent No. 764,649.
3. Hefti, H., *Textile Rundschau* **11**, 82 (1956).
4. Lamborn, B. T., to Hercules Powder Company, U. S. Patent No. 2,810,717 (October 22, 1957).
5. Mosse, P., *Teintex* **19**, 811 (1954).
6. Rosset, J., *Teintex* **22**, 181 (1957); *Melliand Textilber.* **38**, 417 (1957).
7. Rüedi, E., *Melliand Textilber.* **39**, 520 (1958); Stoffel & Co., Belgian Patent 557,828; Swiss Patent 37,596 (1956).

Manuscript received July 27, 1959.

Part II: Bleaching Studies[1]

Introduction

It is well known that sodium chlorite under normal bleaching conditions does not damage cellulose to any noticeable extent. In order to degrade cellulose with chlorite severe treatments are necessary [7]. Sodium chlorite has a distinctly selective oxidation capacity for noncellulosic impurities which makes it possible to bleach very evenly cotton containing heavy motes, provided that suitable operational conditions prevail. The material loss is much lower and the hand is softer than in the conventional hypochlorite and peroxide processes. Also, no scouring is needed and there is practically no danger of catalytic damage. On the other hand, these advantages are accompanied by a serious difficulty: the tendency to corrode stainless-steel bleaching apparatus [3]. The corrosion of stainless-steel equipment can be almost completely eliminated by pH control of the bleach liquor and by addition of sodium nitrate to the bleach solution [16]. In the part of the machinery exposed to gases, corrosion by chlorine dioxide vapors can be eliminated by designing the machine in such a manner that condensation is prevented [4, 9] or by keeping the gaseous phase alkaline [8].

[1] This work was sponsored by Olin Mathieson Chemical Corporation (1957–58).

Experimental Procedure

There are different bleaching units, semi- or fully continuous, on the market that can be used for chlorite bleaching [2, 4, 9, 14, 15]. The working method of these machines can be summarized as follows: (a) impregnation with bleach liquor; (b) warming of the treated material to the chosen temperature, usually by means of steam; (c) rolling or storing of fabric to allow completion of the reaction under unchanged conditions; (d) washing of the bleached goods. In general, this procedure was followed in the present laboratory work. Specifically, the following method was used. A desized huck-toweling fabric, containing many seed husks, was impregnated with the cold bleaching solution on a conventional 2-roll padder. The pick-up was about 100%. After impregnation the cloth was rolled up and put in a preheated jar and sealed. The jars were stored in an oven at 100° C. or at 130° C. in an autoclave under saturated steam atmosphere. As aftertreatment, the bleached cloth was boiled for 5

min. in water, rinsed thoroughly, and dried. The reflectance (MgO as standard) and fluidity (cuprietheylene diamine method) of the bleached samples were measured.

Results and Discussion

The results shown in Figures 1, 2, and 3 were obtained with cotton cloth that had been treated with pure (analytical) chlorite solution and stored at 100° C. or above for different periods of time.

It is clear that good bleaching can be obtained in the absence of any activator with pure chlorite solutions. Bleaching is a function of temperature, time, and chlorite concentration. Tests with commercial chlorite solutions of about pH 10 gave unsatisfactory bleaching results. However, when these bleach liquors were neutralized prior to padding, the bleaching was as good as in the case of pure chlorite solutions. It was found that when activators are not used the pH of the bleach liquors should lie between 6 and 7.

Since the experiments described above were carried out with desized cloth which had no further purification, there was some question as to whether the "neutral" bleaching is "activated" by impurities present in the cloth. Some special tests were made to determine if this was the case.

Cloth containing a large number of seed husks was purified with acid and extracted with benzene. This treatment removed the inorganic constituents (ash) and the waxy materials, but did not remove the husks. No difference in bleaching behavior could be observed with this material. An additional sample was made in which all noncellulosic constituents were removed by appropriate extraction at the

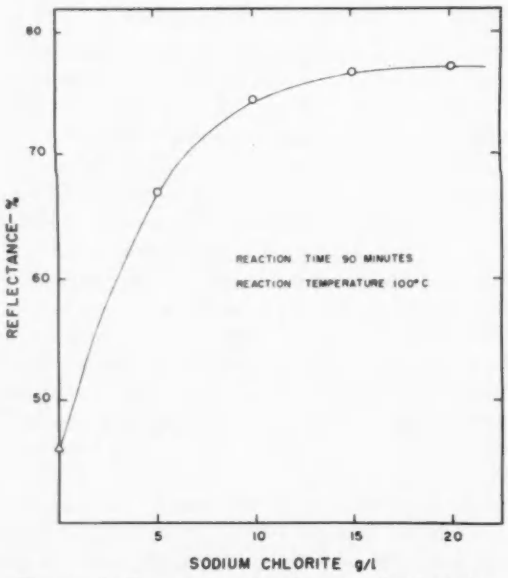

Fig. 1. Reflectance as a function of sodium chlorite concentration at 100° C. and 90 min. bleaching time.

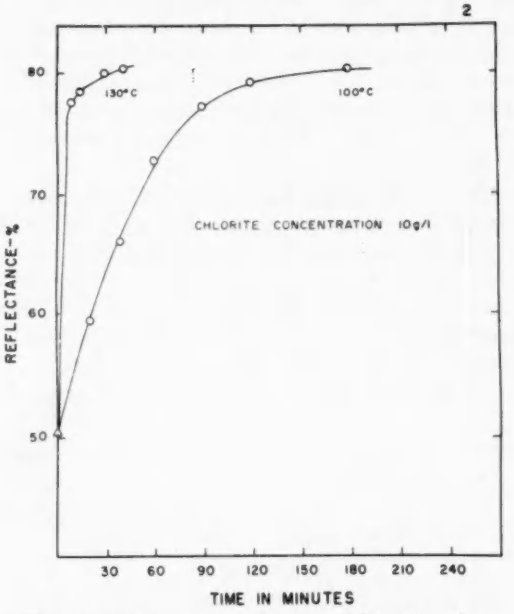

Fig. 2. Reflectance as a function of bleaching time.

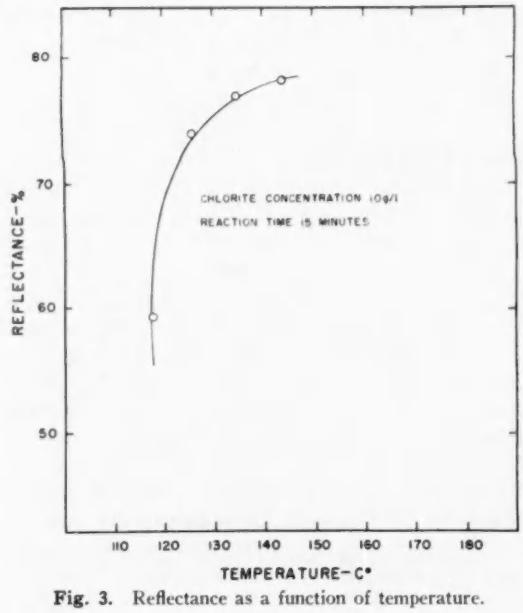

Fig. 3. Reflectance as a function of temperature.

boil with 4% sodium hydroxide solution. As before, the bleaching behavior was similar to that of the unpurified material, and it was concluded that cellulose itself was the "activator." Moreover, bleaching is temperature dependent, and at 130° C. no activator appears to be necessary to achieve good bleaching.

The influence on bleaching of the different activators, studied in Part I [5] was also investigated. In preliminary tests the bleaching results obtained at two chlorite concentrations and two temperatures as a function of activator concentration were determined. Figure 4 shows, as an example, the results obtained with magnesium chloride as the activator.

Almost all activators studied showed the same trend, in that the reflectance increased to a maximum value with increasing activator concentration; the only exception was TEA·HCl (see Figure 5).

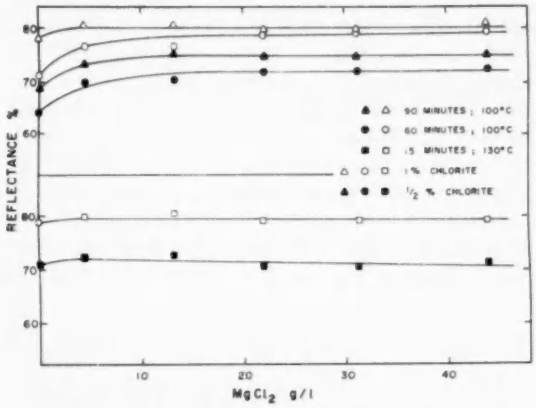

Fig. 4. Reflectance as a function of magnesium chloride concentration.

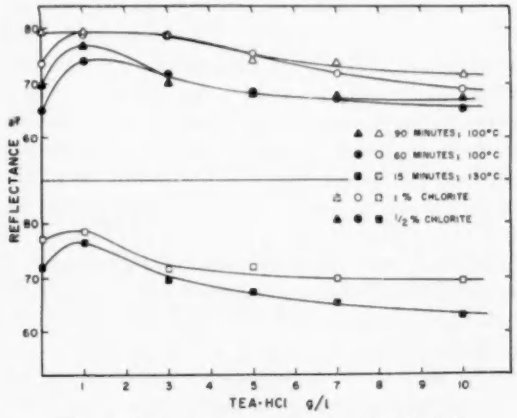

Fig. 5. Reflectance as a function of TEA·HCl concentration.

Some activators gave higher reflectance values than others (Figure 6); these were magnesium chloride, zinc nitrate, and aluminum sulfate. The bleaching tests with 0.5% and 1% sodium chlorite (based on the weight of the cloth) show that small amounts of TEA·HCl give better bleaching results than chlorite alone, although high amounts of TEA·HCl reduce reflectance. This can be easily explained by the fact that TEA·HCl itself is oxidized and consumes a large amount of chlorite when TEA·HCl is present in high concentrations [5]. In the chlorite bleaching with TEA·HCl two competing reactions occur: the bleaching reaction and the oxidation of the activator. The results indicate that the magnitude of the velocity of both reactions is about the same, since some bleaching occurs even above a molar ratio TEA·HCl to chlorite of 1 to 2 (4.2 g./l. TEA·HCl for 0.5% chlorite; 8.4 g./l. TEA·HCl for 1% chlorite).

The effectiveness of the different activators was compared in another test in which the activator concentrations chosen were those that gave maximum reflectance values in the preliminary tests (see Figures 6 and 7). The test conditions were:

Chlorite concentration	10 g./l. (100% chlorite)
Wetting agent[2]	0.75 g./l. Leonil ART
Activator concentration	see Figure 6
Pick-up	100%
Reaction time and temperature	70 min. 100° C.; 15 min. 130° C.

These experiments were done in triplicate and good agreement was obtained. Figure 6 shows the average reflectance values obtained on desized huck toweling cloth. The maximum reflectance obtained with repeated hydrogen peroxide treatments was around 82% on the same cloth. According to Figure 6, all activators give higher reflectance values than chlorite alone at 100° C. and 70 min. bleaching time. The best bleaching results were obtained with TEA·HCl, magnesium chloride, zinc nitrate, and aluminum sulfate. It is interesting to note that magnesium chloride had very little effect on the decomposition of hot chlorite solutions. It was shown in Part I [5] that at 95° C. magnesium chloride at a concentration of 15 g./l. decomposed only 0.5% of the available chlorite. This means that excessive decomposition of a hot chlorite solution and the resulting formation of chlorine dioxide as a main product is not necessarily a criterion for a good activator. With respect to reflectance the following order was

[2] Preliminary tests showed that the wetting agent has no effect on the bleaching itself, but its use results in good absorbency.

observed: TEA·HCl had the highest value, followed by magnesium chloride, zinc nitrate, aluminum sulfate, ethyl *d*-tartrate, ammonium sulfate, ammonium chloride, diacetin, ammonium nitrate, acetic acid–sodium acetate buffer solution of pH 5.6, and pure chlorite solution.

At 130° C. for 15 min. the activators did not improve the bleaching effects; some of them (zinc nitrate, diacetin, TEA·HCl, and aluminum sulfate) even reduced the reflectance considerably.

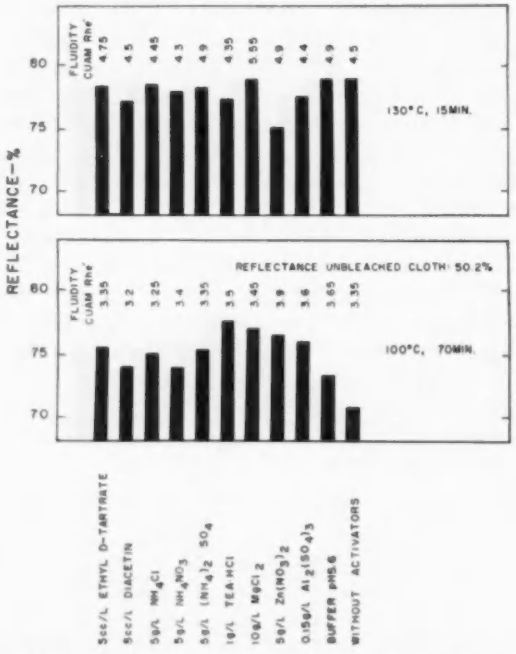

Fig. 6. Reflectance obtained with different activators.

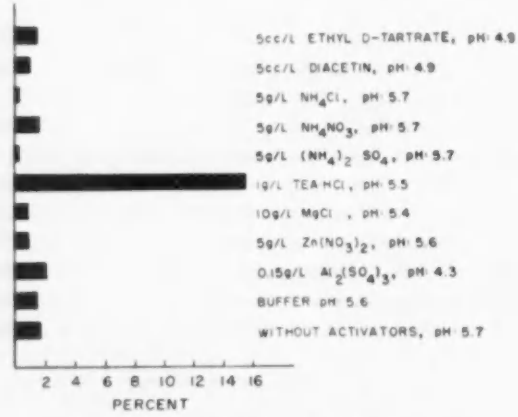
5cc/L ETHYL D-TARTRATE, pH: 4.9
5cc/L DIACETIN, pH: 4.9
5g/L NH4Cl, pH: 5.7
5g/L NH4NO3, pH: 5.7
5g/L (NH4)2 SO4, pH: 5.7
1g/L TEA·HCl, pH: 5.5
10g/L MgCl , pH: 5.4
5g/L Zn(NO3)2, pH: 5.6
0.15g/L Al2(SO4)3, pH: 4.3
BUFFER pH: 5.6
WITHOUT ACTIVATORS, pH: 5.7
2 4 6 8 10 12 14 16
PERCENT

Fig. 7. Chlorite decomposed in bleach liquors after 24 hr. at 30° C.

It was estimated that about 98% of the seed husks were removed when the bleaching was carried out with 1% chlorite at 100° C. for 70 min., but when higher temperatures and shorter reaction times were used, only about 75% of the seed husks were removed. Similar observations have been made in bleaching studies with hydrogen peroxide.

The stability of the different bleach liquors is shown in Figure 7. In most cases, only minor reductions of chlorite concentration were observed after 24 hr. of standing at 30° C. The only exception was TEA·HCl, which showed a loss of about 16%. Thus, when using TEA·HCl as activator in bleach liquors, it should be added shortly before use.

The fluidities of the samples bleached at 100° C. (see Figure 6) lie only slightly above the fluidity of the unbleached cloth (2.8 rhes), indicating that the cotton cloth is for practical purposes undegraded. The different activators do not seem to influence the fluidity values. The fluidity values of the cloth bleached at 130° C. lie slightly above those obtained at 100° C.; however, all the values lie well below the fluidity limit of 10 rhes which is normally accepted in commercial bleaching.

Since it was found that cloth can be bleached in a short time with chlorite at temperatures above 100° C., some tests were conducted to determine whether yarn packages could be bleached in the same way.

The package was impregnated with commercial chlorite solutions (10 g./l. 100% sodium chlorite) in a 1-lb. package-dyeing machine. As a wetting agent 1 g./l. Leonil ART (Hoechst) was added. A series of impregnated packages was then stored in a preheated autoclave at 145° C. in a saturated steam atmosphere for different periods of time. Several things of interest were noted in this first series of experiments. First, there was no uniformity throughout the package with respect to bleaching, the best whiteness being obtained toward the outside of the package. Second, there was apparently a corrosion problem when chlorite was used alone. It is believed that the differences in whiteness can be explained by the steaming system used. The steam was blown into the autoclave and not through the package. Thus, the inside layers needed a much longer time to reach the temperature than the outside layers.

In another test series, a different system was used.

A 1-lb. package-dyeing machine was altered so that direct high-pressure steam could be blown through the package, thereby allowing a rapid and more uniform heating. The package was impregnated on a package-dyeing machine and then transferred to the altered package-dyeing machine after preheating. The machine was closed and steam was blown through the package; during this time the outlet valve was open. After 1 min. the outlet valve was closed and the autoclave brought up to 145° C. About 1–2 min. was needed to reach this temperature. The package was stored at this temperature for 20 min. and then thoroughly rinsed with clean tap water. This time no visual difference in whiteness throughout a dissected yarn package was observed. However, the fluidity of the bleached yarn was relatively high (9.0 rhes). Corrosion damage is shown in Table I.

These results show that the corrosion can be reduced considerably by addition of both ammonium phosphate (dibasic) and sodium nitrate. To minimize the possibility of corrosion it is suggested that impregnation and steaming be carried out in two separate dyeing machines; if only one machine is used it should be rinsed between impregnation and steaming. Since the commercial chlorite solution is slightly alkaline, some ammonia is liberated and enters the gaseous phase of the system and prevents corrosion at the walls.

It was found that in every case where a corrosion point was in contact with the package, the cotton was completely degraded.

Conclusions

The reported work shows that neutral chlorite solutions give acceptable bleaching at temperatures of 100° C. and higher. The possibility of seed husks and waxes acting as activators was excluded, but it appears that cellulose may have an activation action at temperatures above 100° C. In any case, bleaching is temperature dependent, and at 130° C. no added activator appears to be necessary to achieve good bleaching. At temperatures below 100° C., however, bleaching can be improved by addition of different activators.

It was shown that practically no tendering occurs in chlorite bleaching. The fluidities of the bleached cloth were only slightly higher than the fluidity of the unbleached cloth.

As reported in other papers, it was found that corrosion in the part of the bleaching apparatus exposed to liquids is almost completely eliminated by addition of sodium nitrate to the bleach liquor. Corrosion in the part of the bleaching unit exposed to gases can be reduced with activators that liberate practically no chlorine dioxide or, still better, with ammonium salts that react with commercial alkaline chlorite solutions in the following way:

$$NH_4^+ + OH^- \rightarrow NH_3\uparrow + H_2O$$

Thus, ammonium salts appear to act by neutralizing chlorite solutions. Moreover, they appear to improve bleaching, at least at 100° C. The liberated ammonium hydroxide prevents corrosion in the gas phase.

Acknowledgment

The author would like to express his thanks to the management of Olin Mathieson Chemical Corporation for permission to publish these investigations and for useful suggestions, and to H. A. Rutherford and D. M. Cates for the benefit of discussion and advice. The author is indebted to Mrs. L. Kiser for the fluidity determinations.

TABLE I

Bleaching formula	Corrosion
1. 10 g./l. sodium chlorite (100%) 1 g./l. Leonil ART	Autoclave (stainless steel) completely rusted
2. 10 g./l. sodium chlorite (100%) 10 g./l. ammonium phosphate dibasic 1 g./l. Leonil ART	No corrosion on autoclave walls; several corrosion points where metal and package were in contact
3. 10 g./l. sodium chlorite (100%) 10 g./l. sodium nitrate 1 g./l. Leonil ART	Autoclave walls completely rusted; practically no corrosion points where metal and package were in contact
4. 10 g./l. sodium chlorite (100%) 10 g./l. sodium nitrate 10 g./l. ammonium phosphate dibasic 1 g./l. Leonil ART	No corrosion; in one case one small corrosion point found where metal and package were in contact

Literature Cited

1. Anon., *Melliand Textilber.* **38**, 565 (1957).
2. Anon., *Silk and Rayon* **26**, 1040 (1954).
3. Doerfel, E., *Melliand Textilber.* **38**, 285, 413 (1957).
4. Dungler, J., *Melliand Textilber.* **37**, 1312 (1957).
5. Hefti, H., TEXTILE RESEARCH JOURNAL, **30**, 861 (1960).
6. Hefti, H., Dissertation ETH Switzerland (1955).
7. Kocher, F., *Bull. Inst. Textile France* **31**, 32 (1952).
8. Lamborn, B. T., to Hercules Powder Company, U. S. Patent No. 2,810,717 (October 22, 1957).
9. Melbin, B. F., *Textil Rundschau* **10**, 51 (1955); *Am. Dyestuff Reptr.* **44**, 877 (1955); *Textil Praxis* **12**, 370 (1957).
10. Mellgren, P., *Melliand Textilber.* **38**, 911 (1957).
11. Petermann, R., *Deutsche Textiltech.* **7**, 223 (1957).
12. Pierling, H., *Melliand Textilber.* **37**, 1197 (1956).
13. Schmidt, F., *Textil Praxis* **13**, 298 (1958).
14. Strzoda, J., *Melliand Textilber.* **39**, 517 (1958).
15. Vogel, B., *Melliand Textilber.* **37**, 598 (1956).
16. Waibel, W., to Farbwerke Hoechst, Germany, U. S. Patent 2,711,363 (June 21, 1955).

Manuscript received July 27, 1959.

Action of Oxidizing Agents on Cellulose and Hydrocellulose

W. B. Achwal and G. M. Nabar

Department of Chemical Technology, University of Bombay, Bombay 19, India

Abstract

Changes in the properties of cellulose during progressive hydrolysis by dilute sulfuric acid have been studied by measuring the changes in oxidative susceptibility, density, moisture regain, and DP. It is shown that hydrolysis decreases oxidative susceptibility, moisture regain, and DP but the density progressively increases and reaches a constant value at more or less the stage at which DP, moisture regain, and oxygen consumption reach a constant value. From a study of the chemical properties of the products of oxidation of cellulose and the various hydrocelluloses it is shown that the mechanism of oxidation, in spite of the changes indicated above, remains the same in both cases.

CELLULOSE fibers consist of closely packed crystalline regions and less dense noncrystalline or amorphous regions without any line of sharp changes [2, 3, 19, 20]. In the latter, chains are present in a state of random distribution. The physical characteristics and chemical reactions of cellulose are governed by relative amounts of crystalline and noncrystalline portions in a fiber substance. Action of dilute acids on cellulose has been a useful means of providing information about the fine structure of cellulosic fibrous materials [4, 7, 11, 16, 17, 22, 23, 26, 27, 29]. Although kinetics of acid hydrolysis has been studied in great detail with special reference to resultant increase in crystallinity, properties of the products of hydrolysis other than density and moisture regain [11, 17, 26] have received very little attention.

In a recent publication Achwal, Daruwalla, Nabar, and Subramaniam [1] have shown that, during the initial stages of heterogeneous hydrolysis of cellulose with dilute sulfuric acid, a sudden decrease in DP, moisture regain, oxidative susceptibility, and adsorption of dyes and a simultaneous increase in fiber crystallinity and density takes place. They have further shown that continued acid action results in a slower rate of changes in the fiber characteristics; in the final stages of acid action there is a tendency for the leveling-off of all the fiber characteristics.

Present work is undertaken to investigate the characteristics of cellulose modified by treatment with dilute acids and to study action of oxidizing agents on them. Action of oxidizing agents on products of hydrolysis obtained from standard cellulose, standard cellulose mercerized with and without tension, and viscose rayon filament is studied. Chemical properties of resultant "oxyhydrocelluloses" are ex-

amined. An attempt is made to correlate the changes in oxidative susceptibility of the fiber during progressive hydrolysis with the changes in other properties such as DP, moisture regain, density, reducing power, crystallinty, and dye adsorption.

Experimental Methods

Materials used and pretreatments for the preparation of standard cellulose [9], mercerized celluloses, and viscose are similar to those reported earlier [1].

Methods used for the determination of copper number [15], cuprammonium fluidity [14], fiber density [28], degree of polymerization [5], carboxyl content, and moisture regain and conditions used for the preparation of hydrocellulose samples are as described in the above-mentioned publication by Achwal et al. [1].

Treatment of Cellulose and Hydrocellulose Samples with Oxidizing Agents

Potassium dichromate–sulfuric acid [*12*]. All oxidations are carried out using 0.1 *N* potassium dichromate in 0.1 *N* sulfuric acid with a material: liquor ratio 1 : 40. The period of oxidation is varied from 1 to 24 hr. Potassium dichromate shows no self-decomposition during this period. Available oxygen lost from the solution is calculated for each period of treatment. The oxidized samples are thoroughly washed and dried in air.

Potassium dichromate and oxalic acid [*8*]. Various samples are oxidized over a period of 3 hr. with potassium dichromate in the presence of oxalic acid. Different amounts of 2 *N* potassium dichromate are added to 150 ml. of 2 *N* oxalic acid solution at 30° C. in which cellulose samples are suspended with a material : liquor ratio 1 : 50. The treated samples are washed, dried, and carefully stored.

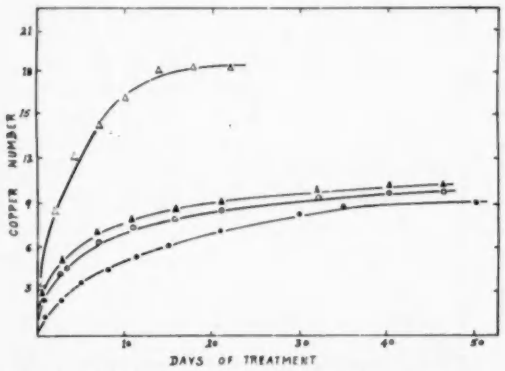

Fig. 1. Relation between copper number and time of treatment with acid for different cellulosic fibers: (●) standard cellulose, (⊙) cellulose mercerized with tension, (▲) cellulose mercerized without tension, and (◬) viscose rayon.

Sodium hypobromite [*12*]. Sodium hypobromite is prepared according to the method described by Birtwell, Clibbens, and Ridge [6]. Cellulose samples are treated with *N*/50 sodium hypobromite solutions for a period of 4 hr. with a material : liquor ratio 1 : 40. Oxidation experiments are carried out in a darkroom. Oxygen consumed by cellulose is estimated as recommended by Nabar and Kulkarni [21]. At the end of oxidation, the samples are freed from hypobromite with repeated changes of distilled water and then with a dilute solution of sodium thiosulfate. The samples are finally washed free of water-soluble materials and stored carefully after drying.

Potassium permanganate [*13*]. Potassium permanganate (0.02 *N*) solutions are used for oxidation treatment with a material : liquor ratio of 1 : 50. Strength of permanganate is estimated at the end of the specified period of treatment and loss in active strength is calculated using a control without any cellulose. Treated samples are thoroughly washed, and deposited oxides of manganese are removed by treatment with an acidified solution of dilute hydrogen peroxide. The samples are finally washed and stored as before after drying.

The pH of various solutions used for oxidation is adjusted as required by using standard buffer mixtures and measured using a glass electrode.

Treatment of the samples with chlorous acid [*12*]. Various oxycelluloses are treated with 0.2 *N* sodium chlorite in 1.5 *N* phosphoric acid for 18 hr. at room temperature on a mechanical shaker. The samples are washed thoroughly with distilled water, dried, and stored.

Shrinkage. Percentage shrinkage measurements of standard cellulose yarns and of modified yarn samples are carried out according to the method used by Kasbekar and Neale [18].

Experimental Results and Discussion

From the results of changes in reducing value during progressive hydrolysis of different cellulosic fibers using 6 *N* sulfuric acid (30° C.), shown in Figure 1, it is seen that the rate of increase in reducing value of the different fibers is rapid in the initial stages of hydrolysis followed by a progres-

sively slower rate; later it reaches a constant value. The highest reactivity towards hydrolysis is shown by viscose and the least by standard cellulose. The copper number of the hydrolyzed samples at the stage where hydrolysis virtually appears to come to a standstill under the conditions studied in this investigation, is different for different fibers. In the case of standard cellulose the maximum copper number reached is 9.0; for mercerized celluloses it is about 10.5 and for viscose it is 18.0.

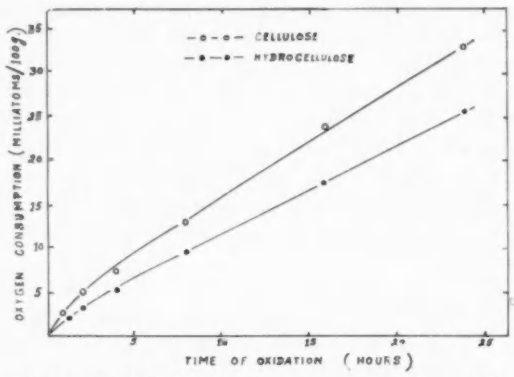

Fig. 2. Relation between oxygen consumption and time of oxidation by a mixture of potassium dichromate and sulfuric acid.

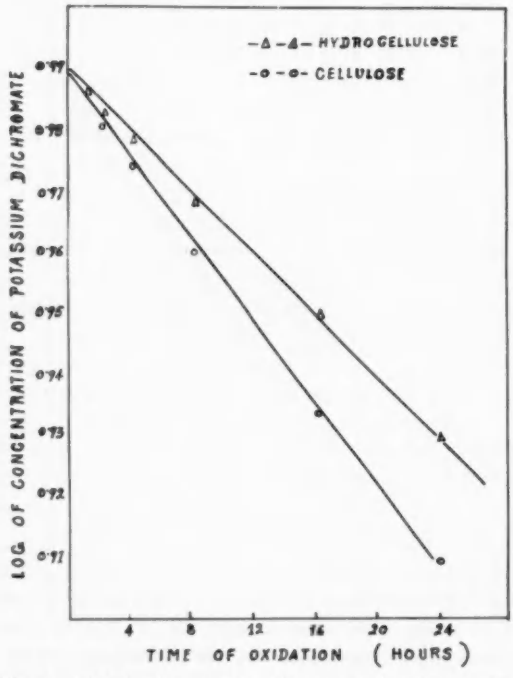

Fig. 3. Relation between log of concentration of potassium dichromate in solution and time of oxidation.

Oxidation of standard cellulose and one hydrocellulose (copper number 3.17) prepared from it is studied using a mixture of potassium dichromate and sulfuric acid. The relation between the amount of oxygen consumed and the period of treatment with the oxidizing agent is shown in Figure 2. It is seen that the relationship for both cellulose and hydrocellulose is of the same type. However, for any given period of treatment, oxygen consumption by standard cellulose is always higher than that by the hydrocellulose. The ratio between oxygen consumption by cellulose and that by hydrocellulose is approximately 1.3. The linear relationship obtained between the log concentration of potassium dichromate and time of reaction, both for cellulose and for hydrocellulose (Figure 3), indicates that a similar mechanism of oxidation reaction takes place with both fiber substances, but rates of reaction for the two fibers are different. Rate of oxidation reaction for any particular concentration of dichromate in solution depends upon the capacity of a fiber substance to become oxidized or, in other words, its oxidative susceptibility. The above results show that hydrolysis of standard cellulose with 6 *N* sulfuric acid has decreased its oxidative susceptibility.

A study of chemical properties of the oxycellulose from standard cellulose and the oxycelluloses from one hydrocellulose formed by action of dichromate–sulfuric acid supports the above conclusions. The relation between increase in copper number and increase in carboxyl content for cellulose and the

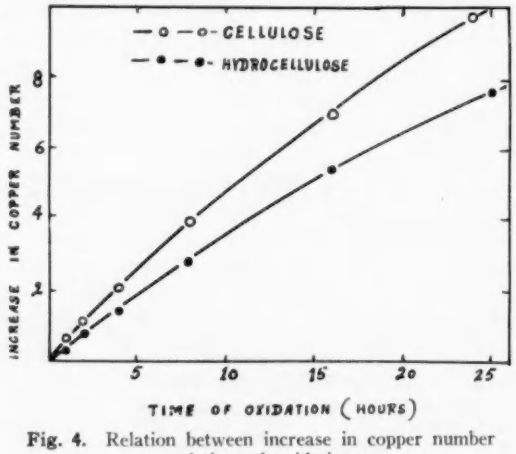

Fig. 4. Relation between increase in copper number and time of oxidation.

hydrocellulose respectively and time of treatment with dichromate is shown in Figures 4 and 5. These figures show good similarity to the relationship shown in Figure 2. Increase in copper number and increase in carboxyl content for various dichromate-oxidized samples is related to oxygen consumption and is shown in Figure 6. It is seen that, for any one of the above properties, the results for both cellulose and hydrocellulose lie on the same straight-line graph. From this figure it is also seen that every milliatom of oxygen consumed by standard cellulose as well as by the hydrocellulose sample during dichromate treatment results in an increase of 0.29 in copper number and of 0.23 milliequivalents of carboxyl groups in the sample. In spite of the presence of a large amount of potential aldehyde groups in the hydrocellulose available for oxidation, the mechanism of oxidation of both the fibers with this reagent appears to be similar, but the extent of oxidation of hydrocellulose is consistently lower than that of standard cellulose. The lowering of oxidative susceptibility of cellulose on progressive hydrolysis is discussed later.

Oxidation of cellulose and hydrocellulose is carried out, replacing potassium dichromate and sulfuric acid by dichromate and oxalic acid; the results are shown in Figure 7. It is seen that increase in copper number in this case also is similar to that in the case of former oxidizing agent. From a study of the chemical properties of the resultant oxycelluloses (described in Table I) it is seen that mechanism of oxidation of both fibers is similar in nature. The exact amount of oxygen uptake in the oxidation reaction with dichromate + oxalic acid cannot be estimated, but from the value of increase in copper number and increase in carboxyl content after oxidation treatment it appears that cellulose takes up more oxygen than hydrocellulose under identical conditions of oxidation.

The oxycelluloses obtained by the action of the above two oxidizing agents on cellulose and hydrocelluloses were treated with chlorous acid and analyzed. From results of analysis, described in Table I, ratio of increase in carboxyl content and decrease in copper number of the oxycellulose sample is calculated. In the case of oxycelluloses obtained by the action of dichromate–sulfuric acid, the value of the ratio is found to be 1.5 but for oxycelluloses formed by the action of dichromate–oxalic acid, the value of the ratio is found to be 1. The amount of

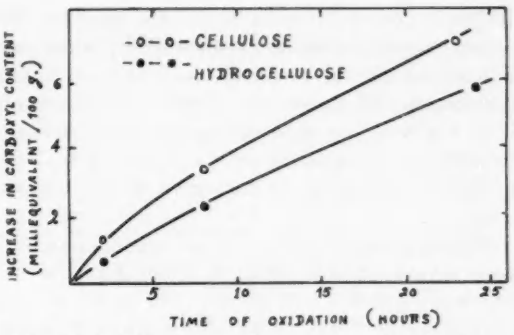

Fig. 5. Relation between increase in carboxyl content and time of oxidation.

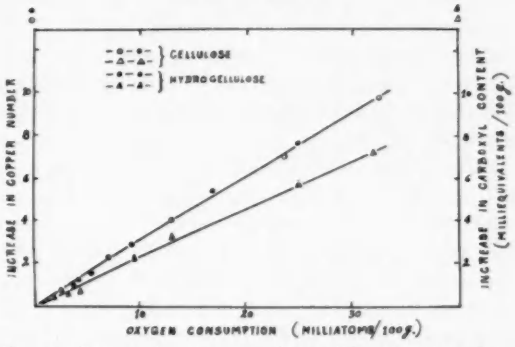

Fig. 6. Increase in copper number and increase in carboxyl content related to the oxygen consumption.

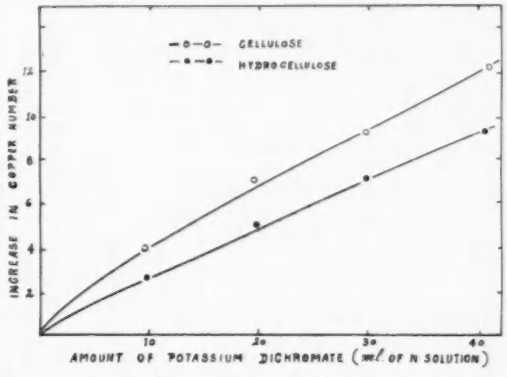

Fig. 7. Relation between increase in copper number and amount of potassium dichromate added to oxalic acid.

copper reduced from cupric to cuprous stage by one free aldehyde group in the two types of oxycelluloses was also calculated from decrease in copper number and increase in carboxyl content after chlorous acid treatment (assuming that oxidation of one free aldehyde group of the oxycellulose by chlorous acid resulted in the formation of one new

carboxyl group). It is found that the quantity, "the copper equivalent of the aldehyde group," for oxycelluloses from standard cellulose and from hydrocellulose by the action of sulfuric acid–dichromate is 10.5 atoms of copper and that for similar products by action of dichromate–oxalic acid is about 14 atoms of copper reduced from the cupric to the cuprous stage.

Results of the action of sodium hypobromite solutions having different pH on cellulose and on hydrocellulose are shown in Figure 8. The curves relating oxygen uptake to pH for both fibers are nearly parallel over the whole pH range examined. Oxidative behavior of the two fibers is similar to that observed earlier with the other two oxidizing agents. With sodium hypobromite as oxidizing agent, the ratio between oxygen consumption by standard cellulose and that by hydrocellulose is approximately 1.4 over the whole pH range. In spite of different chemical natures of the oxidizing agents and the influence of pH on rate of oxygen transfer, similarity in the value of this ratio over the whole pH range with the ratio obtained with dichromate–sulfuric acid appears to be significant. Results of oxygen consumption by cellulose and hydrocellulose using potassium permanganate as the oxidizing agent are shown in Figure 9. Results using these solutions over a wide range of pH, both for cellulose and hydrocellulose, run nearly parallel to one another. The ratio between oxygen uptake by cellulose and that by the hydrocellulose is approximately 1.3. The similarity of the ratios with the three oxidizing agents in spite of their different oxidative mechanisms indicates that in each case the mechanism of oxidation both for cellulose and hydrocellulose is the same. The extent of oxidation is governed by the oxidative susceptibility. If the curves for potassium permanganate in Figure 9 are further examined, it is found that above pH 7 their position slowly alters and after a pH of about 8.5 complete reversal of their positions takes place. The oxygen uptake by hydrocellulose becomes greater than that by standard cellulose. This change in the position of the curves above pH 8.5 might be due to preferential oxidation of the potential aldehyde groups in the hydrocellulose by alkaline permanganate, resulting in a higher consumption of oxygen by hydrocellulose than by standard cellulose. Considerable support to this view is obtained from results given in Figure 10, where effect of the action of alkaline permanganate (pH 9) on a series of hydrocelluloses with increasing copper number is shown. It is found that the oxygen consumption by

TABLE I. Chemical Properties of Dichromate Oxycelluloses Before and After Chlorous Acid Treatment

Material	Conditions of oxidation	Time of oxidation, hr.	Copper number: Before treatment A	Copper number: After treatment B	Copper number: Difference, A − B	Carboxyl content: Before treatment C	Carboxyl content: After treatment D	Carboxyl content: Difference, D − C	Ratio $\frac{D-C}{A-B}$	Copper equivalent	
Standard cellulose (Cu No. 0.03)	0.1 *N* Sulfuric acid +0.1 *N* potassium dichromate	2	1.20	0.19	1.01	1.87	3.35	1.48	1.46	10.78	Mean 10.71
	Same	8	3.93	0.72	3.21	3.94	8.71	4.77	1.49	10.57	
	Same	24	9.76	0.83	8.93	7.70	20.75	13.05	1.46	10.78	
Hydrocellulose (Cu No. 3.17)	Same	2	4.04	1.27	2.77	1.20	5.35	4.15	1.50	10.50	Mean 10.53
	Same	8	5.62	1.27	4.35	2.88	9.38	6.50	1.49	10.57	
	Same	24	10.86	1.82	9.04	6.30	20.10	13.80	1.50	10.50	
Standard cellulose (Cu No. 0.03)	Amounts of 2 *N* dichromate added to 2 *N* oxalic acid										
	10	3	3.96	0.08	3.88	1.68	6.36	4.68	1.19	13.23	
	20	3	6.96	0.25	6.71	3.36	11.10	7.74	1.15	13.70	Mean 14.04
	30	3	9.15	0.62	8.53	4.60	14.80	10.20	1.19	13.23	
	40	3	12.18	0.84	11.34	6.60	18.50	11.90	1.05	15.00	
Hydrocellulose (Cu No. 4.14)	10	3	6.84	2.16	4.68	2.53	7.47	4.94	1.05	15.00	
	20	3	9.18	2.40	6.78	3.98	11.13	7.15	1.06	14.86	Mean 14.81
	30	3	11.16	2.90	8.26	5.53	14.84	9.41	1.13	13.93	
	40	3	13.50	2.90	10.60	6.11	16.97	10.86	1.02	15.44	

a series of hydrocelluloses increases with an increase in their copper number. This means that, under alkaline conditions of treatment at a constant pH, a hydrocellulose sample having higher number of potential aldehyde groups takes up more oxygen than one having a lower number of potential aldehyde groups. This behavior of hydrocelluloses towards alkaline potassium permanganate solutions appears to be contrary to that observed with acidic permanganate solutions (Figure 11). In this case increase in copper number of the hydrocellulose results in a decrease in oxygen consumption; after a copper number of 4.5 is reached oxygen consumption reaches a constant value which is not affected by further increase in copper number.

The study of the oxidation of cellulose and one hydrocellulose was extended to products of progressive hydrolysis obtained from standard cellulose, mercerized standard cellulose, and viscose. The unhydrolyzed fibers and the hydrocelluloses prepared from them were treated with a mixture of 0.1 *N* sulfuric acid and 0.1 *N* potassium dichromate for a period of 24 hr.; oxygen consumed in each case was estimated. Results of these experiments are described in Figures 12, 13, and 14. From these figures it is seen that, with an increase in the degree of hydrolysis, the products of hydrolysis show a decrease in the amount of oxygen consumed. For each of the fiber substances the rate of decrease in oxygen consumption is rapid in the initial stages of hydrolysis, but becomes less pronounced and ultimately reaches a constant value as the hydrolysis proceeds further. In the case of standard cellulose

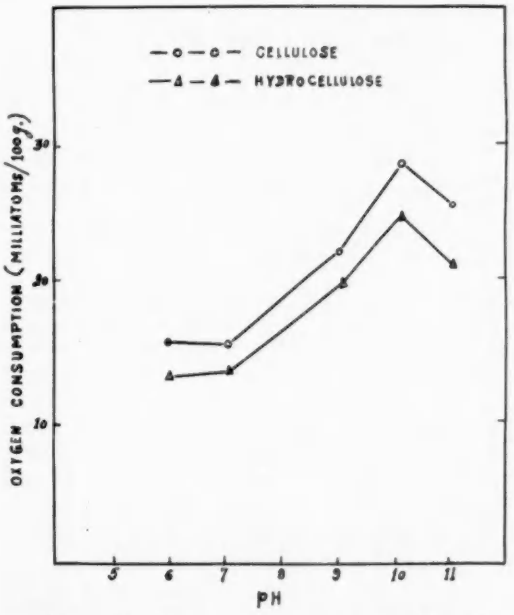

Fig. 8. Relation between oxygen consumption and pH of sodium hypobromite solution.

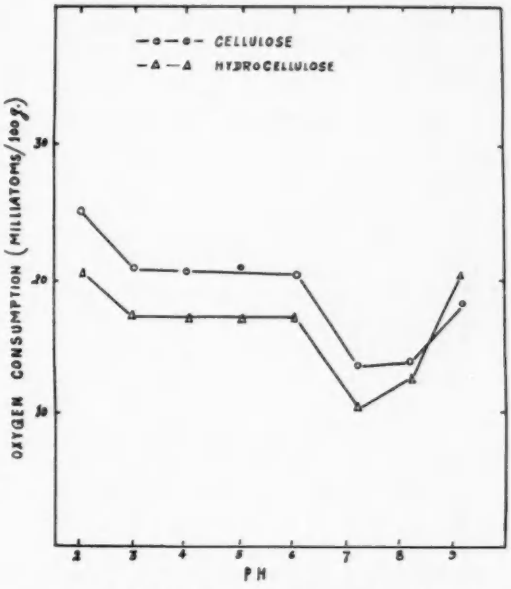

Fig. 9. Relation between oxygen consumption and pH of potassium permanganate solution.

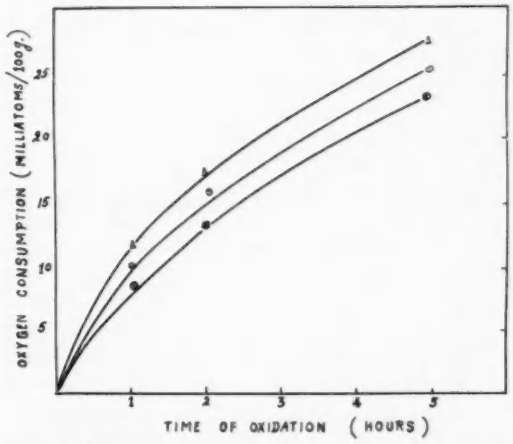

Fig. 10. Relation between oxygen consumption and time of oxidation with alkaline potassium permanganate (pH 9.1) for (×) standard cellulose, (⊙) hydrocellulose (Cu No. 2.5), and (△) hydrocellulose (Cu No. 3.15).

(Figure 12), oxygen uptake comes to a constant value after a copper number of about 4.5 is reached. In the case of mercerized fibers (Figure 13) both with and without tension, oxygen consumption reaches a constant value after a copper number of about 8.2 is reached. In the case of viscose (Figure 14), oxygen consumption reaches a constant value after a copper number of about 16 is reached.

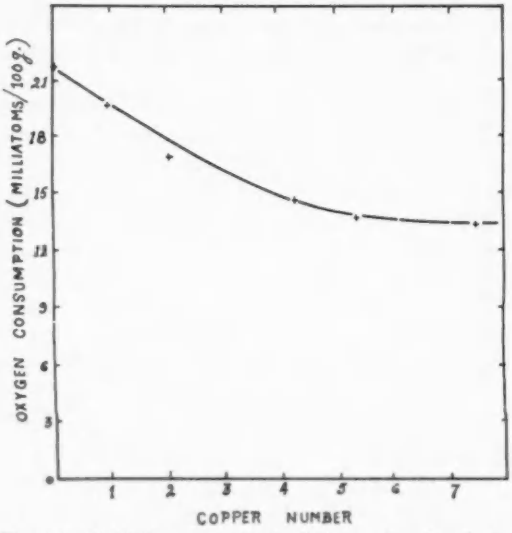

Fig. 11. Oxidation of standard cellulose and various hydrocelluloses by acidic potassium permanganate (pH 5).

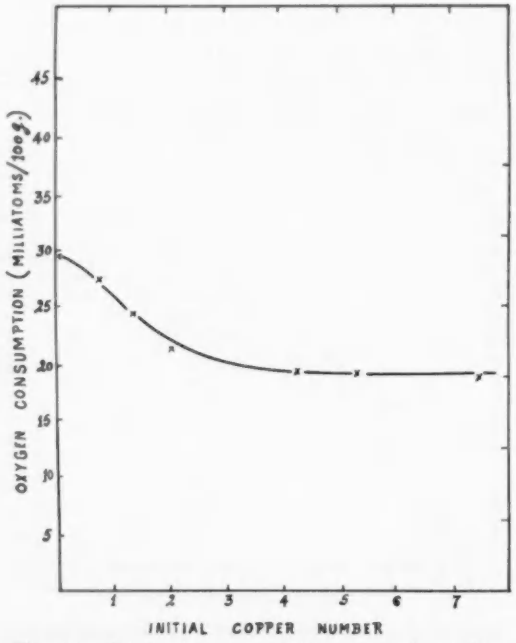

Fig. 12. Relation between initial copper number and oxygen consumption in dichromate oxidation of standard cellulose and hydrocelluloses prepared from it.

Hydrocellulose samples from standard cellulose after treatment with sulfuric acid + potassium dichromate were also examined for increase in reducing value (copper number) and carboxyl content. Relation between the original copper number of these hydrocelluloses and increase in copper number and carboxyl content after oxidation is shown in Figure 15. It is seen that, during oxidation, both increase in copper number and increase in carboxyl content decrease continuously and reach a constant value at a stage where the hydrocellulose sample had an original copper number of about 4.5. The same behavior is observed with oxygen uptake (Figure 12).

In general, oxidative reactivity of the various fibers examined above decreases with progressive hydrolysis, but the stage at which the reactivity comes to a constant value appears to depend on the fiber substance being oxidized.

A detailed investigation of the changes in other properties of standard cellulose (*viz.*, DP, moisture regain, and density) brought about as a result of hydrolysis is also carried out. The results of these experiments are shown in Figure 16. It is seen that the properties (both at 75% RH and 30% RH) reach a constant value at more or less the same stage of hydrolysis at which oxygen consumption also reaches a constant value.

In Table II, results of the effect of progressive hydrolysis on the degree of shrinkage of standard

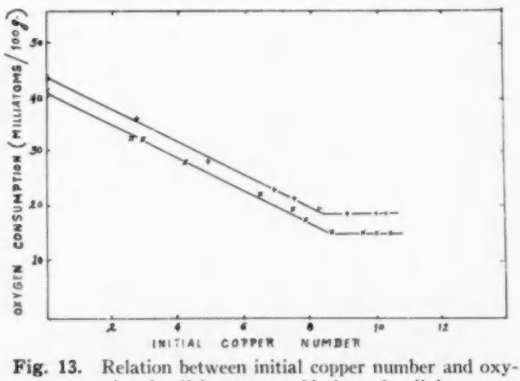

Fig. 13. Relation between initial copper number and oxygen consumption in dichromate oxidation of cellulose mercerized with (×) and without (+) tension and hydrocelluloses prepared from them.

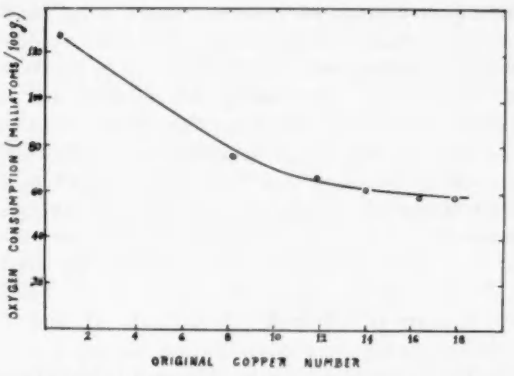

Fig. 14. Relation between initial copper number and oxygen consumption in dichromate oxidation of viscose and hydrocelluloses prepared from it.

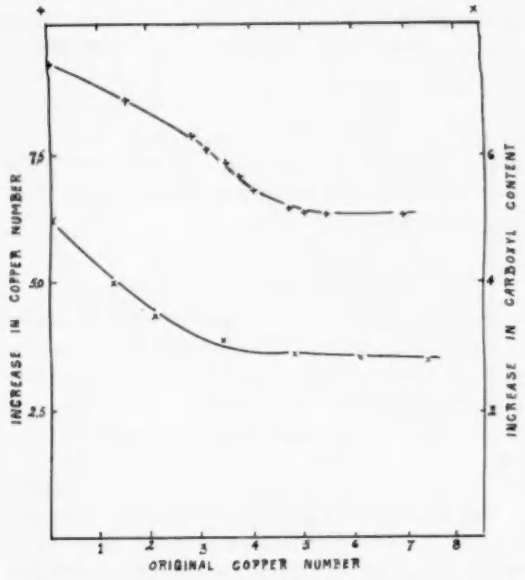

Fig. 15. Increase in copper number (+) and increase in carboxyl content (×) after dichromate oxidation related to the original copper number of the sample.

cellulose yarn in a solution containing 150 g./l. sodium hydroxide are given. Mechanical difficulties in handling hydrocellulose samples in alkaline medium prevented a detailed investigation, but the changes in shrinkage obtained with two hydrocellulose samples having copper number 1.05 and 2.82 respectively and that for standard cellulose yarn (copper number = 0.02) could be examined. The shrinkage of 12.6% and 10.8% for these hydrocelluloses and 15.3% for standard cellulose is significant

TABLE II. Shrinkage of Standard Cellulose Double Yarn in Sodium Hydroxide Solution (150 g./l.)

Temperature 30° C. Time 30 min.

Sample	Copper number	Mean percent shrinkage in length (Mean of 15 separate determinations)
Standard cellulose	0.03	15.32
Hydrocellulose A_1	1.05	12.51
Hydrocellulose B_1	2.82	10.85

and is in accordance with the changes in other properties mentioned above.

Hydrolysis of cellulosic fibers by dilute acids has mainly served as an indirect means for the evaluation of the relative amounts of crystalline and noncrystalline portions in cellulosic fibers. In all reactions such as dyeing, moisture absorption, oxidation, etc. the portion of the fiber substance normally available for reaction under any specified set of conditions is defined as the accessible portion of the fiber substance. The rest is nonaccessible or the crystalline portion. During mild hydrolysis a loss in weight of the fiber substance occurs, probably due to the removal of portions of the accessible regions [1, 10].

The immediate noticeable effect of acid treatment on cellulosic fibers is the loss in tensile properties. Simultaneously, cleavage of the 1:4 linkages in the chain structure results in the formation of new potential aldehyde groups and the reducing value (copper number) of the product increases. Under the specified hydrolysis treatment for standard cellulose described here, the copper number increases to about 9 at the end of a treatment of about 45 days but beyond this time of treatment the copper number remains practically constant. With cellulose mercerized under tension, the copper number reaches a constant value of 10.5 after 37 days of acid treatment; for cellulose mercerized without tension, a copper number of 10 is reached after 32 days of treatment. In the case of viscose, this stage occurs after 14 days of treatment, resulting in a copper number of about 18. Examination of the results of changes in copper number obtained for standard cellulose (Figure 1) and the results of changes in DP during progressive hydrolysis (Figure 16) shows that the copper number continues to increase even after DP reaches a constant value. During progressive acid treatment DP drops from 2540 to 370 at

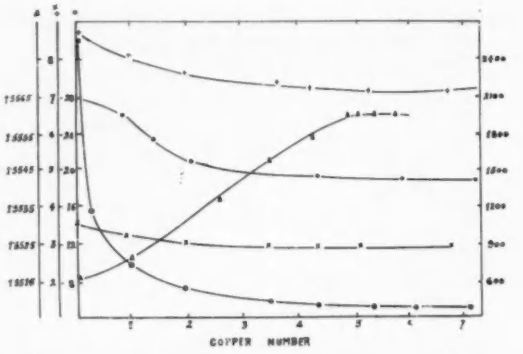

Fig. 16. Relation between copper number and different fiber characteristics of standard cellulose during mild acid hydrolysis: (△) density, (+) moisture regain, percent, at 75% RH, (×) moisture regain, percent, at 30% RH, (●) oxygen consumption during dichromate oxidation (milliatoms/100 g.), and (⊙) DP.

the end of 11 days of treatment and remains practically constant with a continued acid treatment up to a period of 50 days. The stage at which DP reaches a constant value corresponds to a copper number of about 4.5 (Figure 16), which also is the same stage of hydrolysis at which oxygen consumption reaches a constant value (Figure 12).

It is interesting that, during hydrolysis of standard cellulose, the copper number continues to rise (Figure 1) even after the DP has reached a constant value. This means that acid attack on cellulose substance continues to take place with the formation of new reducing groups even after the leveling of DP occurs. During acid treatment, reducing groups can be formed only by splitting of 1:4 glucosidic linkages in cellulose chains. An explanation of this behavior may be found in the following. During continued acid treatment of cellulose, chain segments of certain dimensions may be formed which, though not dissolved by the acid, may not contribute to changes in the viscosity of cuprammonium hydroxide solutions of the residue. Formation of such segments in the substance may result in an increase in copper number due to the presence of potential aldehyde groups. The results of Achwal, Daruwalla, Nabar, and Subramaniam [1] support the above suggestions. These authors have shown that, during progressive hydrolysis of standard cellulose, mercerized cellulose, and viscose loss in weight continues to occur even after DP reaches a constant value. Small but consistent loss in weight during acid attack on the fibers continued to occur even after the copper number reached a constant value. Such a behavior would indicate an attack on the crystallite proper, resulting in a slow etching out of the ends of the crystallite, contributing only to small loss in weight but not to any measurable changes in DP. It is probable that even DP of the product may show noticeable changes if acid attack is continued over much longer periods than those used in the present investigation; after a sufficiently long contact with acid, the substance may become completely dissolved.

From what has been said, it can be concluded that changes in oxidative susceptibility of standard cellulose during progressive hydrolysis are closely connected with simultaneous changes brought about in fiber properties (*viz.*, DP, moisture regain, density, and shrinkage or swelling). Daruwalla and Nabar [10] have shown that progressive hydrolysis of standard cellulose fibers brings about a simultaneous increase in crystallinity and a decrease in dye adsorption and that both these properties reach a constant value at that stage of hydrolysis at which the copper number reaches a value of about 4.5. It is interesting that this stage corresponds to the stage at which oxygen consumption by the fiber substance also comes to a constant value.

Summary and Conclusions

Action of various oxidizing agents on the products of mild acid hydrolysis of cellulosic fibers is investigated. Study of the oxidation of a cellulose and a hydrocellulose by dichromate and sulfuric acid shows that the mechanism of oxidation, both for cellulose and hydrocellulose, is essentially the same, as shown by linear relationships between increase in copper number or carboxyl content with the oxygen consumption and constancy of the ratios of increase in carboxyl content to decrease in copper number after chlorous acid treatment. Hydrocellulose, however, shows a marked reduction in oxidative susceptibility.

Oxidation of cellulose and a hydrocellulose by potassium dichromate in the presence of oxalic acid and by sodium hypobromite over the pH range also shows that in each case the mechanism of oxidation is the same for cellulose and hydrocellulose, the potential aldehyde groups not affecting the course of oxidation.

Oxidation by potassium permanganate up to a pH of 8.5 also follows a similar course, but above this pH the potential aldehyde groups become oxidized,

resulting in a higher oxygen consumption of hydrocellulose than cellulose.

Progressive mild acid hydrolysis of cellulose causes a rapid decrease in oxidative susceptibility in the initial stages of hydrolysis which later becomes less pronounced; ultimately there is a tendency to level off. These changes in oxidative susceptibility are closely connected with simultaneous changes brought about in other fiber characteristics (*viz.* DP, moisture regain, density, and shrinkage).

Literature Cited

1. Achwal, W. B., Daruwalla, E. H., Nabar, G. M., and Subramaniam, P., *J. Polymer Sci.*, **35**, 93 (1959).
2. Astbury, W. T., *Nature* **126**, 913 (1930).
3. Astbury, W. T., *J. Soc. Dyers Colourists* **49**, 169 (1933).
4. Battista, O. A., *Ind. Eng. Chem.* **42**, 502 (1950).
5. Battista, O. A., *Ind. Eng. Chem., Anal. Ed.* **16**, 351 (1944).
6. Birtwell, C., Clibbens, D. A., Geake, A., and Ridge, B. P., *J. Textile Inst.* **21**, T85 (1930).
7. Brenner, F. C., Frilette, V., and Mark, H., *J. Am. Chem. Soc.* **70**, 877 (1948).
8. Clibbens, D. A. and Ridge, B. P., *J. Textile Inst.* **18**, T135 (1927).
9. Committee of the Division of Cellulose Chemistry of American Chemical Society, *Ind. Eng. Chem., Anal. Ed.* **16**, 748 (1944).
10. Daruwalla, E. H. and Nabar, G. M., *J. Polymer Sci.* **20**, 205 (1956).
11. Davidson, G. F., *J. Textile Inst.* **34**, T87 (1943).
12. Davidson, G. F. and Nevelle, T. P., *J. Textile Inst.* **39**, T102 (1948).
13. Doree, C. and Healey, A. C., *J. Soc. Dyers Colourists* **49**, 290 (1933).
14. Fabrics Research Committee, D.S.I.R., "Viscosity of Cellulose Solutions," H.M.S.O., London, 1932.
15. Heyes, T. F., *J. Soc. Chem. Ind.* **47**, T90 (1928).
16. Hiller, L. A. and Pacsu, E., TEXTILE RESEARCH JOURNAL **16**, 490, 564 (1946).
17. Howsmon, J. A., TEXTILE RESEARCH JOURNAL **19**, 152 (1949).
18. Kasbekar, G. S. and Neale, S. M., *Trans. Faraday Soc.* **43**, 517 (1947).
19. Kratky, O. and Mark, H., *Z. Phys. Chem.* **36B**, 129 (1937).
20. Kratky, O., *Kolloid-Z.* **84**, 149 (1938).
21. Kulkarni, V. P. and Nabar, G. M., *J. Sci. Ind. Res. (India)* **15B**, 708 (1956).
22. Millett, M. A., Moore, W. E., and Saeman, J. F., *Ind. Eng. Chem.* **46**, 1493 (1954).
23. Meller, A., *J. Polymer Sci.* **10**, 213 (1953).
24. Nabar, G. M. and Padmanabhan, C. V., *Proc. Indian Acad. Sci.* **31–32**, 371 (1950).
25. Nabar, G. M. and Padmanabhan, C. V., *J. Soc. Dyers Colourists* **69**, 295 (1953).
26. Nickerson, R. F., *Ind. Eng. Chem.* **39**, 1507 (1947).
27. Orr, R. S., Weiss, L. C., Moore, H. B., and Grant, J. N., TEXTILE RESEARCH JOURNAL **25**, 592 (1955).
28. Preston, J. M. and Nimkar, M. V., *J. Textile Inst.* **41**, T446 (1950).
29. Tessler, S., Woodberry, N. T., and Mark, H., *J. Polymer Sci.* **1**, 437 (1956).

Manuscript received April 5, 1960.

The Heat Treatment of Orlon[1] Acrylic Fiber to Render it Fireproof

W. G. Vosburgh

Textile Fibers Department, E. I. duPont de Nemours & Company, Inc.
Wilmington, Delaware

Abstract

A method for preparing a black, fireproof textile fiber candidate (called Fiber AF) from Orlon[1] is described. Fiber AF is prepared by heat treating fibers or fabrics of Orlon, preferably the latter, in air at temperatures in excess of 160° C. The logarithm of the reaction time is inversely proportional to the heating temperature. The important variables found in the process were heating time and temperature, fabric construction, and heating atmosphere.

Fiber AF is *fireproof* and has an unusually high resistance to destruction upon short-time thermal irradiation. Fiber AF can resist thermal irradiation over 100-fold higher than ordinary clothing fabrics. Upon continued exposure to high temperatures, Fiber AF gradually loses its tensile properties. At 900° C., it is completely consumed in 3 hr. While Fiber AF has fair tensile properties, its transverse properties are poor, excluding its possible utility in various types of fireproof garments where good abrasion resistance is required.

Introduction

In recent years the flammability characteristics[2] of both natural [9] fibers and truly synthetic [2] fibers have received considerable attention in civilian and military markets. Although numerous methods are described in the literature for flameproofing natural [2] and synthetic fibers, inorganic fibers such as asbestos, glass, and Fiberfrax[3] remain as the only commercially available *fireproof* fiber candidates.

It was observed in these laboratories that when Du Pont's acrylic fiber, sold under the trademark Orlon, was heated in air above 150° C., an exothermic reaction took place resulting in the formation of a black fireproof textile[4] which retained up to 40% of the initial fabric tenacity. The purpose of this paper is to describe the process for producing AF both in the laboratory and on a semiworks scale

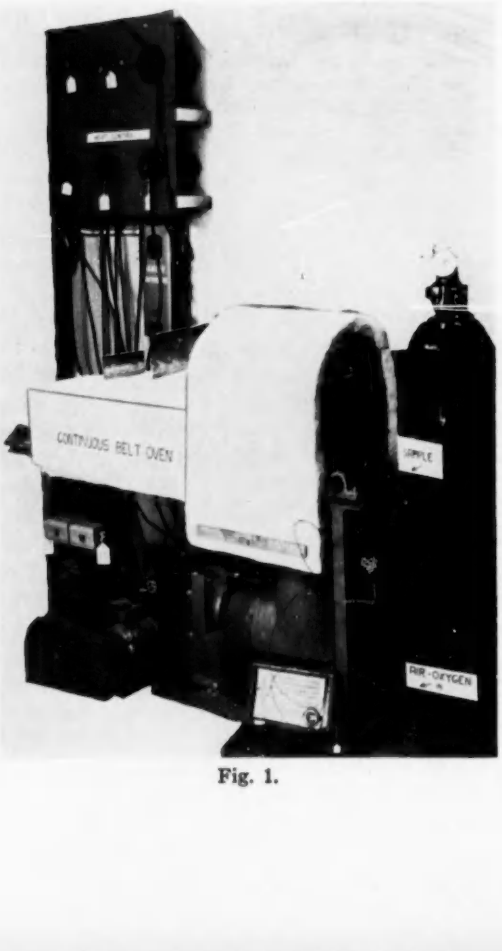

Fig. 1.

[1] Du Pont trademark.

[2] Fireproof will be defined as the total resistance to destruction of a material by fire, flameproof as the resistance of a material to self-combustion once the source of ignition has been removed (the material does not withstand the reaction of the fire without degradation), and flame resistant to materials which, although they may support combustion, burn at a slower rate than the untreated control.

[3] An aluminum silicate fiber manufactured by the Refractories Division of the Carborundum Company.

[4] The black, fireproof product resulting from this heat treatment will be referred to as "AF" in this paper.

together with a comprehensive list of properties and suggested uses for it.

Preparation of AF

For the laboratory preparation of AF in a batch process, almost any type of forced-draft oven capable of operating at temperatures in excess of 200° C. can be used successfully. In this work most of the small laboratory samples were prepared (batch process) by use of a Precision Scientific, No. 845-94, Type A forced-draft oven. For the laboratory preparation of AF in a continuous process, 3-in. strips of Orlon were passed on a moving metal belt at a controlled rate through a hot controlled atmosphere. A picture of this apparatus is shown in Figure 1. Other methods of heat treating Orlon acrylic fiber, such as passing the fabric between heated metal rolls or heating it in a hot inert bath of oil or metal, resulted in only extremely weak and brittle products.

For the pilot-plant preparation of AF, a high-temperature curing tower (Mica Insulator Company) 16 ft. high, consisting of two zones capable of being heated to different temperatures, was used successfully. Orlon fabric was strung up in the curing tower (represented schematically in Figure 2) by means of a glass fabric streamer and started through at 5 yd./hr. output speed with a holdup time of 2 hr. The temperature in Zone 1 was maintained at 250° ± 5° C. and Zone II at 260° ± 5° C. In order to reduce tension on the fabric, the use of tension rolls on the input side was eliminated and the fabric was overfed, so that the only tension on the fabric in Zone 1 was its own weight. By this technique, several samples of AF fabric were prepared for evaluation.

In the detailed study of the laboratory preparation of AF the following reaction conditions were examined and defined.

Temperature–Time

It was found that the logarithm of the time necessary to convert Orlon fabrics to AF was inversely proportional to the environmental temperature in the temperature range of 150–300° C. (Figure 3). This same time–temperature relationship was observed for the rate of thermal decomposition of bulk

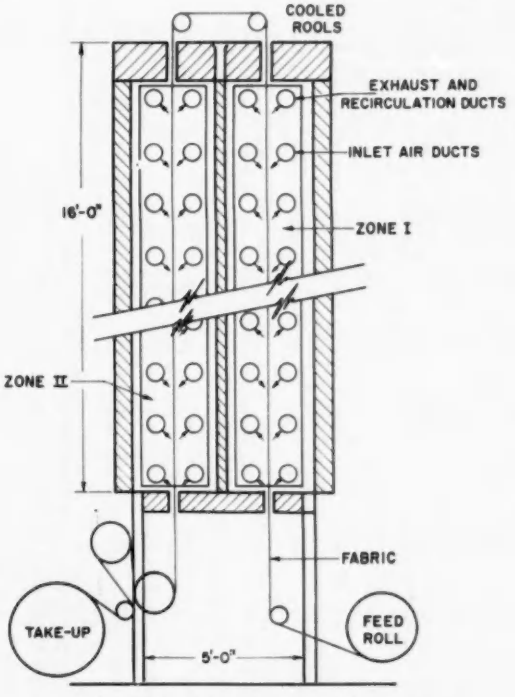

Fig. 2. High-temperature curing tower.

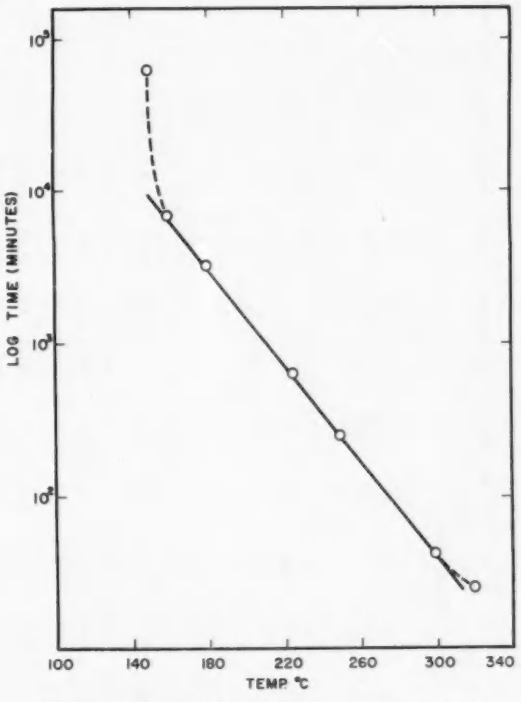

Fig. 3. Effect of oven temperatures on the rate of formation of AF.

TABLE I. The Effect of Fabric Construction on the Physical Properties of AF Yarns and Fabrics

	Fabric construction*																	
	Deering Milliken 4×2 Basket			8-Shaft satin			2×2 Twill			3×1 Twill			2×2 Basket			4×4 Basket			Tricot weave		
Fabric tests	Orig.	AF	% Retained	Orig.	AF	% Retained	Orig.	AF	% Retained	Orig.	AF	% Retained	Orig.	AF	% Retained	Orig.	AF	% Retained	Orig.	AF	% Retained
Wt., oz./yd.²	4.7	9.4	200	6.4	12.1	189	4.9	9.8	200	5.0	10.0	200	4.9	9.6	196	5.0	9.6	192	5.0	7.5	150
Pick count, W×F	84×46	118×60		68×52	88×66		52×40	66×53		52×40	61×54		52×40	68×54		52×40	69×54		52×40	70×52	
Abrasion, Stoll	4115	145	3.5	4037	41	1.0	10,936	91	0.8	8925	49	0.5	6700	62	0.9	1351	69	5.1	5611	165	2.9
Burst strength	>120	116		>120	>120	—	>120	102		>120	87		>120	93		>120	>120		>120	85	
Tongue tear, lb.	30	6.9	23	25	6.3	25	19.2	3.8	20	14.2	2.5	18	27.5	5.0	18	Yarn pulled out	25	—	17.5	2.7	15
Porosity, cfm./ft.² at ½ in. head H_2O	110.0	4.6	4.2	21.0	8.8	42	29.5	2.9	9.8	57.5	5.25	9.1	37.0	1.91	5.2	3000†	100.0	—	16.5	0.9†	—
Grab test	112	87	78	282	95	34	211	94	44	225	72	32	174	72	41	107	72	67	198	79	40
elongation, %	2.4	1.2	50	2.6	1.1	42	2.4	1.4	58	2.5	1.5	60	2.3	1.2	52	2.2	0.71	32	2.1	0.91	43
Flex test		240,000			4700			3600			3000			3600						2400	
Flame resistance	None	Fire proof		None	Fire proof		None	Fire proof		None	Fire proof		None	Fire proof		None	Fire proof		None	Fire proof	
Yarn tests																					
Denier	203	298	147	416	582	140	414	574	139	414	584	141	410	574	140	408	586	143	402	586	146
Ten., dry, g./den.	4.60	0.84	18	3.82	1.09	29	3.93	0.90	23	3.75	0.48	13	3.80	0.84	22	3.89	1.52	39	3.80	0.82	22
Elong., dry, %	17.4	2.8	16	17.1	2.3	13	15.2	1.7	11	14.7	2.2	15	14.8	1.2	8	15.5	2.4	15	14.6	1.3	9
Ten., wet, g./den.	4.46	0.71	16	3.51	1.17	33	4.00	1.09	27	3.82	0.70	18	4.02	1.00	25	3.95	1.20	30	3.94	0.85	22
Elong., wet, %	18.0	5.4	30	15.8	3.3	21	16.7	2.6	16	16.1	1.9	12	16.8	2.4	14	15.9	3.4	21	16.2	2.6	16
Ten., dry, loop	3.53	0.64	18	3.57	1.05	28	3.42	0.59	17	3.46	0.52	15	3.30	0.78	24	3.34	1.18	35	3.65	0.71	19
Elong., %	13.9	1.9	14	15.1	2.1	14	13.5	1.9	14	13.9	1.4	10	13.6	1.9	14	13.0	2.0	15	13.6	1.7	12
Flex abrasion life, cycles	10,000+	31		10,000+	3		10,000+	8		10,000+	0		10,000+	0.5		10,000+	2		10,000+	0.5	
Abrasion, yarn-on-yarn	794	4	0.5	—	6	—	557	13	2.6	482	8	1.7	390	6	1.5	614	5	0.8	127	4	3.1
Impact str., g. cm./den.	2.71	0.18	7	2.75	0.18	7	2.64	0.23	9	2.67	0.20	8	2.67	0.20	8	2.63	0.31	12	2.66	0.30	11
Percent tensile rec. at 1%	88	80		95	89		89	100		84	99		88	100		76	97		85	98	
Percent of work rec. at 3%	25	Broke		26	Broke		25	Broke		23	Broke		23	Broke		23	Broke		23	Broke	
Percent of stress decay at 3%	37.6	Broke		39	Broke		37.6	Broke		39.7	Broke		39.1	Broke		39.7	Broke		39.1	Broke	
Initial modulus	59	25	42	46	24	52	52	18	35	55	16	29	59	20	34	64	29	45	58	16	28
Zero str. temp., °C.																					
At 0.25 g./den. load**	192	620		194			199			196			196			199	605		198	584	
At 0.1 g./den. load	289	653		312	658		302	621		312	636		311	656		302	632		305	654	

* Fabrics were heated 4 hrs. at 275–80° C. in a forced-draft oven.
† Estimate; value outside range of testing apparatus.
‡ Determined on one-half of warp strand.
** The zero-strength temperature varies with the stress applied during the test.

TABLE I. The Effect of Fabric Construction on the Physical Properties of AF Yarns and Fabrics—(Continued)

	8-Shaft dobby			8-Shaft satin			Padduck cloth			Marquisette			Taffeta			Reverse jersey tricot			Plain weave‡‡		
Fabric tests	Orig.	AF	% Retained	Orig.	AF	% Retained	Orig.	AF	% Retained	Orig.	AF	% Retained	Orig.	AF	% Retained	Orig.	AF	% Retained	Orig.	AF	% Retained
Wt., oz./yd.²	5.0	10.8	216	4.9	9.8	200	64.6	139.8	216	6.0	—	—	1.80	3.33	185	6.5	12.1	187	7.2	13.7	191
Pick count, W×F	52×40	70×55		52×40	68×54	—	—	—	—	—	—	—	—	—	—	—	—	—	—	—	—
Abrasion, Stoll	3785	142	3.7	5186	52	1.0	—	—	—	—	—	—	—	—	—	—	—	—	—	—	—
Burst strength	>120	>120		>120	109		—	—	—	—	—	—	117	54	46	—	—	—	—	—	—
Tongue tear, lb.	17.5	4.3	25	20	9.4	47	20	14	70	—	—	—	—	—	—	—	—	—	—	—	—
Porosity, cfm./ft.² at ½ in. head H₂O	120.0	19.2	16	76.0	30.0	39	—	—	—	—	—	—	—	—	—	—	—	—	—	—	—
Grab test	200	112	56	122	98	80	—	—	—	—	—	—	—	—	—	—	—	—	—	—	—
elongation, %	2.5	1.7	68	2.2	1.2	55	—	—	—	—	—	—	—	—	—	—	—	—	—	—	—
Flex test		5100			280,000		—	—	—	—	—	—	—	—	—	—	—	—	—	—	—
Flame resistance	None	Fire proof		None	Fire proof		None	Fire proof		None	Fire proof		None	Fire proof		None	Fire proof		None	Fire proof	
Yarn tests																					
Denier	410	612	149	406	590	145	3020†	4236†	140	193	278	14.5	104	154	148	—	—	—	—	—	—
Ten., dry, g./den.	3.64	1.02	28	4.01	1.51	38	3.95†	0.45†	14	4.61	0.73	15.8	3.98	0.77	19.3	3.95††	—	—	2.1††	—	—
Elong., dry, %	14.6	1.7	12	15.1	3.0	20	18.5†	2.2†	18.7	15.5	3.1	20	15.3	4.1	26.8	16.5††	—	—	—††	—	—
Ten., wet, g./den.	3.74	0.95	25	4.00	1.28	32	—	—	—	—	—	—	—	—	—	—	—	—	—	—	—
Elong., wet, %	15.9	2.8	18	16.2	4.6	28	—	—	—	—	—	—	—	—	—	—	—	—	—	—	—
Ten., dry, loop	3.28	0.91	28	3.53	1.43	40	—	—	—	—	—	—	—	—	—	—	—	—	—	—	—
Elong., %	12.7	2.4	19	13.5	2.5	19	—	—	—	—	—	—	—	—	—	—	—	—	—	—	—
Flex abrasion life, cycles	10,000+	0.5		10,000+	3		—	—	—	6980	90	12.8	8550	80	9.4	—	—	—	—	—	—
Abrasion, yarn-on-yarn	559	6	1.1	602	3	0.5	—	—	—	—	—	—	—	—	—	—	—	—	—	—	—
Impact str., g. cm./den.	2.52	0.29	12	2.55	0.15	6	—	0.16	—	—	—	—	—	—	—	—	—	—	—	—	—
Percent tensile rec. at 1%	80	93		80	91		—	—	—	—	—	—	—	—	—	—	—	—	—	—	—
Percent of work rec. at 3%	23	Broke		22	Broke		—	—	—	—	—	—	—	—	—	—	—	—	—	—	—
Percent of stress decay at 3%	38.1	Broke		39.8	Broke		—	—	—	—	—	—	—	—	—	—	—	—	—	—	—
Initial modulus	53	27	51	57	20	35	—	—	—	—	—	—	—	—	—	—	—	—	—	—	—
Zero str. temp., °C.																					
At 0.25 g./den. load**	198	481		203	615		—	—	—	—	—	—	—	—	—	—	—	—	—	—	—
At 0.1 g./den. load	305	615		302	620		—	—	—	—	—	—	—	—	—	—	—	—	—	—	—

†† Too brittle to test.
‡‡ Staple yarn; all other fabrics are made of continuous filament yarn.

polyacrylonitrile. Hence, the greater the amount of Orlon fabric per unit area exposed to the heated atmosphere and/or the higher the heating temperature, the faster is the rate of conversion to AF and the more difficult it is to control this exothermic reaction. The following examples will suffice to show this effect. A fabric of Orlon (52.4 g.) was packed in an insulated beaker and placed in a hot oil bath maintained at 181° C. After the temperature of the interior of the fabric had reached the bath temperature, the temperature continued to rise and in 7.6 hr. had reached 221° C. Suddenly, a sharp increase in temperature was noted which, after 3 min., attained a maximum of 367° C. Almost immediately the temperature of the fabric dropped until bath temperature was reached. The resulting sample was a black, completely charred mass. This exothermic reaction can be even more dramatically demonstrated at higher oven temperatures. For example, 100-cm. samples of 2-ply 10/1 c.c. of Orlon acrylic staple yarns were wound in 2½-in. diameter skeins containing from 1 to 10 yarns each. The

TABLE II. Additional Physical Property Data of AF Fabrics

Fabric tests	Sample number 1	2	3	4	5	6	7
Weight, ounces per square yard	6.03	10.42	13.0	10.9	22.9	3.97	7.27
Pick count	70×46	80×61	80×64	40×26	96×74	—	—
Abrasion	740–1140*	230–450†	520†	1030†	620†	—	—
Bursting strength	>120	>120	>120	>120	>120	>120	>120
Tongue tear strength, lb.	Did not tear—pulled out	10.5	11	33	14	—	—
Porosity (cfm./sq. ft.; ½ in. H_2O manometer)	80.5	10.7	14.2	—	4.6	—	—
Liveliness, cm./sec.	57	74	65	47	75	—	—
Bending length	2.22	2.44	2.82	2.05	3.26	—	—
Wrinkle resistance	5.1	2.8	4.1	1.7	3.9	—	—
Wrinkle recovery	72	69	46	51	3	—	—
Crease angle	67	75	66	81	55	—	—
Fireproof	No	Yes	Not quite	No	Yes	No	Yes
Yarn tests (warp ends)							
Denier	400	524	551	820	1131	202.9	277.8
Dry tenacity—% elongation	4.1–15.2	1.0–6.4	1.5–7.5	5.1–18.9	1.1–5.4	4.20–16.3	0.66–5.0
Wet tenacity—% elongation	4.3–15.7	0.97–4.7	1.3–13.1	5.1–20.2	0.8–8.4	—	—
Dry loop—% elongation	3.7–13.2	0.88–2.5	1.1–4.3	3.2–12.9	0.8–3.7	—	—
Wet loop—% elongation	3.5–12.8	0.86–4.4	1.0–7.2	3.2–13.3	0.7–7.4	—	—
Dry knot—% elongation	2.5–8.7	0.88–3.5	1.3–4.7	2.2–7.2	0.9–3.4	—	—
Abrasion (yarn on yarn)	450	11	16	835	28	—	—
% Tensile recovery at 1%	85	96	97	96	53	—	—
% Tensile recovery at 3%	50	75	75	61	38	—	—
% Work recovery at 3%	25	48	36	32	45	—	—
% Stress decay at 3%	28	18.5	18	25	18	—	—
Impact strength (g. cm./den. cm.)	2.85	0.19	0.26	2.6	0.14	0.88	0.163
Initial modulus (at 1%)	60	25	26	58	25	—	—
Flex life‡ (0.1 g./den. load)	>2000	9–11	200	>2000	90	—	—
Zero strength temperature (0.5 g./den. load)	155–156° C.	>300° C.	—	—	—	—	—
Twist failure (0.1 g./den. load)	25	10.5	11.5**	18.5**	7.5**	—	—

* Run on Stoll Abrasion machine.
† Run on Taber Abrasion machine.
‡ This test was set up for comparison of these yarns only—not to be compared with other flex tests.
** At 0.2 g./den. load.

No. 1—Control A (8-shaft satin).
No. 2—Control A heated 2 hr. at 285° C. and scoured.
No. 3—Control A heated 4 hr. at 285° C. and scoured.
No. 4—Control B (8-shaft satin).
No. 5—Control B heated 11 hr. at 245° C. plus 2 hr. at 285° C. and scoured.
No. 6—Control C (3 × 1 twill)
No. 7—Control C heated 4 hr. at 285° C.

skeins were supported horizontally and heated for 5 min. at 300° C. in a forced-draft oven. The following observations were made:

Yarns/skein	Tenacity, g./den.	Remarks
1	1.55	Good hand, black, partial flame resistance, no evidence of thermal decomposition
2	1.57	Same remarks
3	1.59	Same remarks
4	1.31	Somewhat stiffer hand; other remarks the same
6	Weak and brittle	Extremely brittle spots in skein where the yarns had been packed together
10	Completely charred and degraded	Complete degradation of the entire skein

Identical Orlon acrylic yarns 50 cm. in length were arranged in parallel rows of 10, 20, and 40 yarns each simulating a fabric warp, clamped at the ends, and heated 5 min. at 300° C. in a forced-draft oven. In all cases, the heat-treated yarn appeared equivalent to the yarns from the 1–3 skeins described above. A single 50-cm. length of this same Orlon staple was completely degraded merely by winding it in a tight ball and subjecting it to the same heat-treating conditions (5 min. at 300° C.).

Fabric Construction

Two important requirements must be considered when choosing the fabric construction of the initial Orlon fiber for conversion to AF.[5] First, the heat from this highly exothermic reaction must be dissipated rapidly during the heat treatment; second, the large area shrinkage (40–45%) must be allowed for in the initial fabric structure. Tables I and II summarize the effect of initial fabric construction on the final properties of the AF yarn and fabric.

In general, the two best fabric constructions found were a 4 × 4 loose basket weave and an 8-shaft satin. Only very weak and brittle AF fabrics were obtained from a plain weave and a knitted fabric. The marquisette and taffeta fabrics had relatively porous constructions but, because of the tightness of the weaves, needed to maintain this construction, restrained shrinkage was encountered, causing excessive yarn tensions within the fabrics, resulting in considerable embrittlement. Staple yarns were more severely degraded during the heat treatment than continuous filament yarns.

[5] Orlon fiber can be converted with the proper heat treatment to AF but, because of the low transverse properties of AF, it is felt that it might be very difficult to weave fabrics from this yarn. Hence, fabrics of Orlon were converted by heat treatment directly to AF fabrics.

TABLE III. The Effect of Napping of Fabric of Orlon Acrylic Fiber on the Properties of AF

Heating time, hr. at 265° C.	Percent strength retained*		Remarks
	Unnapped	Napped	
0	100	100	Controls
8	24	41	Fireproof
10	24	36	Fireproof
16	14	—	Fireproof
24	10	24	Fireproof

* Breaking strength of a 1-in. warp strip of fabric.

A 12.6 oz./yd. 8-shaft satin which, because of its high fabric density, gave a weak AF fabric, was napped using sandpaper. Following an identical heat treatment, the napped fabric of Orlon fiber gave an AF fabric with a greater tenacity and a softer hand than the heat-treated control (Table III). The increased surface area of the napped fabric probably increased the rate of heat dissipation from the fabric during the heat treatment, thus lowering the internal fabric temperature.

Yarn that was raveled from a fabric of Orlon fiber and then converted to AF was always stronger than AF yarn that was raveled from an AF fabric.

Comparable fabrics of bright and semi-dull Orlon gave, under similar heat-treating conditions, similar AF fabrics. Hence, the presence of a delusterant, for example, TiO_2, did not appear to have any deleterious effects.

Heating Atmosphere

It was determined that oxygen was essential in the conversion of Orlon acrylic fiber to AF. Heat treatment in the absence of oxygen (nitrogen) gave only weak, brittle, reddish-yellow, flammable products. If the concentration of oxygen in the heating atmosphere was increased, both the rate of conversion at constant temperature of Orlon to AF and the area shrinkage were increased. The best balance of AF tensile properties was obtained at an oxygen level of 10–20%. The effect of the oxygen concentration on the preparation and properties of AF is shown in Figures 4 and 5.

The heat treatment of Orlon acrylic fiber in an atmosphere of chlorine in an attempt to catalyze the fireproofing reaction resulted in a violent reaction

at 275° C. with complete and immediate charring of the sample. At lower temperatures (175° C.) a weak and brittle AF fabric was obtained (2 hr.). At still lower temperatures (150° C.) no apparent reaction took place. If chlorine was mixed with air, the conversion of Orlon fiber to AF was accelerated. However, the resulting AF fabrics had inferior properties to samples prepared by an air heat treatment.

If a fabric of Orlon was heated (1 hr. at 275° C.) in an atmosphere of trimethylamine, a reddish-orange, partially degraded, flameproof fabric was obtained which resembles the material obtained from a heat treatment in nitrogen. If trimethylamine was mixed with various ratios of air, no change in the rate of formation of AF or change in properties of the resulting AF was noted.

Miscellaneous Process Modifications

If the initial tension on the fabric of Orlon was increased, the warp shrinkage of the resulting AF was reduced. However, both the tenacity and elongation of the AF were adversely affected (Figures 6 and 7).

Fiber AF was best prepared by employing an air velocity in the forced-draft oven of 1.5 to 18 ft./min. If the air velocity was increased above 25 ft./min. or lowered below 0.5 ft./min., a slight decrease in the physical properties of AF was found. Heat treatment in a static atmosphere, even if oxygen was supplied, was much inferior to a circulating atmosphere.

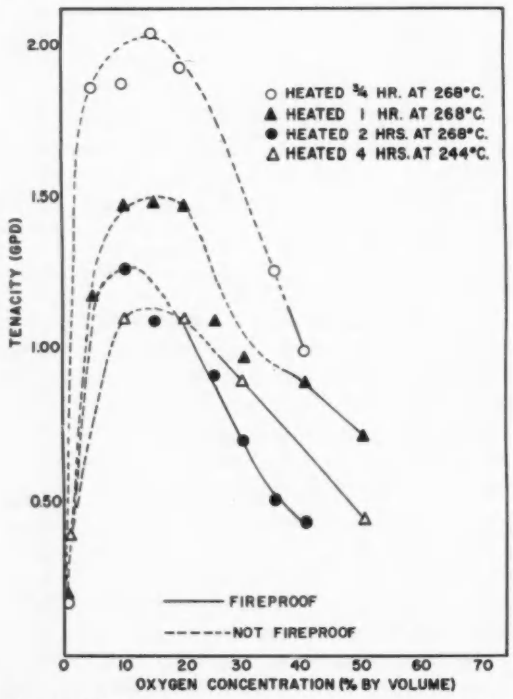

Fig. 4. Effect of oxygen concentration on the properties of heat-treated Orlon acrylic fiber.

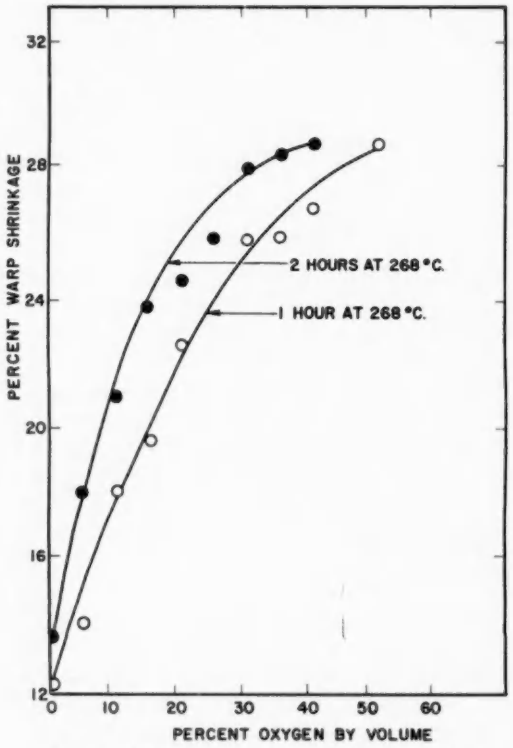

Fig. 5. Effect of oxygen concentration on warp shrinkage of AF fabrics.

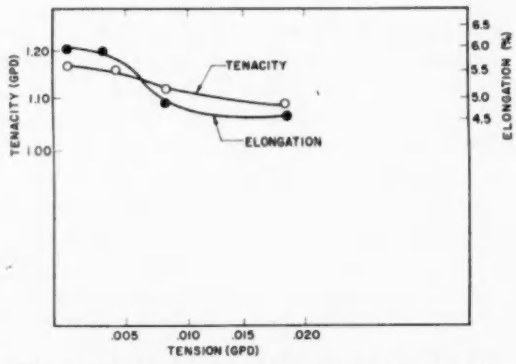

Fig. 6. Effect of tension during heat treatment on the tenacity and elongation of AF.

It was noted that scouring improved the hand of AF fabrics without noticeably changing the physical properties. The mechanical reaction of the scouring treatment probably relieves the internal stresses and strains set up within the fabric during the heat treatment. It is felt that by running the fabric through a button breaker or just mechanically flexing the fabric the same effect might be accomplished.

Catalysis of the Fireproofing Reaction

Since oxygen is essential in the preparation of AF the use of a hot, molten, oxidizing bath might be expected to catalyze the formation of AF and at the same time be a more efficient heat-transfer medium. However, only weak, brittle, flammable products were obtained when fabrics of Orlon acrylic fiber were heated in molten $NaNO_3$-$NaNO_2$ under a variety of conditions. No other heat-treating baths were tested.

Various oxidizing and reducing agents, free-radical scavengers, dehydrogenation agents, inert electrolytes, etc., were tested as possible catalysts for the conversion of Orlon to AF. Short lengths (25 cm.) of 2-ply 10/1 c.c. Orlon yarns were soaked for

TABLE IV. Effect of Catalysts on the Preparation of AF

Catalysts	Tenacity retained, %	Elongation retained, %	Shrinkage, %	Burning time, sec.
Unheated control	100	100	None	11
Heated control	32.6	24.3	15	20.6
Sulfur	54.1	45.6	14	18
o-Nitrophenol	53.7	47.8	11	20.4
p-Thiocresol	53.2	52.1	12	12.2
β-Naphthylamine	48.1	40.0	14	18.5
2,4-Dinitrochlorobenzene	45.7	35.4	15	11.8
Hexachloroethane	45.7	37.8	15	12.2
Maleic anhydride	45.7	36.4	14	8.2
o-Nitrophenol + hydroquinone (1:1)	44.2	34.7	14.5	15
Copper sulfate	43.8	28.1	16	17
Benzalazine	43.8	36.2	15	17
Malonic acid	42.0	33.3	15	12
Ferrous ammonium oxalate	39.8	30.8	16	13
Nickel oxalate (in dilute acetic acid)	39.6	35.0	16	17
Hydroxylamine	38.8	45.2	13	11.6
Boric acid	38.2	25.8	17	16.6
Ceric nitrate	38.0	32.1	14	13.2
Resorcinol	37.2	35.8	14.5	16
p-Methyl cyclohexanone	37.2	28.8	17	8
Diethyl malonate	37.2	28.0	17	23
m-Cresol	36.4	26.2	15	13.2
p-Phenylene diamine	35.8	20.3	13	15
p-Nitroaniline	34.2	33.4	14.5	14.5
Cobalt naphthenate	32.6	19.2	14	12.4
Urea	32.6	23.7	15	16
m-Phenylene diamine	31.2	19.5	14	15.6
Strontium oxide	30.7	20.6	14.5	7.2
Ferrous ammonium sulfate	30.7	17.8	15	11.2
Thiourea	28.2	16.2	14	14
Ammonium sulfate	27.0	16.4	17	22
Potassium dichromate	23.6	17.6	15	8
Sodium phosphite	21.1	9.2	13	25.2
Stannous chloride	19.2	10	14	17.4
Fluoboric acid	16.5	8.4	14	15.5
Nickel oxalate (in ammonium carbonate sol'n)	15.5	9.2	15	18
Chromic acid	15.5	3.8	12	12.4
Sodium hypophosphite	8.7	0.6	12	21.5
Hydroquinone	7.4	4.2	17	13.6
Sodium chloride	7.1	0.6	14	19
p-Nitrophenol	7.1	4.2	11	20.4
Sodium carbonate	5.9	3.8	15	11.2
Zinc chloride	4.3	2.5	17	21
Phosphorus pentasulfide	2.0	0.60	15	Flame resistant
Diethyl malonate + zinc chloride (3:1)	2.0	0.60	12	Flameproof

30 min. at room temperature in a 1–2% alcohol or water solution of the test reagents. The impregnated yarns were dried at room temperature and heated in air under conditions where the control yarn would not be converted to fireproof AF (10 min. at 300° C. in a forced-draft oven) in warp-type skeins of 4 yarns each. The burning time of the heated yarns was determined by measuring the length of time in seconds necessary for a 15-cm. length of yarn supported vertically to burn completely upon ignition of its free end. The average value of four determinations is reported. As summarized in Table IV, only phosphorus pentasulfide and zinc chloride + diethyl malonate appeared to have any catalytic effect on the rate of formation of AF from Orlon fiber. In both cases, the treated yarn was completely degraded. Sulfur, *o*-nitrophenol, and *p*-thiocresol appeared to improve the physical properties of the heat-treated Orlon; however, no improvement in the flammability characteristics was noted. Generally, the catalysts that gave heat-treated Orlon acrylic fiber with the best tensile properties were free-radical scavengers while catalysts that gave heat-treated Orlon with the poorest tensile properties were strong oxidizing or reducing agents.

Heat Treatment of Copolymers

The thermal stability of copolymers of polyacrylonitrile is considerably lower than the homopolymer. Hence, any heat treatment to convert copolymer compositions to AF should be carried out for shorter reaction times at slightly reduced temperatures. All the copolymers that were examined and that contained at least 85% acrylonitrile could be converted to AF by a heat treatment in air. It was felt that copolymers which contain less than 85% acrylonitrile could also be rendered fireproof by a proper heat treatment provided the melting or sticking point of the copolymer was above 165° C., the apparent lower limit of this fireproofing reaction.

TABLE V. Heat of Wetting of AF

Progressive heat treatment*	Heat of wetting, cal./g.
2½ hr. at 275° C.	21.6
½ hr. at 275° C.	20.4
½ hr. at 275° C.	19.3
Desiccator 1 hr.	15.2
Desiccator 17 hr.	18.2
6 hr. at 200° C.	21.6
16 hr. at 180° C.	21.6
8 hr. at 275° C.	21.7

* Progressive tests on the same sample of AF. Fabric was air-dried at 25° C. prior to each run.

Analytical Results

Since freshly prepared AF is extremely hygroscopic, analyses were made on an as-received basis and were corrected according to a Karl Fischer water determination [10]. As evidence of hygroscopicity, the heat of wetting of anhydrous AF has been measured and found to be approximately 21.5 calories/g. (Table V).

A sample of polyacrylonitrile which had been con-

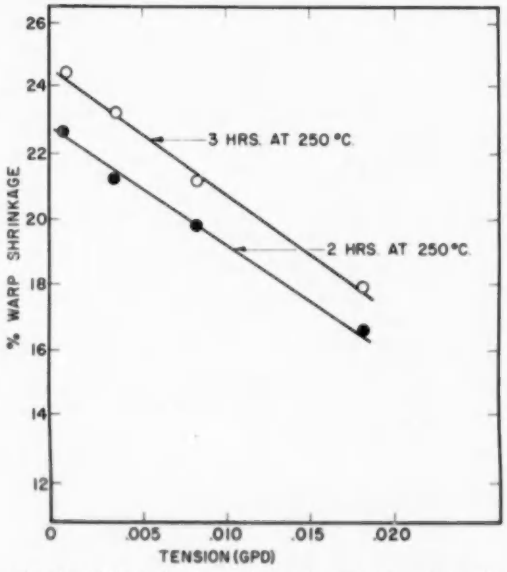

Fig. 7. Effect of tension during heat treatment on the warp shrinkage of Orlon acrylic fiber.

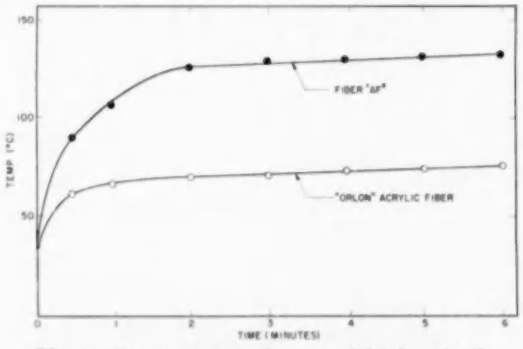

Fig. 8. Temperature at the rear of fabrics of AF and Orlon acrylic fiber.

TABLE VI. Thermal Properties of AF

Exposure Time	Degrees Centigrade	Remarks
5 min.	500	Sample glowed red, no flame, withdrawn whole.
5 min.	540	Sample glowed red, no flame, slight deterioration.
5 min.	820	Sample completely destroyed.
27 sec.	600	Sample lost rigidity in 4 sec., did not glow red or flame in 27 sec.
10 sec.	620	Longitudinal edges of sample glowed red in 7 sec. Did not flame.
10 sec.	650	Longitudinal edges of sample glowed red in 5 sec. Did not flame.
10 sec.	680	Longitudinal edges of sample glowed red in 4 sec. Did not flame.
10 sec.	705	$\frac{3}{16}$ in. of sample (longitudinal edge) glowed red. Did not flame.
10 sec.	735	$\frac{3}{4}$ in. of sample (longitudinal edge) glowed red. Did not flame.
10 sec.	760	Entire sample glowed red immediately; did not flame. No apparent change in tensile properties.
10 sec.	790	Entire sample glowed red immediately; flamed in 1 sec.
3 hr.	900	Completely consumed.

verted to AF by heating 24 hr. at 200° C. was analyzed as follows: C, 62.44; H, 3.45; N, 21.80; O, 12.31. This analysis can be explained by assuming that dehydrocyanation occurs in about 15% of the monomer units; oxidation occurs in the other 85% followed by dehydration of half of the oxidized units.

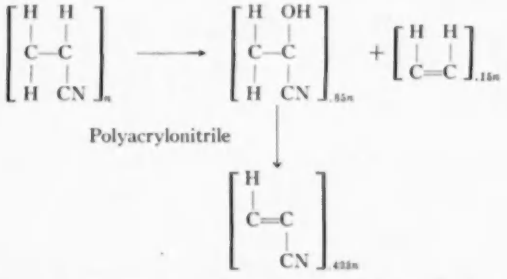

The above explanation applies only to the reactions of the monomer units. As suggested earlier by Houtz [8], a possible structure for AF could be represented by the condensed heterocyclic ring structure shown in Figure 10.

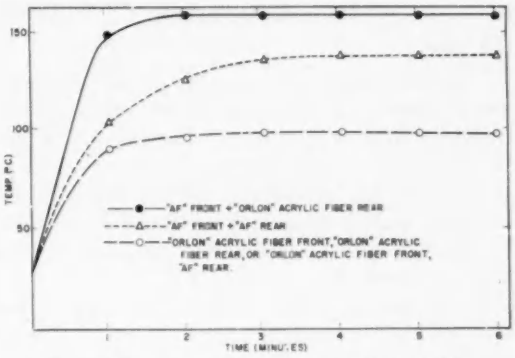

Fig. 9. Temperature between two layers of fabric of AF Orlon and acrylic fiber.

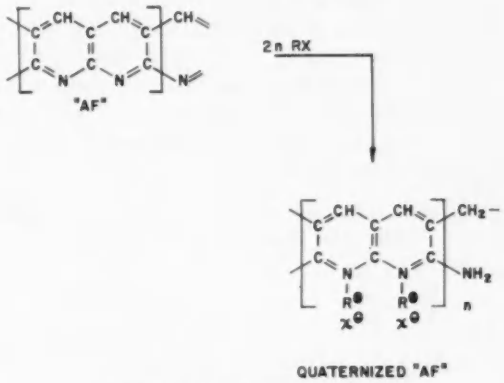

Fig. 10. Quaternization of AF.

A discussion of the structure of AF and the thermal degradation products of polyacrylonitrile is given elsewhere [1, 2, 4, 5, 6, 7].

Off-Gases During Heat Treatment

When polyacrylonitrile is heated below 120° C. in air or vacuum, no hydrogen cyanide and only trace amounts of ammonia can be found in the volatile components. However, as the heating temperature is increased, the amount of volatile components increases, resulting after pyrolysis in about 7% by weight of off-gases being released. The composition of the off-gases and the temperature range at which each is preferentially released is as follows:

Temp. range, °C.	NH_3, mole %	HCN, mole %	CH_4, mole %
Room temp.–200	1.3	0.7	0
250–370	3.9	3.0	0
390–500	4.8	2.2	3.4
Total	10.0	5.9	3.4

Properties of AF

Thermal

The most outstanding property of AF is its superior resistance to degradation on short-time exposures to high temperatures. For example, a piece of AF heated to over 750° C. for 10 sec. exhibited no apparent loss in tensile properties and only after extended heating times at high temperatures (3 hr. at 900° C.) was AF completely consumed. These data are summarized in Table VI.

It was found at the Naval Material Laboratory that AF had an unusually high resistance to destruction upon thermal irradiations. AF withstood exposures up to 5500 cal./cm.^{2} delivered in 60 sec., while all ordinary clothing fabrics of comparable weight were destroyed with only 50 cal./cm.^{2} exposures at similar delivery rates. The above rates were obtained by point focusing a standard Navy searchlight, having a calibrated emissivity measured in calories/sq. cm./sec., a standard distance onto a standard thickness of the test specimen.

Although AF was found to be extremely resistant to destruction for short-time, high-temperature exposures, it was further found that AF would offer somewhat less protection than wool, cotton, or Orlon against thermal radiation burns not only because of its high thermal conductivity, but also because of its higher absorptivity and higher optical transmittance.[6] When AF (fabric) was exposed to the infrared radiations of a GE heat lamp (250 watts, 5 in. from the fabric), the back surface of the fabric reached a temperature of 135–140° C. whereas Orlon acrylic fabric under comparable conditions reached a temperature of only 75–80° C. A combination of Orlon with AF showed that when the AF fabric was in front of the Orlon the temperature between the layers was higher than when the Orlon was in front of the AF. These data are summarized in Figures 8 and 9.

Since AF is a good conductor of heat, attempts were made to coat AF fabrics with a resin emulsion

[6] These data were obtained by the Naval Material Laboratory.

TABLE VII. The Effect of Temperature on the Physical Properties of Heat-Treated Orlon Acrylic Fiber

	Heat treatment				
	Control	1 hr. at 250° C.	2 hr. at 250° C.	3 hr. at 250° C.	3½ hr. at 250° C.
Original properties					
Denier, warp	398	467	539	567	584
Tenacity, g./den.	4.4	1.9	1.5	1.2	1.1
Elongation, %	16.1	9.4	8.2	6.8	5.6
Shrk. during prep.,					
% warp	—	14.0	22.6	24.6	25.4
% area	—	25.3	38.4	40.5	42.7
Fireproof	No	No	No	No	Yes
After 240 hr. at 165° C.					
Denier	442	492	537	574	533
Tenacity, g./den.	2.2	1.8	0.71	0.15	0.12
Ten., % retained	50	96	48	12	12
Elongation, %	9.6	8.0	3.3	2.0	2.0
Elong., % retained	60	90	40	30	36
Flex-abrasion life, cycles	5000	471	54	1	*
Shrinkage, % warp	6.3	5.4	3.9	2.6	2.5
Shrinkage, % area	15.7	10.7	7.9	4.6	6.8
After 500 hr. at 165° C.					
Denier	482	505	534	*	*
Tenacity, g./den.	0.64	0.82	0.14	*	*
Ten., % retained	15	44	9.4	*	*
Elongation, %	2.2	2.6	4.1	*	*
Elong., % retained	14	28	50	*	*
Flex-abrasion life, cycles	116	49	3	*	*
Shrinkage, % warp	15.6	9.8	5.6	3.6	3.2
Shrinkage, % area	30.7	18.8	11.2	6.7	7.2

* Too brittle to test.

TABLE VIII. Chemical Resistance of Fabrics of Orlon Acrylic Fiber Partially Converted to AF

Property	Heat treatment				
	Control	1 hr. at 250° C.	2 hr. at 250° C.	3 hr. at 250° C.	3½ hr. at 250° C.
Denier	410	468	535	567	578
Tenacity, g./den.	3.3	2.3	1.4	1.2	1.0
Elongation, %	14.5	13.2	9.0	7.2	5.9
Resist. to 10% NaOH at 50° C.					
% Retent. after 8 hr.,					
Tenacity	104	29	85	66	88
Elongation	104	20	31	184	83
% Retent. after 1 day,					
Tenacity	98	0	48	67	76
Elongation	113	0	15	36	46
% Retent. after 2 days,					
Tenacity	84	0	23	29	11
Elongation	94	0	10	17	19
Resist. to 37% HCl at 50° C.					
% Retent. after 8 hrs.,					
Tenacity	†	58	76	70	82
Elongation	†	230	48	78	79
% Retent. after 1 day,					
Tenacity	105	25	72	76	89
Elongation	109	14	32	70	64
% Retent. after 2 days,					
Tenacity	95	0	64	76	76
Elongation	105	0	28	57	66
Resist. to 58% H_2SO_4 at 50° C.					
% Retent. after 8 hrs.,					
Tenacity	†	98	89	73	78
Elongation	†	102	231	69	141
% Retent. after 1 day,					
Tenacity	108	97	76	73	84
Elongation	—	104	94	76	65
% Retent. after 2 days,					
Tenacity	106	94	74	70	87
Elongation	110	121	36	62	66
Properties after 500 hr. at 165° C.					
Denier	497	513	*	*	*
Tenacity, g./den.	0.74	1.0	—	—	—
Elongation, %	2.1	3.1	—	—	—
Resist. to 10% NaOH at 50° C., after 8 hr.	Disintegrated	Disintegrated	—	—	—
Resist. to 37% HCl at 50° C., after 8 hr.	Disintegrated	Disintegrated	—	—	—
Resist. to 58% H_2SO_4 at 50° C.					
% Retent. after 8 hr.,					
Tenacity	55	73	—	—	—
Elongation	224	106	—	—	—
After 1 day	Disintegrated	Disintegrated	—	—	—

* Too brittle to test.
† Exceeded range of instrument.

of TiO_2 in an effort to obtain a white heat-reflecting surface. No satisfactory white surface could be obtained by applying resin-bonded TiO_2 pigment. When a 50% aqueous slurry of TiO_2 was padded on AF followed by a resin-bonding treatment, white AF fabrics were obtained. However, due to the thick coating of the flammable bonding agent, the fabrics would support combustion.

Mechanical Properties

As shown in Table I and II, the initial construction of the fabric of Orlon greatly influenced the mechanical properties of the resulting AF fabric. Generally, the best AF fabrics had fair strength properties; for example, a warp yarn tenacity of 0.8–1.5 g./den., a 55–80% retention of the initial fabric grab strength, and a 25–50% retention of the initial fabric tongue tear strength. However, the transverse properties of AF were inferior to those of Orlon. All AF fabrics exhibited a low abrasion resistance and a low elongation; for example, a sample of Orlon which initially was flexed over 1400 flex abrasion cycles when converted to AF failed after 25 flex abrasion cycles.

When AF fabrics were held at elevated temperatures, a gradual loss of tensile properties occurred (Table VII). At 135° C. this property loss was very gradual; after one month an AF fabric dropped in tensile properties from a tenacity–elongation of 1.25/3.7 to .52/1.5. At 165° C. the loss in tensile properties was faster, while at 900° C. the fabric was completely consumed in 3 hr. If AF was heated to incandescence with a Bunsen or a Meeker burner (flaming) and held at this red heat (700 or 800° C.) for a few seconds, only a slight loss in tenacity could be noted.

Chemical Properties

The resistance of AF yarn to acids and bases is less than Orlon yarn. Generally, the chemical resistance of AF is dependent upon the previous heating cycle. The more severe the heat treatment, the poorer the chemical resistance. These data are tabulated in Table VIII.

TABLE IX. Mildew Resistance of AF

Fabric	Unleached: Reference strength in lb.	Unleached: Visible growth from *Chaetomium*	Unleached: Lb. of strength after test	Unleached: % Strength retained	Leached: Visible growth of *Chaetomium*	Leached: Lb. of strength after test	Leached: % Strength retained	Soil burial: Strength in lb. after test	Soil burial: % Strength retained
Orlon control A	220	1 1 1 1	203.7	93	1 1 1 1	226.5	103	185.7	83
Orlon control B	128.3	1 1 1 1	130.2	101	0 1 1 1	140.6	109	146.5	114
Fiber AF from control A	119.3	2 1 2 2	104.7	88	2 3 2 2	112.7	94	124.1	104
Fiber AF from control B	94.7	3 3 3 2	89	94	1 2 2 2	88.7	94	90.3	95
Cotton duck control	90	5 5 5 5	0	0	5 5 5 5	0	0	0	0

Visible Growth of *A. niger* U.S.D.A. No. 6275 and *P. citrinium* AATCC No. 9849

Fabric and construction style	Unleached: Visible growth	Leached: Visible growth
Orlon control A	1 1 1 1	1 1 1 1
Orlon control B	1 1 1 1	1 1 1 1
Fiber AF from control A	1 0 1 2	1 1 1 1
Fiber AF from control B	0 0 1 1	1 0 1 2
Cotton duck control	5 5 5	5 5 5

Key to visible growth:

Numerical designation	Fungal resistance	Amount of fungal growth
0	Excellent	No growth of fungi evident.
1	Good	Traces of fungi, observable with hand lens.
2	Fair	Slight growth, covering up to 25% of sample.
3	Poor	Moderate growth, covering 25–75% of sample.
4	Very poor	Profuse growth, covering 75–100% of sample.
5	Very poor	Profuse growth, covering all of sample, and also heavily fruited (spores).

AF is black not only on the surface of the fiber but through the entire yarn sample. If fabric of Orlon is heated in the absence of oxygen (for example, in nitrogen) for a time and temperature calculated to give AF (see Figure 3), a reddish-yellow, flammable product is obtained. If this material is allowed to stand at room temperature in air, it gradually darkens; however, no change in the flammability characteristics can be noted.

AF is not soluble in any common solvent. As noted in Table VIII, degradation does occur in hot caustic or hot mineral acids after extended exposure.

In visible growth tests using *Chaetomium*, some mildew was observed on the surface of AF after 14 days of incubation. Although a slight amount of growth was also observed when a mixture of *Aspergillus niger* and *penicillium citrinum* spores was sprayed on the sample, it retained essentially all of its tensile properties. Table IX summarizes these observations.

Since AF is slightly basic [7] and this basicity may be due to a tertiary nitrogen atom [8], it was felt that the reaction of AF with an alkyl halide might produce a quaternary salt (Figure 10) which would have an increased electrical conductivity. The conductivity of AF initially in the range of Dacron [8] polyester fiber (resistivity = 10^{18} ohms) was increased 1000-fold upon treatment with benzyl bromide so that its conductivity was now in the range of glass (resistivity = 10^{15} ohms).

Miscellaneous Properties

AF has less lateral order as well as less orientation than the polyacrylonitrile control. These data were obtained by the visual comparison of x-ray diagrams of AF and Orlon fibers from both drawn and undrawn yarns.

The density of AF was found to be between 1.57 and 1.60, while polyacrylonitrile has a density of 1.17.

Possible Uses for AF Fibers and Fabrics

The most remarkable property of AF is its superior resistance to high-temperature degradation upon short-time exposures; that is, its high critical energy input value. Fabrics and fibers of AF are fireproof. The 40–45% area shrinkage that occurs during the preparation of AF minimizes any additional shrinkage at elevated temperatures in either hot air or boiling water. Approximately 40% of the inherently good tensile properties of Orlon acrylic fiber are retained by AF. The most serious deficiencies of AF are its poor yarn-on-yarn abrasion resistance and its decreased flex life; that is, its poor transverse properties. In uses (military or civilian) where fireproofing clothing is desired, for example, flight clothing, flame throwers' clothing, proximity suits, fire-fighting suits, etc., it is felt that fabric properties such as abrasion resistance and seam strength cannot be sacrificed just to achieve fireproofing. However, the high critical energy input value of AF may suggest uses where this property is desired at the sacrifice of transverse properties.

Other possible applications for AF are:

1. High-temperature-resistant electrical insulators.
2. Hydrolytic filtration fabrics (provided flexing is a minimum).
3. Fireproof laminate for heat-resistant plastics; for example, conveyor belts, brake linings, etc.
4. Welders' curtains and sleeves.
5. Fireproof sewing thread.

Properties of "AF" Sewing Thread

	Denier	Tenacity, g./den.	% Elongation	Flex life, Cycles
Control	690	3.3	20	1300
AF	872	1.5	15	1200

6. Fireproof carrier and/or reinforcing agent for nonfireproof materials.
7. Mixed fibers and fabrics with other fireproofing materials.

Summary

AF is prepared by heat-treating yarns or fabrics of Orlon acrylic fiber, preferably the latter, in air at temperatures in excess of 160° C. The logarithm of the reaction time is inversely proportional to the heating temperature. The important variables in the process are (1) heating time and temperature; (2) fabric construction—due to the exothermic nature of the reaction and the excessive shrinkage which accompanies this heat treatment, it is necessary to dissipate the heat of reaction rapidly and to allow the yarn to shrink freely; and (3) heating atmosphere—oxygen is essential; the optimum concentration is 15–20%.

[7] Attempts were made to determine the basicity of AF, but due to its insolubility, only very erratic results were obtained. However, it was shown that flamed AF was generally more basic than AF itself.

[8] Registered Du Pont trademark.

AF is fireproof and has an unusually high resistance to destruction upon short-time thermal irradiation. In fact, AF can resist thermal radiations over 100-fold higher than ordinary clothing fabrics. Upon continued exposure to high temperatures, AF gradually loses its tensile properties; at 900° C. it is completely destroyed in 3 hr. AF has slightly higher thermal conductivity, optical transmittance, and absorptivity than wool or cotton. While AF has fair tensile properties, its transverse properties are poor, excluding its possible utility in various types of fireproof garments where good abrasion resistance is required. However, the above failings of AF as an ordinary clothing fabric should not preclude its use in applications where its more advantageous qualities, such as fireproofing and unusual resistance to thermal radiation, is required.

Acknowledgment

Grateful acknowledgment is made to the following members of the Du Pont research staff whose contributions made this paper possible: Dr. M. Q. Webb, Dr. D. L. Green, Mr. C. R. Humphreys, and Mr. A. W. Riester, for early scouting work on the preparation and properties of Fiber AF; Mr. R. A. Kasey, for early process development work on Fiber AF (Figures 6 and 7) and for the development of the larger-scale preparation of AF (Figure 2); Dr. E. F. Evans, for the fabric construction data (Tables I and II), heating atmosphere data (Figures 4 and 5), chemical resistivity studies (Table VIII), and temperature–physical property relationships (Table VII); Dr. O. H. Bullitt and Dr. R. Zbinden, for the determination of off-gases; Dr. R. L. Krause and Dr. S. H. Davidson, for the soil burial and mildew resistance data (Table IX); Mr. J. A. Roetling, for the determination of the thermal radiation characteristics (Figures 8 and 9); and Mr. C. A. Shoecraft and Mr. J. S. H. Cruice, for furnishing the fabrics of Orlon acrylic fiber studied in this work.

Acknowledgment is also made to Mr. Thomas I. Monahan of the Materials Laboratory of the New York Naval Shipyard for allowing us to use their data on the thermal radiation characteristics of AF and to the Mica Insulator Company for allowing us to include in this publication a schematic representation of their high-temperature curing tower (Figure 2).

Literature Cited

1. Burlant, W. J. and Parsons, J. L., *J. Polymer Sci.* **22**, 249–56 (1956).
2. Church, J. M., *Chem. Eng. News* **31**, 325–9 (1953).
3. Drake, G. M., *Electronic News* **1**, January 11 (1960).
4. Grassie N. and McNeill, I. C., *J. Chem. Soc.* **1956**, 3929–33 (1956).
5. Grassie, N. and McNeill, I. C., *J. Polymer Sci.* **27**, 207–18 (1958).
6. Grassie, N. and McNeill, I. C., *J. Polymer Sci.* **30**, 37–46 (1958).
7. Grassie, N. and McNeill, I. C., *J. Polymer Sci.* **39**, 211–222 (1959).
8. Houtz, R. C., TEXTILE RESEARCH JOURNAL **20**, 796 (1950).
9. Little, R. W., "Flameproofing Textile Fabrics," New York, Reinhold Publishing Company (1947).
10. Siggia, S., "Quantitative Organic Analysis *via* Functional Groups," New York, John Wiley & Sons (1949).

Manuscript received February 11, 1960.

The Mechanical Properties of the Ortho- and Para-Like Components of Lincoln Wool Fibers

M. Feughelman and A. R. Haly

C.S.I.R.O. Wool Research Laboratories, Division of Textile Physics, Ryde, N.S.W., Australia

Abstract

The mechanical properties of Lincoln wool fibers in which the para-like portion of the wool fiber has been removed by abrasion have been compared with the properties of the same fibers unabraded. Results of tests in water at 20° C. indicate that the stress–strain curve in the yield region is considerably different in slope for an unabraded as against an abraded fiber. This result, together with other lesser mechanical differences, can be explained in terms of a difference of packing between the para-like and ortho-like components of a wool fiber. At pH 1 mechanical tests show a major reduction in these mechanical differences, suggesting that the packing in para-like wool components is mainly dependent on salt linkages.

Introduction

Thorsen [7], in an analysis covering a wide range of wool types from Merino to Lincoln, has shown a general mechanical stiffening of fibers (tested in water) with increase in the proportion of paracortex present in the fiber. This survey required the careful examination and testing of a large number of fibers both for proportion of paracortex and mechanical properties. With the development by Snaith [4] of a centerless grinding technique, which enabled Lincoln wool fibers to be uniformly ground to constant-diameter cylinders over many centimeters length, it has become possible to measure more directly the mechanical properties of the para- and ortho-like sections of fibers where these sections are radially disposed across the fiber cross section.

Experimental

Medulla-free Lincoln wool fibers were selected for uniformity of diameter along their length. These fibers were cut into half-lengths. Each pair of half-fibers was kept together and one half-fiber of the pair was ground down by the technique described by Snaith [4] to a uniform-diameter cylinder of cross-sectional area between $\frac{1}{4}$ and $\frac{1}{3}$ of the original area. Previous checks using dyeing techniques showed that this amount of removal of the outside of these wool fibers left only the ortho-like portion. The mechanical properties of the abraded half-fiber were compared with the properties of the corresponding untouched half-fiber.

The load–extension curves of these fibers in distilled water (pH 6.5) and in aqueous HCl (pH 1) were determined at a constant rate of loading by use of a standard Cambridge Textile Extensometer. The fibers were in the form of a loop with the two ends held by a tapering plug holder, the looped end being passed over a hook. All the experiments were carried out at a temperature of 20° ± 1° C. Prior to each test each fiber was relaxed in water at 52° ± 1° C. for 1 hr. The rate of loading for the double fiber during load–extension tests was 1.03 g./min.

Load–extension curves were obtained in water for ten pairs of fiber halves. The first four pairs were extended well beyond the yield region so that estimates could be made of the turnover point between the yield and post-yield regions. These fibers were then rejected for further test because the excessive strain [2] they had undergone made their original mechanical properties irreproducible. Load–extension curves were then obtained for the remaining six pairs of fibers in HCl solution at pH 1. After these fibers were tested at pH 1, a repeat experiment was carried out in distilled water. The repeat test was used as a check to show that reproducibility was obtained between the first and last tests in distilled water. There was no measurable difference between the curves.

Results in Distilled Water

As would be expected from the results obtained by Thorsen [7], the unabraded wool fiber in water,

which contains both ortho- and para-like components, is generally stiffer in load–extension tests than the purely ortho-like abraded fiber. Figure 1 illustrates the general relationship in terms of stress and strain between an abraded and unabraded pair of fiber halves tested in distilled water at pH ~ 6.5. Although the Hookean region for the abraded fiber (OA′) in general appeared weakened relative to the unabraded fiber (OA), the experimental technique used did not lend itself to an accurate assessment of this difference. However, in the slope of the yield regions a major difference was observed. The slope for the unabraded fiber averaged 2.72×10^8 dynes/cm.^{2} while the abraded fiber averaged 4.15×10^8 dynes/cm.^{2} (see Table I).

Also, a significant difference was obtained in the value of the stress at 15% extension. For the unabraded fiber this stress had an average value of 3.72×10^8 dynes/cm.^{2} and for the abraded fiber, a value of 3.30×10^8 dynes/cm^2.

TABLE I. Values of the Yield Region Slope of the Stress–Strain Curve of the Unabraded and Corresponding Abraded Wool Fibers in Distilled Water (pH about 6.5), Together With the Values of the Stress in Each Case at 15% Extension

	Slope of yield region			Stress over 15% extension	
Fiber no.	Unabraded, $\times 10^8$ dynes/cm.^{2}	Abraded, $\times 10^8$ dynes/cm.^{2}	Ratio of yield slopes	Unabraded, $\times 10^8$ dynes/cm.^{2}	Abraded, $\times 10^8$ dynes/cm.^{2}
1	3.28	6.17	0.53	3.46	3.43
2	1.86	4.35	0.43	3.54	3.33
3	2.64	4.25	0.62	3.41	3.40
4	2.60	3.14	0.83	3.63	3.13
5	3.19	3.88	0.82	3.96	3.42
6	2.55	3.88	0.66	4.30	3.46
7	3.42	3.85	0.89	4.37	3.69
8	3.05	3.40	0.90	4.59	3.11
9	2.51	4.31	0.58	3.76	3.15
10	2.08	4.24	0.49	3.22	2.86
Mean	2.72	4.15	0.66	3.72	3.30
Standard deviation of mean	0.17	0.26	0.05	0.05	0.07

TABLE II. Strain at Turnover from Yield to Post-Yield Regions

Fiber no.	Unabraded, %	Abraded, %	Difference, %
1	28.0	29.5	+1.5
2	27.9	29.0	+1.1
3	26.4	28.9	+2.5
4	28.2	29.3	+1.1

The strain at the turn-over point between the yield and post-yield regions (B and B′ in Figure 1) showed a general increase for the abraded wool fiber as against the unabraded fiber (see Table II).

Results at pH 1

Speakman and Hirst [5] have indicated a stability of mechanical properties of wool fibers from pH 7 down to pH 4. Below pH 4 is a region of mechanical weakening of fibers until pH 1 is reached. At pH 1 a new region giving stable mechanical properties begins. In a later paper [6] these authors claim that the weakening of the wool fiber between pH 4 and pH 1 is due to breakdown of salt linkages.

Load–extension curves on fiber pairs No. 5–10 (see Table III) at pH 1 gave for the slope in the yield region of unabraded fibers an average of 4.06 $\times 10^8$ dynes/cm.^{2} and for the abraded fibers, 4.65×10^8 dynes/cm^2. These values indicate that the slope of yield region for an unabraded fiber is affected much more by the change from pH 6.5 to a pH 1 medium than the abraded fiber. The change in the stress at 15% extension going from pH 6.5 to pH 1 for both abraded and unabraded fibers showed an almost identical drop of about 40% (see Table IV).

TABLE III. Values of the Yield Region Slope of the Stress–Strain Curves of an Unabraded Wool Fiber and the Corresponding Abraded Fiber in an HCl Solution at pH 1

Fiber no.	Unabraded, $\times 10^8$ dynes/cm.^{2}	Abraded, $\times 10^8$ dynes/cm.^{2}	Ratio of yield slopes
5	4.82	4.56	1.06
6	4.32	5.25	0.82
7	4.30	5.12	0.84
8	4.17	4.35	0.96
9	3.92	4.78	0.82
10	2.84	3.86	0.79
Mean	4.06	4.65	0.87
Standard deviation	0.27	0.22	0.08

TABLE IV. Ratio of Stresses at pH 1 and pH 6.5 for Abraded and Unabraded Fiber Halves Both at 15% Strain

Fiber no.	Unabraded	Abraded
5	0.63	0.56
6	0.60	0.62
7	0.58	0.60
8	0.61	0.59
9	0.61	0.65
10	0.61	—
Average	0.61	0.60

Discussion

In distilled water the major mechanical difference between the abraded and unabraded fibers is in the slope of the yield region. If the part of the fiber which is abraded away is considered to be purely para-like and the part remaining, which is almost ¼ of the unabraded fiber, to be purely ortho-like, the slope in the yield region for the para component can be calculated from the average values given in Table I of this slope for the abraded and unabraded fibers. It was assumed that ortho- and para-like parts are in parallel and the yield region slope of the para-like part of the fiber was calculated to be 2.0×10^8 dynes/cm.^{2} This value is less than half the value for the ortho-like component of 4.15×10^8 dynes/cm.^{2} A simple explanation of this considerable difference in yield region slope can be based on a postulated difference in organization of the mechanical units forming the ortho- and para-like portion of the fiber.

Let us consider the ortho-like part of the wool fiber to consist of mechanical units which vary slightly in their stress–strain relation, as indicated in Figure 2, Curves a, b, and c. Three such units acting in series would give an average stress–strain curve with a slope in the yield region very different from that of the original units (see Figure 2, dotted curve). For the para-like section of the wool fiber it would be necessary to postulate that all the mechanical units act almost identically. It is known [3] that the ortho- and para-like components of a wool fiber are dissimilar in the lateral packing of their microfibrils, the paracortex appearing more crystalline. Experiments [1] on the torsional properties of wools with radial and bilateral distribution of the ortho-like and para-like material have already shown the effect of this packing on these properties of the fiber. Better packing with more accurate alignment of microfibrils and more cross-linkages in the paracortex would be consistent with the idea that this part of the structure acts mechanically more nearly like a single unit, hence giving a yield region over a narrow band of stress. In the orthocortex, where the microfibrillar packing is inferior, it is possible that the microfibrillar alignment is not as accurate. This latter proposition is supported by the fact that the ortho-like portion of the wool fiber must be extended further (see Table II) than the para-like portion to reach the turnover strain between the yield and post-yield regions (Points B′ and B in Figure 1). This may mean that some strain is taken up in bringing the microfibrils into alignment in the ortho-like portion of the wool fiber.

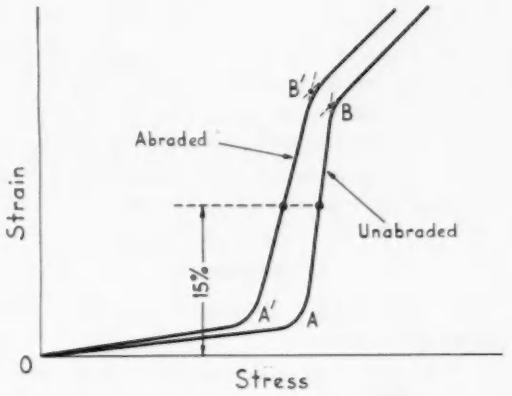

Fig. 1. The stress–strain curves of the abraded and unabraded halves of the same Lincoln wool fiber in water, converted from the load–extension curves drawn by the Cambridge Textile Extensometer.

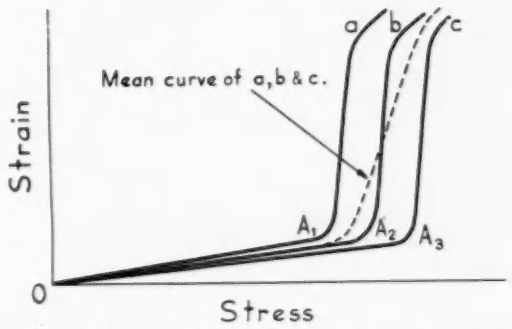

Fig. 2. The stress–strain curves of three proposed mechanical units, a, b, and c in series, and the stress–strain curve (dotted) of the resultant of these units.

The mechanical tests at pH 1 indicate a great reduction in the difference between the yield regions for the ortho- and para-like portions of the wool fibers tested. The breakdown of salt linkages at pH 1 results in a 50% change in the slope of the yield region for an abraded fiber and only a 12% change for the ortho-like abraded fiber. The fact that the value of the yield region slope of the para-like section of the wool approaches the value of the ortho-like section at pH 1 and that the change from pH ~ 6.5 to pH 1 has only a relatively minor effect on the value of this slope for the ortho-like section means that the salt linkages that are broken in the

para-like section when the pH is changed from ~ 6.5 to 1 play a vital part in the organization of the para-like structure. Further, the major difference between the ortho- and para-like portions of the wool fiber may be due to these salt linkages being present in the para- but not in the ortho-like portion of the fiber.

Acknowledgment

The authors thank J. W. Snaith for preparing the abraded fiber specimens.

Literature Cited

1. Andrews, M. W., Feughelman, M., and Mitchell, T. W., in preparation.
2. Feughelman, M., *J. Textile Inst.* **45**, T630 (1954).
3. Rogers, G. E., *J. Ultrastructure Res.* **2**, 309 (1959).
4. Snaith, J. W., TEXTILE RESEARCH JOURNAL **30**, 543 (1960).
5. Speakman, J. B. and Hirst, M. C., *Nature* **127**, 665 (1931).
6. Speakman, J. B. and Hirst, M. C., *Nature* **128**, 1073 (1931).
7. Thorsen, W. J., TEXTILE RESEARCH JOURNAL **28**, 185 (1958).

Manuscript received April 15, 1960.

Letter to the Editor

Short communications in the form of Letters to the Editor are intended to provide prompt publication of significant new research results and to permit an exchange of views on papers previously published in the JOURNAL. These communications are not submitted to formal review as are research papers, and the editors do not assume any share of the author's responsibility for the information given or the opinions expressed. When work previously published in the JOURNAL is the subject of critical comment, the authors of the original paper are given an opportunity to submit a reply, which will be published concurrently when possible.

Setting Wool Textiles with Ethanolamine

Western Regional Research Laboratory[1]
Albany 10, California
June 6, 1960

To the Editor
TEXTILE RESEARCH JOURNAL

Dear Sir:

Various reducing and alkaline agents have been suggested and employed for permanent setting of waves, pleats, and creases in materials composed of keratin fibers [1, 2, 4, 5]. During an investigation of setting agents, we have observed that highly effective setting of creases in wool textiles is accomplished simply by steam pressing fabrics treated with very dilute solutions of ethanolamine. Durable creases and pleats can thereby be imparted to wool garments without significant damage to the hand, strength, or other properties of the material.

In the above process, a dilute solution of ethanolamine is applied to the textile, which is then heated while constrained in the desired pattern. It is believed that heating the fabric in the presence of ethanolamine disrupts certain chemical bonds in the wool and that these bonds are then re-formed in the constrained position. Because ethanolamine is nonvolatile, it remains in the fabric; in the small amount used, it causes no apparent wool damage. The ethanolamine process avoids the use of reducing agents such as thioglycolates and bisulfites, which are often accompanied by objectionable odors.

The ethanolamine is usually applied to the textile as a 0.25–2% aqueous solution. The solution may be applied to the entire textile by spraying or immersion; it may also be applied only to the area to be creased or set into a pattern. The textile is heated at temperatures between 100° C. and 150° C. by a tailor's steam press or other heating device. The time for setting is decreased with increasing temperature, and may vary from several seconds to a few minutes. When the process is properly carried out, the pleats are durable to both dry cleaning and mild laundering.

As an illustration of the process, strips of wool flannel (7 oz./sq. yd.) were folded over and steam pressed for about ½ min. Each cloth was treated with a solution containing a particular concentration of ethanolamine and 0.01–0.05% of isooctyl phenyl ether of polyethylene glycol wetting agent. The solutions were applied along the crease at about 0.1 ml. of solution per inch. The cloths were then pressed in a tailor's flat bed press with the steam supply at a temperature of 140–145° C. Pressing was continued for a period up to 30 sec. while the steam flowed onto the cloths. Suction was then applied for 30 sec. to exhaust the steam from the cloths.

To test the durability of the creases, the strips were washed in a household agitator-type washer for 4 min. at 38° C. in water containing 0.1% of detergent. After being washed, the cloths were tumble-dried for 20 min. at 65° C. in a household dryer. A control sample which was not treated with ethanolamine solution was steam pressed and washed with the other samples. The dried strips were visually examined and the creases rated on the following scale: excellent, good, fair, poor, no crease. The results are tabulated in Table I.

Breaking strength tests by the cut-strip method

[1] A laboratory of the Western Utilization Research and Development Division, Agricultural Research Service, U.S. Department of Agriculture.

TABLE I

Conc'n of ethanolamine in treating sol'n, %	Time of steaming, sec.	Crease rating
0.25	15	poor
0.25	30	excellent
0.5	5	poor
0.5	15	excellent
0.5	30	excellent
1.0	5	good
1.0	30	excellent
None (control)	30	poor

(ASTM D 39-49) indicated that the process causes no significant loss in fabric strength. Durable creases have also been imparted to dyed fabrics shrinkproofed by polyamide-epoxide resins [3] without loss of shrinkproofing or adverse effect on the dye. Since fabrics vary, it is advisable to employ test swatches to check for possible dyeshade alteration and to determine optimum ethanolamine concentration and pressing time. In general, the ethanolamine process shows promise of being an economical and successful method for durably creasing a variety of wool fabrics.

Acknowledgment

The authors wish to thank Helen Kivela for skilled technical assistance.

Literature Cited

1. C.S.I.R.O. (Aust.) Wool Textile Res. Lab., "Durable Creasing and Pleating of Pure Wool Fabrics," Report No. G6, Geelong (1957).
2. Farnworth, A. J., TEXTILE RESEARCH JOURNAL **27**, 632 (1957).
3. Pardo, C. E. Jr. and O'Connell, R. A., *Am. Dyestuff Reptr.* **47**, P333 (1958).
4. Speakman, J. B. and Marks and Spencer, Ltd., British Patent 775,486 (1957).
5. Wool Bureau, Inc., Wool Science and Technology Report No. 4, "Durable Pleating and Creasing of All-Wool Apparel with Si-Ro-Set Solution" (1959).

N. H. KOENIG
W. L. WASLEY
C. E. PARDO, JR.